MODELING OF DIFFUSIONAL LIMITATIONS IN STYRENE ACRYLONITRILE (SAN) BULK COPOLYMERIZATIONS AND MULTI-OBJECTIVE OPTIMIZATION OF SAN REACTORS

by

RAJESHWAR MAHAJAN

COLLEGE OF ENGINEERING STUDIES

under the guidance of

Dr. SANTOSH K. GUPTA

PROFESSOR, DEPARTMENT OF CHEMICAL ENGINEERING

and

Dr. ASHOUTOSH PANDAY

PROFESSOR, DEPARTMENT OF CHEMICAL ENGINEERING

submitted

IN PARTIAL FULFILLMENT OF THE REQUIREMENT OF

THE DEGREE OF DOCTOR OF PHILOSOPHY

to the

UNIVERSITY OF PETROLEUM AND ENERGY STUDIES
DEHRADUN
December, 2014

DECLARATION BY THE SCHOLAR

I hereby declare that this submission is my own work and that, to the best of my knowledge and belief, it contains no material previously published or written by another person nor material which has been accepted for the award of any other degree or diploma of the university or other institute of higher learning, except where due acknowledgment has been made in the text.

Place: UPES, Dehradun   (Rajeshwar Mahajan)

Date: 30-11-14

THESIS COMPLETION CERTIFICATE

This is to certify that the thesis on "**Modeling of Diffusional Limitations in Styrene Acrylonitrile (SAN) Bulk Copolymerizations and Multi-Objective Optimization of SAN Reactors**" by **Rajeshwar Mahajan** in partial completion of the requirements for the award of the Degree of Doctor of Philosophy (Engineering) is an original work carried out by him under our joint supervision and guidance.

It is certified that the work has not been submitted anywhere else for the award of any other diploma or degree of this or any other university.

Dr. Santosh K. Gupta   **Dr. Ashoutosh Panday**

Professor   Professor

Dept. of Chemical Engineering   Dept. of Chemical Engineering

UPES, Dehradun – 248007   UPES, Dehradun – 248007

Date: 30-11-14

ACKNOWLEDGEMENTS

I sincerely appreciate the inspiration; support and guidance of all my friends and colleagues for aspiring guidance, constructive criticism and friendly advice during this work.

Last but not the least, a special thanks to my family for their continuous encouragement. They are my eternal source of inspiration. Without their encouragement and understanding, it would have been impossible for me to finish this work.

Rajeshwar Mahajan

EXECUTIVE SUMMARY

Polymers have become an integral part of our life due to their lower cost and better properties. In copolymerization, two or more monomers are combined in a desired proportion in the presence of some initiator to produce copolymers having the desired physical and chemical properties. The control of these properties requires a thorough knowledge of the polymerization kinetics as well as the associated transport processes. The desired properties of the polymers can be obtained by maintaining the optimal temperature history in industrial reactors. The present study focuses on the modeling and multi-objective optimization of diffusional limitations in random bulk copolymerization of styrene-acrylonitrile (SAN).

Chapter 1 gives the insights of the kinetic scheme and the diffusion controlled transport of random bulk copolymerization of SAN. Diffusional limitations (the gel, glass and cage effects) are manifested in several bulk free radical homopolymerizations as well as in random copolymerizations. These are associated with a decrease of several orders of magnitude of the rate constants of termination, propagation and initiation (the initiator efficiency), respectively.

Chapter 2 describes the literature review on the modeling and optimization of homopolymerization and copolymerization systems. Most of the work in the literature gives information about the modeling of diffusional limitations in

homopolymerizations under isothermal/non-isothermal operations in batch/semi-batch reactors. However, most of the modeling and optimization work in copolymerization is on solution polymerizations, where diffusional limitations are not manifested. The earlier models developed for bulk copolymerizations focus only on isothermal batch reactors. Some of the work in the literature is on their multi-objective optimization (MOO). The objective functions are selected to produce a copolymer with desired physical properties and with minimal post separation costs. Commonly used objective functions in MOO include minimization of the reaction time, maximization of the overall monomer conversion, the copolymer product having a desired value of the styrene mole fraction and having a desired value of the number average molecular weight.

Chapter 3 highlights important aspects of the kinetics of SAN copolymerization. The method of moments is used to define the growing radicals and resulting dead copolymer molecules. Diffusional limitation phenomena have been modeled earlier using the free volume theory for the diffusivities of the primary radicals, macro-radicals and monomer molecules, and have been applied to homopolymerizations. In this study, a similar model is developed for random bulk copolymerizations using the free volume theory of Vrentas and Duda.[1, 2] The model developed for copolymerization is along the lines used by Ray et al. [3] and Seth and Gupta [4] for homopolymerizations. The kinetic model of SAN copolymerization consists of mass balance equations, moment equations, gel, glass and cage effect (and other associated) equations.

In Chapter 4, the kinetic model of the SAN bulk copolymerization is used to carry out single and multi-objective optimization of these reactors under non-isothermal batch conditions. The objectives are selected from among: minimization of the reaction time, maximization of the overall monomer conversion and maximization of the number average molecular weight of the product. Constraints are used for the mole fraction of styrene in the copolymer produced (so as to produce copolymer having desired properties), and on the permissible range of temperature in the reactor. The purpose is to generate optimal temperature histories in order to achieve these objectives using genetic algorithm.

Results and discussion are presented in Chapter 5. The parameters of the model are fitted using *isothermal* data on styrene acrylonitrile (SAN) random copolymerization carried out in small ampoules using AIBN initiator. The model is tuned by minimizing the *normalized* sum of square errors between the experimental data of Garcia-Rubio et al. [5] and the model-predicted values to obtain the individually optimized parameters (IOPs). Thereafter, best-fit global correlations have been developed for this system where these parameters are expressed as a function of temperature, initial mole fraction of styrene in the feed and initial molar concentration of the initiator. This enables the model to be used for studying non-isothermal copolymerizations. The model is then used to optimize SAN bulk copolymerization reactors using single and multiple objective functions. In single objective optimization, the temperature history is obtained which minimizes the total reaction time while maintaining the overall monomer conversion, number average molecular

weight and the mole fraction of styrene in the copolymer at a specified (desired) value. In the two objective optimization problem, the objective functions are the minimization of the total reaction time and the maximization of the number average molecular weight of the product. The overall monomer conversion and the mole fraction of styrene in the copolymer produced are taken as constraints. In the three objective problem, the objective functions are the minimization of the total reaction time, the maximization of the number average molecular weight of the product and the maximization of the overall monomer conversion. The constraint used in this problem is the desired mole fraction of styrene in the copolymer produced. The optimization toolbox of MATLAB with genetic algorithm as the solver is used. Pareto optimal solutions are obtained for the 2- and 3- objective optimization problems. Different points in the Pareto set are associated with different optimal temperature histories, some of which are presented.

Finally, the conclusions derived from the present investigation are summarized in Chapter 6. An improved model is developed for SAN copolymerizations which can be used for non-isothermal batch reactors. Optimal temperature histories are generated using MOO to produce a copolymer having desired physical properties. Recommendations for future studies have also been included here.

References:

1.   Vrentas, J. S. and Duda, J. L. (1977), Diffusion in Polymer-Solvent Systems. II. A Predictive Theory for the Dependence of Diffusion Coefficients on Temperature, Concentration and Molecular Weight.

Journal of Polymer Science - Polymer Physics Edn., Vol. 15. pp. 417-439.

2.   Vrentas, J. S. and Duda, J. L. (1979), Molecular Diffusion in Polymer Solutions. AIChE Journal, Vol. 25. pp. 1-24.

3.   Ray, A. B., Saraf, D. N., and Gupta, S. K. (1995), Free Radical Polymerizations Associated With the Trommsdorff Effect Under Semibatch Reactor Conditions. I: Modeling. Polymer Engineering and Science, Vol. 35. pp. 1290-1299.

4.   Seth, V. and Gupta, S. K. (1995), Free Radical Polymerizations Associated with the Trommsdorff Effect Under Semi-Batch Reactor Conditions: An Improved Model. Journal of Polymer Engineering, Vol. 15. pp. 283-326.

5.   Garcia-Rubio, L. H., Lord, M. G., MacGregor, J. F., and Hamielec, A. E. (1985), Bulk Copolymerization of Styrene and Acrylonitrile: Experimental Kinetics and Mathematical Modelling. Polymer, Vol. 26. pp. 2001-2013.

CONTENTS

xi

LIST OF SYMBOLS

$(AN)_m$ mole fraction of acrylonitrile in copolymer

D_I diffusivity of the initiator in the monomer copolymer mixture

D_m diffusivity of the monomer in the monomer copolymer mixture

D_p diffusivity of the copolymer in the monomer copolymer mixture

$D_{n,\,m}$ dead polymer molecule having n repeat units of monomer 1 and m repeat units of monomer 2

E_d, E_{I1}, E_{I2} activation energies for the initiation reaction, J mol^{-1} K^{-1}

E_{pij}, E_{fij} activation energies for the propagation reaction and chain transfer to monomer, J mol^{-1} K^{-1}

E_{tcij}, E_{tdij} activation energies for the termination reaction, J mol^{-1} K^{-1}

f initiator efficiency

f_0 initiator efficiency in the limiting case of zero diffusional resistance

f_{10} initial mole fraction of styrene in feed

I, I_i^*, I_i objective function, objective functions (i = 1, 2 and 3)

I_0 initial molar concentration of initiator, mol m^{-3} or mM

k_d, k_{I1}, k_{I2} rate constants for initiation at any time t, s^{-1} or m^3 mol^{-1} s^{-1}

k_p rate constants for propagation, m^3 mol^{-1} s^{-1}

k_{pij} rate constants for propagation at any time t, m^3 mol^{-1} s^{-1} (i, j = 1, 2)

k_t rate constants for termination, m^3 mol^{-1} s^{-1}

k_{tcij}, k_{tdij} rate constants for termination by combination and by disproportionation at any time t, m^3 mol^{-1} s^{-1} (i, j = 1, 2)

k_{fij}	rate constants for chain transfer to monomer at any time t, m³ mol⁻¹ s⁻¹ (i, j =1, 2)
$k_{I1,o}$, $k_{I2,o}$	k_{I1}, k_{I2} in absence of the gel, glass and cage effects, m³ mol⁻¹ s⁻¹
$k_{pij,o}$	k_{pij} in absence of the gel, glass and cage effects, m³ mol⁻¹ s⁻¹ (i, $j = 1, 2$)
$k_{tcij,o}$, $k_{tdij,o}$	k_{tcij} and k_{tdij} in absence of the gel, glass and cage effects, m³ mol⁻¹ s⁻¹ (i, $j = 1, 2$)
$k_{fij,o}$	k_{fij} in absence of the gel, glass and cage effects, m³ mol⁻¹ s⁻¹ (i, $j = 1, 2$)
k_d^0, $k_{pij,0}^0$, $k_{fij,0}^0$, $k_{tcij,0}^0$, $k_{tdij,0}^0$	frequency factors for the intrinsic rate constants, s⁻¹ or m³ mol⁻¹ s⁻¹
M_i	moles of monomer i in liquid phase, mol ($i = 1$: styrene, i = 2: acrylonitrile)
M_{jp}	molecular weight of polymer jumping unit, kg mol⁻¹
$\bar{M}_n$	number average molecular weight, kg mol⁻¹
$\bar{M}_w$	weight average molecular weight, kg mol⁻¹
$(MW)_I$	molecular weight of initiator, kg mol⁻¹
$(MW)_{mi}$	molecular weight of the monomer i, kg/mol
$P_{n,m}$	growing polymer radical having n repeat units of monomer 1 and m repeat units of monomer 2 with monomer 1 at terminal end
$Q_{n,m}$	growing polymer radical having n repeat units of monomer 1 and m repeat units of monomer 2 with monomer 2 at terminal end
r_1, r_2	reactivity ratios
r_{I1}, r_{I2}	radius of initiator reaction sphere and diffusion sphere, m

r_D	radius at which the concentration of the radical approaches the unperturbed bulk concentration
r_m	effective reaction radius, m
R	primary radical
R^*	the average number of both monomer 1 and 2 chain sequence occurring in a copolymer per 100 monomer units
R_g	universal gas constant, J mol^{-1} K^{-1}
St_c	mole fraction of styrene in the copolymer
St_{rm}	mole fraction of styrene in the (unreacted reaction) mixture
t	time, s
T	temperature of the reaction mixture at time t, K or ^{o}C
T_{gm1}, T_{gm2}	glass transition temperature of the monomers 1 and 2, K
T_{gp}	glass transition temperature of the copolymer, K
$\bar{T}_{gp}$	mean glass transition temperature of the two copolymers, K
T_{gp1}, T_{gp2}	glass transition temperatures of the copolymers 1 and 2, K
T_{gp12}	glass transition temperature of the strictly alternating copolymer, K
V_L	volume of liquid at time t , m^3
$\hat{V}_I^*$	specific critical hole free volume of initiator, m^3 kg^{-1}
$\hat{V}_{m1}^*, \hat{V}_{m2}^*$	specific critical hole free volume of monomers 1 and 2, m^3 kg^{-1}
$\hat{V}_{p1}^*, \hat{V}_{p2}^*$	specific critical hole free volume of homopolymers 1 and 2, m^3 kg^{-1}
$\hat{V}_p^*$	specific critical hole free volume of copolymer, m^3 kg^{-1}
V_{pj}	molar volume of the copolymer jumping unit, m^3 mol^{-1}
V_{fm1}, V_{fm2}	fractional free volume of monomer 1 and 2
V_{fp}	fractional free volume of copolymer

$x_m(t)$	total molar conversion at time t
x_w	overall mass conversion

Greek letters

γ_p, γ_m, γ_I	overlap factors for copolymer, monomer and initiator
θ_{tcii}, θ_{pii}, θ_f	adjustable parameters in the model, s
$\lambda_{p,q}$	moment of live $(P_{n,m})$ polymer radicals $\left[\equiv \sum_{n=1}^{\infty}\sum_{m=0}^{\infty}(n^p m^q P_{n,m})\right]$, mol
$\mu_{p,q}$	moment of live $(Q_{n,m})$ polymer radicals $\left[\equiv \sum_{n=0}^{\infty}\sum_{m=1}^{\infty}(n^p m^q Q_{n,m})\right]$, mol
$\tau_{p,q}$	moment of dead $(D_{n,m})$ polymer chains $\left[\equiv \sum_{n=0}^{\infty}\sum_{m=0}^{\infty}(n^p m^q D_{n,m}); \; n = m \neq 0 \text{ (simultaneously)}\right]$, mol
ξ_{m1p}, ξ_{m2p}	ratio of volume of monomer1 (or monomer 2) to the volume of a copolymer jumping unit
ξ_{Ip}	ratio of volume of initiator to the volume of a copolymer jumping unit
ρ_{m1}, ρ_{m2}	density of pure liquid monomer1 and monomer 2 at temperature T (kg m^{-3})
ρ_{p1}, ρ_{p2}	density of homopolymer 1 and homopolymer 2 at temperature T (kg m^{-3})
ρ_p	density of co- polymer at time t (kg m^{-3})
ϕ_{m1}, ϕ_{m2}, ϕ_p	volume fractions of monomers and copolymer in liquid at time t
ϕ_t	cross termination rate parameter
Ψ, Ψ_{ref}, Ψ'_{ref}	defined in Appendix A2
Ψ', Ψ'', Ψ''_{ref}	defined in Appendix A2

Δt	time interval, s
ΔT	temperature interval, K or ^{o}C

Subscripts/Superscripts

d	desired value
f	final value
I	initiator
min	minimum value
max	maximum value
m1	momomer 1
m2	monomer 2
p	copolymer
p1	homopolymer 1
p2	homopolymer 2
$_0$	initial value (unless otherwise specified)
ref	reference

LIST OF ABBREVIATIONS

AIBN	2,2′-azobisisobutyronitrile
BFCs	Best-fit correlations
GA	genetic algorithm
IOPs	Individually optimized parameters
MMA	methylmethcrylate
MOO	multi-objective optimization
MWD	molecular weight distribution
NSGA-I	non-dominated sorting genetic algorithm
PDI	polydispersity index
PMMA	polymethylmethcrylate
SAN	styrene acrylonitrile copolymer
TOL	user-specified tolerance

LIST OF FIGURES

LIST OF TABLES

Chapter 1

INTRODUCTION

Polymers have a large impact on every aspect of our day to day life. Due to their low cost and superior properties, polymers are replacing traditional materials. New polymeric materials are being developed to meet specific requirements of end user applications. However, the scope of inventing new polymers is limited. Therefore, the focus of researchers is to improve existing polymers by optimizing their production (decreasing cost of production, increasing yield, etc.) or improving product properties. One of the techniques in the latter category is copolymerization. Here, two or more monomers are reacted to produce copolymers which have the desired physical, chemical and mechanical properties. Also, optimization of reactors producing this copolymer needs to be studied, particularly, because of the diffusional limitations being present. This would enable economic production of this important copolymer, while maintaining its important physical properties.

An important property of polymers is the molecular weight distribution (MWD). From an applications point of view, it is desirable to have a high (average) molecular weight product with a narrow MWD, which improves thermal properties, impact resistance, hardness and strength of the polymer. Another property is the (mean) composition of one of the monomeric components in the copolymer. A small change in the copolymer composition

will yield a product having poor properties. The control of these properties requires a thorough knowledge of the polymerization kinetics as well as the associated transport processes. The number average molecular weight, $\bar{M}_n$, and the overall monomer conversion, x_m, will depend on the temperature, T, for isothermal batch reactors, or, for industrial reactors, on the temperature history, $T(t)$, where t is the time. Higher temperatures give higher values of x_m but lower values of $\bar{M}_n$. Higher conversions are preferred because it decreases the post-separation and recycling costs. Therefore, the process parameters are optimized to meet the end use properties.

Styrene acrylonitrile random copolymer (SAN) is a rigid and transparent plastic material which is produced by the copolymerization of styrene and acrylonitrile in the presence of free-radical generating initiators like 2,2′-azobisisobutyronitrile (AIBN). SAN combines the clarity and rigidity of polystyrene with the hardness, strength, and heat- and solvent-resistance of polyacrylonitrile. It is used in automotive parts, battery cases, kitchenware, appliances, furniture, plastic optical fibers, medical supplies, etc.

Commercially, SAN is produced worldwide by emulsion, suspension, and continuous bulk polymerizations technologies. Finished products of SAN are almost exclusively made by bulk polymerization since it results in superior optical properties. Also, of the three methods, bulk polymerization technology is the most cost efficient and generates the least waste.

1.1   KINETIC SCHEME

The kinetic scheme of free radical random bulk copolymerization of styrene and acrylonitrile, using AIBN as the initiator, is summarized in Table 1.1. $P_{n,m}$

Table 1.1 Kinetic Scheme for the Copolymerization of SAN

Initiation
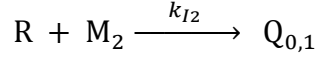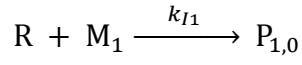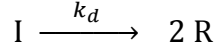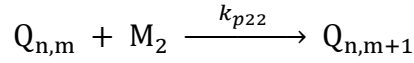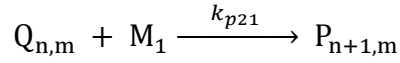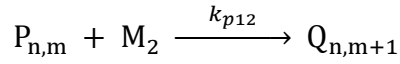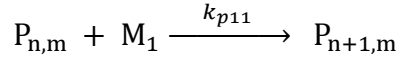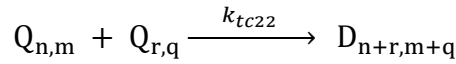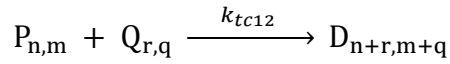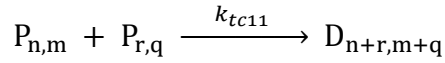
$$I \xrightarrow{k_d} 2R$$

$$R + M_1 \xrightarrow{k_{I1}} P_{1,0}$$

$$R + M_2 \xrightarrow{k_{I2}} Q_{0,1}$$

Propagation

$$P_{n,m} + M_1 \xrightarrow{k_{p11}} P_{n+1,m}$$

$$P_{n,m} + M_2 \xrightarrow{k_{p12}} Q_{n,m+1}$$

$$Q_{n,m} + M_1 \xrightarrow{k_{p21}} P_{n+1,m}$$

$$Q_{n,m} + M_2 \xrightarrow{k_{p22}} Q_{n,m+1}$$

Termination by combination

$$P_{n,m} + P_{r,q} \xrightarrow{k_{tc11}} D_{n+r,m+q}$$

$$P_{n,m} + Q_{r,q} \xrightarrow{k_{tc12}} D_{n+r,m+q}$$

$$Q_{n,m} + Q_{r,q} \xrightarrow{k_{tc22}} D_{n+r,m+q}$$

Termination by disproportionation

$$P_{n,m} + P_{r,q} \xrightarrow{k_{td11}} D_{n,m} + D_{r,q}$$

$$P_{n,m} + Q_{r,q} \xrightarrow{k_{td12}} D_{n,m} + D_{r,q}$$

$$Q_{n,m} + Q_{r,q} \xrightarrow{k_{td22}} D_{n,m} + D_{r,q}$$

Chain transfer to monomer

$$P_{n,m} + M_1 \xrightarrow{k_{f11}} P_{10} + D_{n,m}$$

$$P_{n,m} + M_2 \xrightarrow{k_{f12}} Q_{01} + D_{n,m}$$

$$Q_{n,m} + M_1 \xrightarrow{k_{f21}} P_{10} + D_{n,m}$$

$$Q_{n,m} + M_2 \xrightarrow{k_{f22}} Q_{01} + D_{n,m}$$

---

* * *
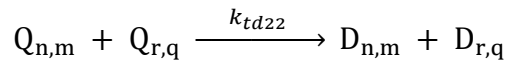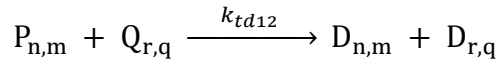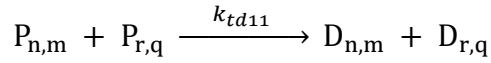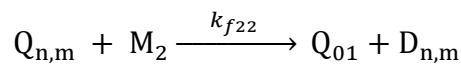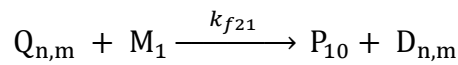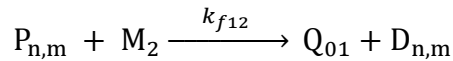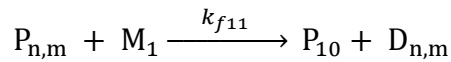
is a macro-radical having n units of M_1 (styrene) and m units of M_2 (acrylonitrile) ($n + m$ monomer units in all), but having an M_1 unit at its end. Similarly, $Q_{n,m}$ is a macro-radical having n units of M_1 (styrene) and m units of M_2 (acrylonitrile) ($n + m$ monomer units in all), but having an M_2 unit at its end. The dead macromolecular chains, $D_{n,m}$, are defined in a similar manner. Initiation, propagation and termination (by combination, disproportionation and chain transfer to monomer) reactions are all shown in Table 1.1.

1.2 DIFFUSION-CONTROLLED TRANSPORT

In bulk polymerizations, three diffusion-controlled processes affect the rate of the chemical reactions at high monomer conversions due to the increase in viscosity of the reaction mass. These are the cage, gel and glass effects. These effects (for chain-growth polymerizations) are related to the initiation, termination and propagation reactions, respectively.

1.2.1 Cage Effect

The cage effect has been attributed to the free radicals generated (from the decomposition of the initiator), being unable to escape out of the 'cage' of the reaction mass (primarily, monomers) surrounding them. This leads to the free radicals reacting further to give unreactive side products, thus leading to a waste of initiator molecules. This is represented in terms of an empirically-determined initiator efficiency, f, which decreases at high monomer conversions as the viscosity of the reaction mass increases.

1.2.2 Gel Effect

The gel or Trommsdroff-Norrish [1, 2] effect represents the decrease in the termination rate constants, k_ts, due to the increasing viscosity of the reaction mass. This was first reported in the literature by Norrish and Smith [2] and

Trommsdroff et al. [1] This decreases the mobility of the growing macro-radicals towards each other and, thus, decreases the rate of termination, leading to a significant increase in the concentration of the growing macro-radicals in the reaction mass and to the rate of polymerization.

1.2.3 Glass Effect

At higher monomer conversions, the propagation reaction also becomes diffusion-controlled. In this late stage of polymerization, the reaction mass becomes glassy in nature because the glass transition temperature of the reaction mass becomes higher than the polymerization temperature. This is known as the glass effect. This restricts the diffusion of monomer molecules towards the macro-radicals and the reaction stops short of 100% conversion. The glass effect is associated with the decrease in the propagation rate constants, k_ps.

1.3 RESEARCH MOTIVATION

The properties of the polymer produced depend on several parameters, but, for a *given* feed (fraction of the two monomers and the initiator concentration) it is the variation of temperature with time, $T(t)$, for a batch industrial reactor, that controls the properties (namely, the average molecular weights, copolymer composition and the monomer conversion) of the final product. The models developed in the past have focused primarily on *isothermal* copolymerizations and have not been generalized to model non-isothermal operations, which are a norm in industrial reactors. Therefore, these models cannot be used for studying industrial copolymerization reactors. In the present work, the earlier isothermal models have been extended so as to be

5

applicable for non-isothermal conditions as well. The parameters of the present model have been 'tuned' (parameters have been curve-fitted) using the isothermal experimental data of Garcia-Rubio et al. [3] The tuned model is then used for the optimization of SAN reactors and optimal temperature histories obtained so as to obtain copolymers having the desired properties (number average molecular weight, styrene composition in the copolymer produced and the overall monomer conversion) using single and multi-objective optimization.

Chapter 2

LITERATURE REVIEW

2.1   MODELING OF FREE RADICAL POLYMERIZATION

A considerable amount of work on diffusion-controlled phenomena in free radical *homo*polymerizations has been published in the open literature. However, the number of studies on diffusion-controlled free radical *co*polymerizations is somewhat limited.

2.1.1   Studies Related to Free Radical Homopolymerization

Chiu et al. [4] developed a mathematical model to describe the gel effect exhibited by free radical homopolymerization reactions. They used the Fujita-Doolittle free volume theory [5] for the diffusivity. The effect of diffusional limitations on the overall rate of termination gradually (and continuously) increases with the monomer conversion. The model also considered the glass effect, which occurs at higher monomer conversions. The model predictions for polymethylmethcrylate (PMMA) were found to be in reasonable agreement with experiments on the monomer conversion and the average molecular weights for isothermal polymerization of methylmethcrylate. The model ignored the decrease in the initiator efficiency. Hui and Hamielec [6] studied diffusional effects in the polymerization of styrene in the temperature range, $100 - 200°C$. They developed an *empirical*, free volume [5] based

kinetic model expressing $k_p/k_t^{1/2}$ (which is related to the average chain length of the polymer formed in the absence of diffusional limitations) in terms of a third degree polynomial involving the monomer conversion, x_m, and temperature, T, as

$$\frac{k_p}{k_t^{1/2}} = \left[\frac{k_p^0}{k_t^{o^{1/2}}}\right] \exp(A_1 x_m + A_2 x_m^2 + A_3 x_m^3) \qquad (2.1)$$

In Eqn. 2.1, superscript, ^{0}, indicates values in the absence of diffusional limitations. The empirical parameters, $A_1 - A_3$, in this equation were expressed as linear functions of temperature. Hui and Hamielec [6] tuned their model parameters for a few homopolymerizations. Curteanu and Bulacovschi [7] extended the relations given by Hui and Hamielec [6] and related k_t and k_p, *individually*, to x_m as

$$k_t = k_t^o \exp(A_1 + A_2 x_m + A_3 x_m^2 + A_4 x_m^3) \qquad (2.2)$$

$$k_0 = k_p^o \exp(B_1 + B_2 x_m + B_3 x_m^2 + B_4 x_m^3) \qquad (2.3)$$

The *individual* sets of model parameters, A_i and B_i, were obtained by tuning the experimental data of Balke and Hamielec [8] at different (isothermal) temperatures and initiator loadings, as well as experimental data of Srinivas et al. [9] under non-isothermal conditions and Dua et al. [10] under semi-batch conditions. Sangwai et al. [11] assumed a linear dependence of the eight parameters in Eqns. (2.2) and (2.3), on temperature. They tuned these parameters using earlier as well as their own experimental data on PMMA. The model of Chiu et al. [4] was extended by Achilias and Kiparissides [12]. Their model used the Vrentas and Duda [13, 14] model for the free volume and the theory of excess chain-end mobility. There was only one curve-fit

parameter in their model, the remaining parameters being obtained by independent measurements on *non-reacting* systems. The model parameters were obtained by curve-fitting experimental data on methylmethacrylate polymerization under isothermal conditions. Seth and Gupta [15] and Ray et al. [16] developed an improved semi-empirical model to account for diffusional limitations in homopolymerizations. The free volume theory of Vrentas and Duda [13, 14] was used to account for the variation of the diffusion coefficients with time. The model parameters were tuned using the experimental data of Balke and Hamielec [8] on isothermal bulk polymerization and experimental data of Schulz and Harborth [17] on solution polymerizations of methylmethacrylate in batch reactors. Unlike earlier models, this model did not incorporate the *initial* value of the number average chain length or of the initial value of the initiator concentration and was, thus, applicable for non-isothermal polymerizations as well as for polymerizations under semi-batch conditions. They predicted the effects of instantaneous addition or flashing of the solvent, initiator and/or monomer and of near-step increase or decrease in temperature on the conversion and molecular weights. Industrial polymerizations are usually carried out under non-isothermal conditions. The experimental data of Srinivas et al. [9] and Dua et al. [10] under idealized experimental conditions of non-isothermal and semi-batch reaction conditions were well explained using model parameters tuned using *only* isothermal data, thus confirming the tuned models for all reactor conditions. It may be added that the models like in Eqns. 2.2 and 2.3 have been more successful than the models developed from the studies of the groups of Soong and Kipparisides.

2.1.2   Studies Related to Free Radical Copolymerization

Garcia-Rubio et al. [3] investigated the random bulk *co*polymerization of polystyrene and acrylonitrile experimentally over a wide range of temperatures, initiator and monomer concentrations and obtained data on the rates of polymerization and copolymer properties. They extended the free volume homopolymerization models of Marten and Hamielec [18, 19] to model the diffusion-controlled termination and propagation reactions. They ignored the decrease of initiator efficiency. Their predictions of the overall monomer conversion, copolymer composition and sequence-length were in reasonable agreement with experimental data up to a limiting conversion, but there was significant discrepancy at higher conversions. Sharma and Soane [20] extended the basic homopolymerization model of Chiu et al. [4] to describe the styrene-methylmethacrylate random bulk copolymerization system. They used the Fujita-Doolittle free volume theory [5] for the diffusivity of molecules and radicals. They assumed the initiator efficiency to be independent of the monomer conversion. Their high conversion diffusion-controlled copolymerization model considered the composition drift in regions near the glass effect, resulting from reactivity differences between the two monomers. The product formed during copolymerization becomes progressively depleted in the faster reacting monomer. In addition, the diffusional processes exert a strong influence on the instantaneous molecular weight and composition of the copolymer produced, especially at higher overall monomer conversions. Proper consideration of diffusional limitations at higher conversions is an integral part of any optimization scheme for controlling composition drift. Their model predictions were in accord with

experimental data of Marten and Hamielec [19] on polymethylmethacrylate. Hwang et al. [21] developed a mathematical model for free radical bulk copolymerization of styrene and acrylonitrile with AIBN initiator in a batch reactor. The free volume theory of Marten and Hamielec [18, 19] was used to describe the diffusion-controlled features of the propagation and termination reactions. The pseudo-kinetic rate constant method as well as the terminal model was applied to reduce the complex rate expressions for the copolymerization system to those for the corresponding homopolymerization systems. It was observed that the molecular weight distribution became broader with the increase in monomer conversion, because the weight-average molecular weight increases at a faster rate than the number-average molecular weight. However, the comparison of the model with available experimental data was not reported. Keramopoulos and Kiparissides [22] modified the model of Sharma and Soane [20]. They extended the earlier development of Achilias and Kiparissides [12] and used the generalized free volume theory of Vrentas and Duda [13, 14] for ternary systems and an effective reaction radius. The initiator efficiency, propagation and termination rate constants were modeled in terms of diffusion- and reaction-limited terms. They presented a very comprehensive model to predict the overall monomer conversion, average molecular weights and copolymer composition for three free radical copolymerization systems, namely, styrene-methylmethacrylate, styrene-acrylonitrile and p-methyl-styrene-methylmethacrylate. Though the models of Garcia-Rubio and Keramopoulos and Kiparissides, in principle, account for non-isothermal effects (the parameters are temperature dependent) these effects were not validated. Scorah et al. [23] investigated the free radical

11

copolymerization of styrene-methyl methacrylate by using a tetrafunctional initiator. The predictions of conversion and molecular weights were in agreement with the experimental data over a range of temperature and initiator concentrations. This model can be used for batch, bulk or solution polymerizations and can be modified to account for flow terms as well. Jalili et al. [24] developed a comprehensive model using the free volume theory proposed by Marten and Hamielec [18, 19], to describe the copolymerization of styrene-methyl methacrylate system. The model predictions are in agreement with the experimental data on conversion, composition and average molecular weights upto limiting conversions. Costa et al. [25] developed a kinetic model for the copolymerization of vinylidene fluoride and hexafluoropropylene in supercritical carbon dioxide in both continuous and a dispersed polymer rich phase. The effect of monomer feed composition, interphase area, reaction time and pressure on conversion and molecular weight distribution was described by their model. Li et al. [26] discussed a heterogeneous model with an initial solution polymerization model and then a two phase model for the graft copolymerization of styrene and acrylonitrile in the presence of poly(propylene glycol). The continuous phase became the disperse phase at monomer conversions of 3 to 5 percent, which leads to an abrupt decrease in the molecular weight, polymerization rate and graft efficiency and broadening of the molecular weight distribution.

2.2   OPTIMIZATION STUDIES

Several optimization studies on polymerization in batch reactors involving single and multiple objective functions have been reported in the last few

decades using evolutionary algorithms, particularly genetic algorithm (GA).

2.2.1 Optimization Studies for Homopolymerizations

Chakravarthy et al. [27] adapted GA to obtain optimal temperature *histories* for methylmethacrylate polymerizations. The reaction time, t_f, was minimized, while simultaneously requiring the attainment of design values of the final monomer conversion and the number average chain length. GA was used by these workers to obtain global-optimal temperature histories for MMA polymerization. Garg and Gupta [28] used the non-dominated sorting genetic algorithm (NSGA-I) for developing a multi-objective optimization (MOO) technique for free radical bulk homopolymerization reactors. They studied the polymerization of MMA in a batch reactor. They used the temperature history as the decision/control variable for minimizing the reaction time, t_f, and the final value of the poly-dispersity index (PDI_f) of the polymer, while constraining the monomer conversion and $\bar{M}_n$ at the end of polymerization to desired values. Mitra et al. [29] adapted NSGA-I for obtaining Pareto optimal solutions for three grades of nylon 6 produced in an *industrial* semi-batch reactor. The two objective functions used for multi-objective optimization were the minimization of the reaction time and the concentration of the undesirable cyclic dimer in the product, while meeting the end point constraints on the final values of the monomer conversion and $\bar{M}_n$. The vapor release rate history and the jacket fluid temperature were used as the two decision variables. Merquior et al. [30] carried out the multi-objective optimization of the free radical polymerization of styrene in a batch reactor. The objective functions included the monomer conversion, molecular weight

13

and the poly-dispersity index of the polymer product. The decision variables were the reactor temperature and the quantity of initiator. They generated the optimal Pareto solutions for producing different grades of polymer. Bhat et al. [31] studied the multi-objective optimization of an industrial polystyrene reactor (the Tower process). Mitra et al. [32] used the elitist non-dominated sorting genetic algorithm (NSGA-II) to obtain Pareto solutions for an isothermal semi-batch epoxy polymerization process. The objective functions used were to minimize the poly-dispersity index and to maximize the value of $\bar{M}_n$ of the pre-polymer product. The decision variables were the addition profiles of monomer, sodium hydroxide and epichlorohydrin. Minimizing the addition of NaOH to maximize the preferential formation of lower oligomers was also studied.

2.2.2 Optimization Studies for Copolymerization

Similar multi-objective optimization studies have been carried out on copolymerizations. Tsoukas et al. [33] studied the multi-objective optimization of the free radical solution copolymerization of SAN copolymer to obtain Pareto sets using two objectives: minimizing the difference between the average value of the copolymer composition of the product and the deviation of the final value of the molecular weight distribution (through the PDI) from desired values. The effects of various decision variables such as the temperature and/or monomer/initiator addition, on the performance of the copolymerization reactor were investigated. Monomer addition was found to be a more effective manipulated variable than the temperature for the narrowing of the copolymer composition distribution. The reverse was true for

the molecular weight distribution. They neglected the Trommsdorff or gel effect in their kinetic model. They used the ε-constraint technique along with Pontryagin's minimum principle. Farber [34] used multi-objective optimization for simulating two copolymerization systems, methyl methacrylate-vinyl acetate and SAN in *c*ontinuous *s*tirred *t*ank *r*eactors (CSTR*s*) under steady state conditions. The objectives selected were the maximization of $\bar{M}_n$ of the product, maximization of the conversion of monomer 1 and minimization of the deviation of the average copolymer composition of the product from a desired value. The decision variables were temperature and residence time. The gel effect was not incorporated. The technique used was the ε-constraint technique along with the Kuhn-Tucker equations for non-linear programming. Butala et al. [35] used CONSOLE, an optimization package of user interactive computer-aided design (CAD), for developing the open-loop strategies for batch and semi-batch solution copolymerization of SAN. The objective functions were to minimize the deviations of the average copolymer composition and of the molecular weight of the product from specified values. The reactor temperature and the flow rate of the feed (a mixture of initiator, monomer and solvent) were used as decision variables. They parameterized the decision variables to obtain optimal solutions. Nayak and Gupta [36] used the ϕ-factor kinetic model for the multi-objective optimization of the solution copolymerization of SAN using the elitist non-dominated sorting genetic algorithm, NSGA-II. The multiple objectives used for the optimization of a semi-batch reactor were the average composition of the copolymer product, the value of $\bar{M}_n$, the conversion of monomers attained in the reactor and the poly-dispersity index. The rate of

15

continuous addition of a monomer-solvent-initiator mixture (having a specified and fixed composition) and the history, $T(t)$, of the temperature were used as control variables. Amaro et al. [37] presented an optimization formulation for the bulk copolymerization of butyl methacrylate and butyl acrylate using a model with the pseudo-homopolymerization approximation and using an empirical model for the diffusional effects. The objective function was to minimize the reaction time to achieve a target copolymer composition and the molecular weight distribution. They used the feed rates of the monomer and the initiator as the decision variables. Toledo and Castellanos [38] studied the multi-objective optimization of free radical solution copolymerization of acrylonitrile and vinyl acetate in a CSTR. The objective function was to maximize the final value of the monomer conversion and to minimize the breadth of the molecular weight distribution. The monomer feed rates were taken as decision variables. Anand et al. [39] used differential evolution (DE) to obtain the optimal control policies for the temperature and the rate of addition of monomer to obtain copolymer of a desired average composition and of the molecular weight distribution in a semi-batch solution copolymerization reactor.

The model of Garcia-Rubio et al. [3] ignored the decrease in the initiator efficiency and is not validated for non-isothermal operation of batch reactors. The model developed by Keramopoulos and Kiparissides [22] considers diffusional limitations, but was not validated for non-isothermal conditions. Therefore, the models developed in the past, *in their present forms*, are not validated for non-isothermal conditions, which is a requirement of industrial operations. In the present study, we extend the homopolymerization model

16

presented by Seth and Gupta [15] and Ray et al. [16] to SAN bulk copolymerizations under non-isothermal conditions. In the present work, the parameters, θ_{tc11}, θ_{p11}, θ_{p22} and θ_f, for the gel, glass and cage effects are obtained by tuning (curve-fitting) them using *isothermal* data on styrene acrylonitrile (SAN) random copolymerization (data by Garcia-Rubio et al. [3] in small ampoules) under a variety of experimental conditions. It is assumed that the same model parameters will apply to non-isothermal and semi-batch conditions as well, as was the case with PMMA homopolymerization (for which this has been confirmed experimentally, too). The tuned model is then used for optimization studies involving the temperature history, $T(t)$, as the decision variable. The present work focuses on the single- and multi-objective optimization of free radical random *bulk* copolymerization of SAN using the temperature history, $T(t)$, as the optimization/decision variable. The objective functions and constraints used for optimization studies are:

   a. Minimization of the reaction time, t_f

   b. Maximization of the overall monomer conversion, x_m

   c. Maximization of $\bar{M}_{nf}$ or the copolymer product having a desired value, $\bar{M}_{nd}$, of $\bar{M}_{nf}$

   d. The copolymer produced having a desired average value, St_{cd}, of the styrene mole fraction, St_c

Chapter 3

MODELING OF SAN BULK COPOLYMERIZATIONS

The kinetic scheme of free radical random bulk copolymerization of SAN is summarized in Table 1.1. The reaction mass in the batch reactor consists of the growing radicals and resulting dead copolymers. Mass balance equations are written for each of the *molecular species* and are given in Appendix A-1a. These 'species' equations [40] are summed up appropriately to give the equations for the several zeroth, first and second moments of the macro-radicals and dead macromolecular species defined by

$$\lambda_{p,q} \equiv \sum_{n=1}^{\infty} \sum_{m=0}^{\infty} n^p m^q P_{n,m} \tag{3.1}$$

$$\mu_{p,q} \equiv \sum_{n=0}^{\infty} \sum_{m=1}^{\infty} n^p m^q Q_{n,m} \tag{3.2}$$

$$\tau_{p,q} \equiv \sum_{n=0}^{\infty} \sum_{m=0}^{\infty} n^p m^q D_{n,m} \; ; \; n = m \neq 0 \text{ (simultaneously)} \tag{3.3}$$

3.1   KINETICS OF SAN COPOLYMERIZATION

The reaction order is assumed to be first order with respect to both the reactants. All the reactions are assumed to be elementary and irreversible. The termination by disproportionation reactions has been ignored in the model calculations. The kinetics of SAN copolymerization consists of the mass

balance equations, moment equations, gel, glass and cage effect (and other associated) equations. The balance equations comprise of a set of first order ordinary differential equations of the initial value kind (ODE-IVPs) and are given in Appendix A-1b. These are written in terms of the total moles of the various species and the total volume, V_L. This enables the use of varying density of the reaction mass (as also for semi-batch operation of the reactors through the addition and vaporization terms which may easily be incorporated).

The balance equations in Appendix A-1b are identical to the more general expressions given by Keramopoulos and Kiparissides [22] but in the absence of chain transfer to the modifier, chain transfer to polymer and terminal double-bond polymerization. The total number of moles of either styrene or acrylonitrile in the unreacted reaction mixture and in the copolymer should not change with time, i.e., their derivatives with respect to time should be zero. This has been used as a check of our balance equations, both analytically (to check the correctness of the equations in Appendix A-1) as well as numerically (to check our computer code).

The *overall* molar conversion, x_m, the total mass conversion, x_w, the mole fraction, St_c, of *st*yrene in the *c*opolymer and its mole fraction, St_{rm}, in the (unreacted) reaction mass are given by

$$x_m = 1 - \frac{(M_1 + M_2)}{(M_{1,0} + M_{2,0})} \tag{3.4}$$

$$x_w = 1 - \frac{(M_1 (MW)_{m1} + M_2 (MW)_{m2})}{(M_{1,0} (MW)_{m1} + M_{2,0} (MW)_{m2})} \tag{3.5}$$

19

$$St_c = \frac{M_{1,0} - M_1}{(M_{2,0} - M_2) + (M_{1,0} - M_1)} \tag{3.6}$$

$$St_{rm} = \frac{M_1}{M_1 + M_2} \tag{3.7}$$

The number average molecular weight, $\bar{M}_n$, and the weight average molecular weight, $\bar{M}_w$, are given by

$$\bar{M}_n = \frac{(MW)_{m1}(\lambda_{1,0} + \mu_{1,0} + \tau_{1,0}) + (MW)_{m2}(\lambda_{0,1} + \mu_{0,1} + \tau_{0,1})}{(\lambda_{0,0} + \mu_{0,0} + \tau_{0,0})} \tag{3.8}$$

$$\bar{M}_w = \frac{(MW)_{m1}^2(\lambda_{2,0} + \mu_{2,0} + \tau_{2,0}) + (MW)_{m2}^2(\lambda_{0,2} + \mu_{0,2} + \tau_{0,2}) + 2(MW)_{m1}(MW)_{m2}(\lambda_{1,1} + \mu_{1,1} + \tau_{1,1})\}}{(MW)_{m1}(\lambda_{1,0} + \mu_{1,0} + \tau_{1,0}) + (MW)_{m2}(\lambda_{0,1} + \mu_{0,1} + \tau_{0,1})} \tag{3.9}$$

The expressions for $\bar{M}_n$ and $\bar{M}_w$ are the same as those used by Sharma and Soane. [20] The expression for $\bar{M}_n$ also matches with the equation given by Keramopoulos and Kiparissides. [22] The cumulative M_w in the Keramopoulos et al. model is calculated on the basis of the double moments of the "dead" chain length-copolymer composition (CLCC) distribution whereas in the Sharma and Soane [20] model the M_w is calculated based on the second moments of the growing and the dead radicals. The expression for $\bar{M}_w$ given by Keramopoulos and Kiparissides [22] appears to be in error.

3.2   MODELING OF DIFFUSION-CONTROLLED TRANSPORT

The most important part of the present model is the equations for the cage, gel and glass effects. In the present study, an adaptation of the model of Sharma and Soane [20] and of Keramopoulos and Kiparissides [22] is developed for copolymerizations, along the lines used by Seth and Gupta [15] and Ray et al. [16] for homopolymerizations.

Chiu et al. [4] and Sharma and Soane [20] used a simple model for the diffusional effects on the rate constants. In the present work, the equivalent of their equations in terms of moments is used. As polymerization begins, the polymer radicals are far apart from each other. These radicals diffuse through the reaction mixture by translational motion and come closer to each other. Then, the segmental motion orients these radicals to facilitate the collision of the reactive ends of the radicals. This leads to termination, when the radicals migrate within one molecular diameter, as shown in Fig. 3.1. [4, 20]

Termination takes place only after their proper orientation and collision. Thus, the termination rate depends upon the chain mobility (diffusion), molecular weight of the diffusing species, composition of the medium and the temperature. These considerations are incorporated in the mathematical description of the termination rate constants, k_{tcii}; i = 1, 2, as given by Sharma and Soane [20] as
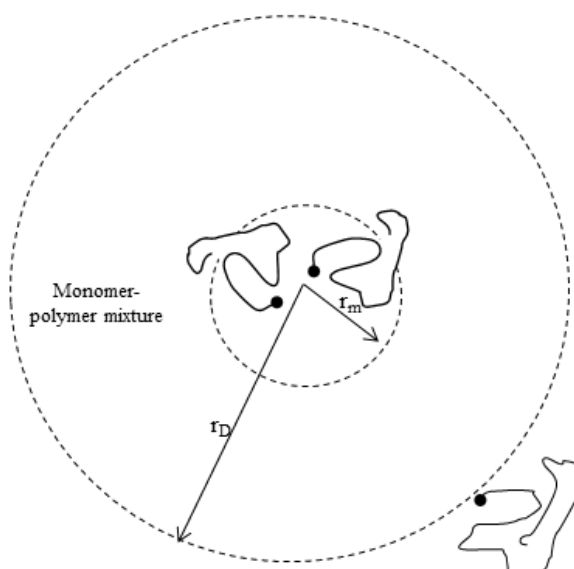
Figure 3.1. Schematic diagram illustrating the diffusion of one macroradical towards another during termination [4, 20]

$$\frac{1}{k_{tc11}} = \frac{1}{k_{tc11,0}} + \frac{r_m^2}{3D_p} \frac{\lambda_{0,0}^2}{V_L\,(\lambda_{0,0} + \mu_{0,0})} \qquad (3.10)$$

$$\frac{1}{k_{tc22}} = \frac{1}{k_{tc22,0}} + \frac{r_m^2}{3D_p} \frac{\mu_{0,0}^2}{V_L\,(\lambda_{0,0} + \mu_{0,0})} \qquad (3.11)$$

where r_m is the effective reaction radius around a macro-radical within which the 'true' rate constants, $k_{tc11,0}$ and $k_{tc22,0}$, unencumbered by diffusional limitations, characterize the reaction process, and D_p represents the effective migration coefficient representing both diffusive and propagational motion of a neighboring macro-radical to this reaction sphere having $r = r_m$, as shown in Fig. 3.1. It was assumed by Sharma and Soane [20] that r_m is a constant and D_p depends on temperature, concentration and molecular weight. Both r_m and D_p are the same for all i. Eqn. (3.10) can be re-written as

$$\frac{1}{k_{tc11}} = \frac{1}{k_{tc11,0}} + \frac{r_m^2}{3D_{p,ref}} \frac{\lambda_{0,0}^2}{V_L\,(\lambda_{0,0} + \mu_{0,0})} \frac{D_{p,ref}}{D_p} \qquad (3.12)$$

In the above equation, *ref* represents a reference state ($\phi_{m1} = 0$, $\phi_{m2} = 0$, $\phi_p = 1$), the same for all i. The variable ϕ denotes the volume fraction in liquid at time t. The term, $D_p/D_{p,ref}$, can be written using the free volume theory of Vrentas and Duda [13, 14] as discussed by Ray et al. [16]

$$\frac{D_p}{D_{p,ref}} = \frac{\bar{M}_{w,ref}^2\, exp(\Psi_{ref})}{\bar{M}_w^2\, exp(\Psi)} \qquad (3.13)$$

where Ψ and Ψ_{ref} are given by

$$\Psi = \frac{\gamma_p \left\{ \frac{\rho_{m1}\,\phi_{m1}\hat{V}_{m1}^*}{\xi_{m1p}} + \frac{\rho_{m2}\phi_{m2}\hat{V}_{m2}^*}{\xi_{m2p}} + \rho_p\phi_p\hat{V}_p^* \right\}}{\rho_{m1}\,\phi_{m1}\hat{V}_{m1}^* V_{fm1} + \rho_{m2}\phi_{m2}\hat{V}_{m2}^* V_{fm2} + \rho_p\phi_p\hat{V}_p^* V_{fp}} \qquad (3.14)$$

$$\Psi_{ref} = \frac{\gamma_p}{V_{fp}} \qquad (3.15)$$

In Eqns. (3.14) and (3.15) , γ_p is an overlap factor (accounts for the free volume being available to more than one molecule) for the copolymer, ρ is the density at temperature T, $\hat{V}^*$ represent the specific critical hole free volume and V_f is the fractional free volume. Subscripts $m1$, $m2$ and p denote monomer 1, monomer 2 and the copolymer, respectively. The parameter, ξ_{mip}, used in Eqn. (3.14) is defined as the ratio of the critical molar volume of the jumping unit of monomer, i, to that of the jumping unit of the copolymer, $\hat{V}_p^* M_{jp}$

$$\xi_{mip} \equiv \frac{\hat{V}_i^* (MW)_i}{\hat{V}_p^* M_{jp}}; i = 1, 2 \qquad (3.16)$$

Because of the inherent difficulty in determining the molecular weight of the polymer jumping unit, an empirical expression has been proposed by Suzuki and Mathot [41] for its calculation in terms of the glass transition temperature of the copolymer

$$\hat{V}_p^* M_{jp} = (0.6224 \, \mathrm{T}_{gp} - 86.95) \times 10^6, \ T_{gp} \geq 295K \qquad (3.17)$$

$$\hat{V}_p^* M_{jp} = (0.0025 \, \mathrm{T}_{gp} + 69.47) \times 10^6, \ T_{gp} \leq 295K \qquad (3.18)$$

The glass transition temperature, T_{gp}, of the copolymer depends on its composition and the glass transition temperatures, T_{gp1} and T_{gp2}, of the respective homopolymers. T_{gp} can be calculated from the Suzuki and Mathot [41] relationship

$$T_{gp} = (1 - (AN)_m)T_{gp1} + (AN)_m T_{gp2} + \frac{R^*}{100}(T_{gp12} + \bar{T}_{gp}) \qquad (3.19)$$

23

where $(AN)_m$ is the mole fraction of acrylonitrile in the copolymer ($= 1 - St_c$).

$\bar{T}_{gp}$ is the mean glass transition temperature of the two homopolymers

$$\bar{T}_{gp} = \frac{(T_{gp1} + T_{gp2})}{2} \tag{3.20}$$

T_{gp12} is the glass transition temperature of the corresponding strictly-alternating copolymer and R^*, the average number of both 1 and 2 monomer chain sequences occurring in a copolymer per 100 monomer units. R^* can be estimated from the following relation from Suzuki et al. [41]

$$R^* = \frac{400 \, (AN)_m \, (1 - (AN)_m)}{[1 + \{1 + 4 \, (AN)_m (1 - (AN)_m)(r_1 r_2 - 1)\}^{1/2}]} \tag{3.21}$$

where r_1 and r_2 are the monomer reactivity ratios.

Eqns. (3.12) – (3.15) are combined to give

$$\frac{1}{k_{tc11}} = \frac{1}{k_{tc11,0}} + \left(\frac{r_m^2}{3D_{p,ref}\bar{M}_{w,ref}^2} \right) \frac{\bar{M}_w^2 \, \lambda_{0,0}^2}{V_L \, (\lambda_{0,0} + \mu_{0,0})} \frac{1}{exp(-\Psi + \Psi_{ref})}$$

$$\equiv \frac{1}{k_{tc11,0}} + \theta_{tc11} \frac{\bar{M}_w^2 \, \lambda_{0,0}^2}{V_L \, (\lambda_{0,0} + \mu_{0,0})} \frac{1}{exp(-\Psi + \Psi_{ref})} \tag{3.22}$$

A similar development carried out for k_{tc22} gives

$$\frac{1}{k_{tc22}} = \frac{1}{k_{tc22,0}} + \theta_{tc22}\bar{M}_w^2 \frac{\mu_{0,0}^2}{V_L(\lambda_{0,0} + \mu_{0,0})} \frac{1}{exp(-\Psi + \Psi_{ref})} \tag{3.23}$$

In the above analysis, the fitting parameter, θ_{tcii}, has dimensions of time and can be viewed as a characteristic migration time of a growing radical. θ_{tcii} is given by

$$\theta_{tcii} = \frac{r_m^2}{3D_{p,ref}\bar{M}_{w,ref}^2}; \quad i = 1, 2 \tag{3.24}$$

which is similar to the θ_{tii} ($\equiv r_m^2/3D_0$, where D_0 depends on temperature and molecular weight) used by Sharma and Soane [20] for copolymerizations and θ_t used by Ray et al. [16] for homopolymerizations. Since it was assumed that r_m and the two parameters, $D_{p,ref}$ and $\overline{M}_{w,ref}^2$, at the reference state ($\phi_{m1} = 0$, $\phi_{m2} = 0$, $\phi_p = 1$) are the same for all i and j ($i, j = 1, 2$), we obtain

$$\theta_{tc11} = \theta_{tc22} \tag{3.25}$$

$k_{tcii,0}$ has a strong temperature dependence but lacks the concentration and molecular weight dependence, whereas $D_{p,ref}$ has a strong dependence on temperature and concentration. Therefore, θ_{tcii} is dependent on the temperature, composition and the initiator loading (feed value), I_0.

The cross termination rate constants (e.g., $k_{tc12} = k_{tc21}$) are calculated using the correlation given by Keramopoulos and Kiparissides [22] as

$$k_{tc12} = \phi_t \left[2(k_{tc11} \, k_{tc22})^{1/2} \right] \tag{3.26}$$

where the cross termination rate parameter, ϕ_t, is defined as

$$\phi_t = 16 \frac{\{0.625 \, (1 - f_{10}) + r_1 f_{10}\}}{(1 - f_{10}) + r_1 f_{10}} \tag{3.27}$$

At high conversions, the diffusion of monomers is hindered. The diffusion limited propagation rate constants, k_{pii}, as reported by Sharma and Soane [20] are

$$\frac{1}{k_{p11}} = \frac{1}{k_{p11,0}} + \theta_{p11} \frac{\lambda_{0,0}}{V_L} \frac{1}{exp\left[\xi_{m1p}\left(-\Psi' + \Psi'_{ref}\right)\right]} \tag{3.28}$$

$$\frac{1}{k_{p22}} = \frac{1}{k_{p22,0}} + \theta_{p22} \frac{\mu_{0,0}}{V_L} \frac{1}{exp\left[\xi_{m2p}\left(-\Psi' + \Psi'_{ref}\right)\right]} \tag{3.29}$$

where Ψ' and Ψ'_{ref} are given by

$$\Psi' = \frac{\gamma_m \left\{ \frac{\rho_{m1} \phi_{m1} \hat{V}_{m1}^*}{\xi_{m1p}} + \frac{\rho_{m2} \phi_{m2} \hat{V}_{m2}^*}{\xi_{m2p}} + \rho_p \phi_p \hat{V}_p^* \right\}}{\rho_{m1} \phi_{m1} \hat{V}_{m1}^* V_{fm1} + \rho_{m2} \phi_{m2} \hat{V}_{m2}^* V_{fm2} + \rho_p \phi_p \hat{V}_p^* V_{fp}} \tag{3.30}$$

$$\Psi'_{ref} = \frac{\gamma_m}{V_{fp}} \tag{3.31}$$

Here, γ_m is the overlap factor for the monomer. The parameter, θ_{pii}, is the characteristic monomer diffusion time and is given by

$$\theta_{pii} = \frac{r_{m,i}^2}{3 D_{m_i,ref}}; \quad i = 1, 2 \tag{3.32}$$

The parameters, θ_{pii}, are similar to θ_p used by Ray et al. [16] for homopolymerizations. They are functions of temperature alone.

The cross propagation rate constants (k_{p12} and k_{p21}) are expressed in terms of the reactivity ratios, r_1 and r_2, as done by Keramopoulos and Kiparissides [22]

$$k_{p12} = k_{p11}/r_1 \tag{3.33}$$

$$k_{p21} = k_{p22}/r_2 \tag{3.34}$$

At low monomer conversions, the rate of diffusion of the primary radicals from the cage is very fast. The expressions for the initiator efficiency, f, can be developed using a combination of the homopolymerization model of Seth and Gupta [15] and the copolymerization model of Keramopoulos and Kiparissides [22] as

$$\frac{1}{f} = \frac{1}{f_0} \left(1 + \frac{r_{I2}^3}{3 \, r_{I1} D_I} \frac{\left(k_{I1,0} M_1 + k_{I2,0} M_2 \right)}{V_L} \right)$$

$$= \frac{1}{f_0} \left[1 + \left(\frac{r_{I2}^3}{3 \, r_{I1} D_{I,ref}} \right) \frac{\left(k_{I1,0} M_1 + k_{I2,0} M_2 \right)}{V_L} \frac{D_{I,ref}}{D_I} \right]$$

$$\equiv \frac{1}{f_0}\left(1 + \theta_f(T) \frac{(k_{I1,0}M_1 + k_{I2,0}M_2)}{V_L} \frac{1}{exp[\xi_{Ip}(-\Psi'' + \Psi''_{ref})]}\right) \qquad (3.35)$$

where f_0 is the initiator efficiency at zero monomer conversion, and r_{I1} and r_{I2} are the radius of the initiator reaction sphere and the diffusion sphere, respectively. Ψ'' and Ψ''_{ref} are given by

$$\Psi'' = \frac{\gamma_I\left\{\frac{\rho_{m1}\,\phi_{m1}\hat{V}^*_{m1}}{\xi_{m1p}} + \frac{\rho_{m2}\phi_{m2}\hat{V}^*_{m2}}{\xi_{m2p}} + \rho_p\phi_p\hat{V}^*_p\right\}}{\rho_{m1}\,\phi_{m1}\hat{V}^*_{m1}V_{fm1} + \rho_{m2}\phi_{m2}\hat{V}^*_{m2}V_{fm2} + \rho_p\phi_p\hat{V}^*_pV_{fp}} \qquad (3.36)$$

$$\Psi''_{ref} = \frac{\gamma_I}{V_{fp}} \qquad (3.37)$$

In Eqn. (3.37), γ_I is the overlap factor for the initiator. The parameter, θ_f, is given by

$$\theta_f = \frac{r^3_{I2}}{3\,r_{I1}D_{I,ref}} \qquad (3.38)$$

and is somewhat similar to the θ_f used by Seth and Gupta [15] for homopolymerizations. The molar concentration of the initiator is very small as compared to monomers concentration in the reaction mass, so the terms the radius of the diffusion sphere (r_{I2}) and the radius of the initiator reaction sphere (r_{I1}) are independent of monomer conversion and temperature. Therefore, the terms, r^3_{I2} and r_{I1}, are expected to be insensitive to monomer conversions and temperature. θ_f is a function of the temperature alone. The complete set of equations for the cage, gel and glass effects is given in Appendix A-2.

The rate constants, k_d, $k_{p11,0}$, $k_{p22,0}$, $k_{tc11,0}$, $k_{tc22,0}$, $k_{f11,0}$, $k_{f12,0}$, $k_{f21,0}$ and $k_{f22,0}$, are written in terms of Arrhenius equations as:

$$k_d = k_d^0 \, exp\left[-E_d/R_gT\right] \tag{3.39}$$

$$k_{p11,0} = k_{p11,0}^0 \, exp\left[-E_{p11}/R_gT\right] \tag{3.40}$$

$$k_{p22,0} = k_{p22,0}^0 \, exp\left[-E_{p22}/R_gT\right] \tag{3.41}$$

$$k_{tc11,0} = k_{tc11,0}^0 \, exp\left[-E_{tc11}/R_gT\right] \tag{3.42}$$

$$k_{tc22,0} = k_{tc22,0}^0 \, exp\left[-E_{tc22}/R_gT\right] \tag{3.43}$$

$$k_{f11,0} = k_{f11,0}^0 \, exp\left[-E_{f11}/R_gT\right] \tag{3.44}$$

$$k_{f21,0} = k_{f21,0}^0 \, exp\left[-E_{f21}/R_gT\right] \tag{3.45}$$

$$k_{f12,0} = k_{f12,0}^0 \, exp\left[-E_{f12}/R_gT\right] \tag{3.46}$$

$$k_{f22,0} = k_{f22,0}^0 \, exp\left[-E_{f22}/R_gT\right] \tag{3.47}$$

where k_d^0, $k_{p11,0}^0$, $k_{p22,0}^0$, $k_{tc11,0}^0$, $k_{tc22,0}^0$, $k_{f11,0}^0$, $k_{f21,0}^0$, $k_{f12,0}^0$, $k_{f22,0}^0$ are the

frequency factors for the intrinsic rate constants, s^{-1} or m^3 mol^{-1} s^{-1}.

The values of k_{f11}, k_{f12}, k_{f21} and k_{f22} are calculated using

$$\frac{k_{fij}}{k_{fij,0}} = \frac{k_{pij}}{k_{pij,0}}; \text{ where } i,j = 1,2 \tag{3.48}$$

The parameters used for copolymerization of SAN with AIBN have been

taken from Seth and Gupta [15] Keramopoulos and Kiparissides [22] and

Nayak and Gupta [36] and are summarized in Table 3.1. The balance

equations in Appendix A-1b along with those given in Appendix A-2 are

solved using the code, ODE15s, of MATLAB. The initial conditions used are

at $t = 0$ (only monomer 1, monomer 2 and initiator are present)

$$R = 0 \tag{3.49}$$

$$I = I_0 \tag{3.50}$$

$$\lambda_{0,0} = \lambda_{1,0} = \lambda_{0,1} = \lambda_{1,1} = \lambda_{2,0} = \lambda_{0,2} = 0 \tag{3.51}$$

Table 3.1 Parameters Used for the Copolymerization of SAN with AIBN

		Parameters	Ref.
ρ_{m1}	=	$923.6 - 0.887(T - 273.15)$ kg m^{-3}	[22]
ρ_{m2}	=	$806 - 1.052(T - 293.15)$ kg m^{-3}	[22]
ρ_{p1}	=	$1085 - 0.605(T - 273.15)$ kg m^{-3}	[22]
ρ_{p2}	=	1150 kg m^{-3}	[22]
f_0	=	0.58	[22]
k_d^o	=	8.6907×10^{14} s^{-1}	This work
$k_{p11,0}^o$	=	1.06×10^4 m^3 mol^{-1} s^{-1}	[22]
$k_{p22,0}^o$	=	3.0×10^4 m^3 mol^{-1} s^{-1}	[22]
$k_{f11,0}^o$	=	2.31×10^3 m^3 mol^{-1} s^{-1}	[36]
$k_{f21,0}^o$	=	6.93×10^3 m^3 mol^{-1} s^{-1}	[36]
$k_{f21,0}^o$	=	1.856×10^3 m^3 mol^{-1} s^{-1}	This work
$k_{f22,0}^o$	=	100 m^3 mol^{-1} s^{-1}	This work
$k_{tc11,0}^o$	=	1.25×10^6 m^3 mol^{-1} s^{-1}	[36]
$k_{tc22,0}^o$	=	3.3×10^9 m^3 mol^{-1} s^{-1}	[36]
E_d	=	128.281×10^3 J mol^{-1}	[36]
E_{p11}	=	29.59×10^3 J mol^{-1}	[36]
E_{p22}	=	17.17×10^3 J mol^{-1}	[36]

$$E_{tc11} \quad = \quad 7.022 \times 10^3 \, \text{J mol}^{-1} \qquad\qquad [36]$$

$$E_{tc22} \quad = \quad 22.61 \times 10^3 \, \text{J mol}^{-1} \qquad\qquad [36]$$

$$E_{f11} \quad = \quad 53.05 \times 10^3 \, \text{J mol}^{-1} \qquad\qquad [36]$$

$$E_{f12} \quad = \quad 53.05 \times 10^3 \, \text{J mol}^{-1} \qquad\qquad [36]$$

$$E_{f21} \quad = \quad 24.44 \times 10^3 \, \text{J mol}^{-1} \qquad\qquad [36]$$

$$E_{f22} \quad = \quad 24.44 \times 10^3 \, \text{J mol}^{-1} \qquad\qquad [36]$$

$$r_1 \quad = \quad 0.36 \qquad\qquad [22]$$

$$r_2 \quad = \quad 0.078 \qquad\qquad [22]$$

$$R_g \quad = \quad 8.314 \, \text{J mol}^{-1} \, \text{K}^{-1} \qquad\qquad \text{X}$$

$$\hat{V}_I^* \quad = \quad 9.12 \times 10^{-4} \, \text{m}^3 \, \text{kg}^{-1} \qquad\qquad [22]$$

$$\hat{V}_{m1}^* \quad = \quad 9.12 \times 10^{-4} \, \text{m}^3 \, \text{kg}^{-1} \qquad\qquad [22]$$

$$\hat{V}_{m2}^* \quad = \quad 1.135 \times 10^{-3} \, \text{m}^3 \, \text{kg}^{-1} \qquad\qquad [22]$$

$$\hat{V}_{p1}^* \quad = \quad 8.35 \times 10^{-4} \, \text{m}^3 \, \text{kg}^{-1} \qquad\qquad [22]$$

$$\hat{V}_{p2}^* \quad = \quad 9.49 \times 10^{-4} \, \text{m}^3 \, \text{kg}^{-1} \qquad\qquad [22]$$

$$V_{fm1} \quad = \quad 0.04 + 6.2 \times 10^{-4}[T(\text{K}) - T_{gm1}] \qquad\qquad [22]$$

$$V_{fm2} \quad = \quad 0.025 + 1.25 \times 10^{-3}[T(\text{K}) - T_{gm2}] \qquad\qquad [22]$$

$$V_{fp} \quad = \quad 0.025 + 2.5 \times 10^{-4}[T(\text{K}) - T_{gp}] \qquad\qquad [22]$$

$$\hat{V}_p^* M_{jp} \quad = \quad 0.6224 \, T_{gp} - 86.95, \ T_{gp} \geq 295K$$

$$[22]$$

$$= \quad 0.0925 \, T_{gp} + 69.47, \ T_{gp} \leq 295K$$

$(MW)_{m1}$ = 0.10414   kg mol^{-1} [22]

$(MW)_{m2}$ =   0.05306   kg mol^{-1} [22]

$(MW)_{I}$ =   0.0681   kg mol^{-1} [22]

γ_p =   1.0   [15]

γ_m =   1.0   [15]

γ_I =   1.0   [15]

T_{gm1} =   185 K   [22]

T_{gm2} =   190.38 K   [22]

T_{gp1} =   378.2 K   [41]

T_{gp2} =   373.2 K   [41]

T_{gp12} =   384.7 K   [41]

****

$$\mu_{0,0} = \mu_{1,0} = \mu_{0,1} = \mu_{1,1} = \mu_{2,0} = \mu_{0,2} = 0 \qquad (3.52)$$

$$\tau_{0,0} = \tau_{1,0} = \tau_{0,1} = \tau_{1,1} = \tau_{2,0} = \tau_{0,2} = 0 \qquad (3.53)$$

$$V_L = 1 \; m^3 \; \text{(arbitrarily)} \qquad (3.54)$$

$$V_{L1} = \frac{f_{10} \, \rho_{m2,0} \, (MW_{m1})}{(1 - f_{10})\rho_{m1,0}(MW_{m2}) + f_{10}\rho_{m2,0}(MW_{m1})} \qquad (3.55)$$

$$V_{L2} = V_L - V_{L1} \qquad (3.56)$$

$$M_{1,0} = \frac{\rho_{m1,0} \, V_{L1,0}}{(MW_{m1})} \qquad (3.57)$$

$$M_{2,0} = \frac{\rho_{m2,0} \, V_{L2,0}}{(MW_{m2})} \qquad (3.58)$$

with I_0, f_{10} and T_0 specified.

The parameters, $\theta_{tc11}, \theta_{p11}, \theta_{p22}, \theta_f$, characterizing the diffusional effects are *tuned* using experimental data [3] on isothermal polymerizations. This is discussed in Chapter 5.

Chapter 4

OPTIMIZATION OF SAN BULK COPOLYMERIZATION REACTORS

After tuning the model discussed in Chapter 3, optimization of non-isothermal SAN bulk copolymerization in batch reactors is studied using the model equations developed. The properties of the SAN depend upon the temperature history, because increase in temperature results in faster conversion but the number average molecular weight decreases. Single- as well as multiple-objective optimizations are studied.

4.1   SINGLE-OBJECTIVE OPTIMIZATION

A simple problem involving a single objective function, *I*, which is a function of the temperature history, $T(t)$, is first solved. A few important end-point constraints are also incorporated. The problem solved is to obtain the optimal temperature *history* which minimizes the total reaction time, t_f. The associated end-point constraints are: a specified (*d*esired) value, x_{md}, of the overall monomer conversion in the polymer product is attained, the product has a specified (*d*esired) value, $\bar{M}_{nd}$, of the number average molecular weight, and the average composition in the copolymer product has a *d*esired value, St_{cd}, of the mole fraction of styrene. This single-objective optimization problem can be represented mathematically as

$$\text{Min } I^* \left[T(t) \right] = \ t_f \tag{4.1}$$

subject to (s. t.)

$$x_{mf} = x_{md} \tag{4.2}$$

$$\bar{M}_{nf} = \bar{M}_{nd} \tag{4.3}$$

$$St_{cf} = St_{cd} \tag{4.4}$$

$$T_{min} \leq T(t) \leq T_{max} \tag{4.5}$$

In these equations, subscript, f, represents the final values at t_f. The first constraint (Eqn. 4.2) ensures that recycling of the unreacted monomer is limited (minimizes the post reaction separation and recycling costs). The second and third constraints [Eqns. (4.3) and (4.4)] ensure desired physical properties of the copolymer produced. A similar single objective optimization problem was formulated for homopolymerization reactors exhibiting diffusional limitations [27]. Minimizing I leads to an increase in the production capacity through a reduction of t_f, while simultaneously providing solutions satisfying the end requirements of conversion, number average molecular weight and styrene mole fraction in the copolymer.

The end-point constraints in Eqns. (4.2) – (4.5) can be incorporated as penalty functions [42] in Eqn. (4.1) to give a modified objective function, $I[T(t)]$. The final single objective optimization problem is then

$$\text{Min } I[T(t)] = t_f + w_1 \left(1 - \frac{x_{mf}}{x_{md}}\right)^2 + w_2 \left(1 - \frac{\bar{M}_{nf}}{\bar{M}_{nd}}\right)^2 \\ + w_3 \left(1 - \frac{St_{cf}}{St_{cd}}\right)^2 \tag{4.6}$$

s.t.

$$T_{min} \leq \mathrm{T}(t) \leq T_{max} \qquad\qquad (4.7)$$

In Eqn. (4.6), w_1, w_2 and w_3 are (large) penalty parameters, specified by the user to satisfy the three end-point constraints.

GA, as normally used for optimization, involves the use of several *values* of the decision variable, *T*. In contrast, in Eqn. (4.6), the decision variable, *T*, is a *function* of time (history or trajectory), and so we need to adapt the available codes for GA for such trajectory-optimization problems. We follow the methodology used by Chakravarthy et al. [27] For ***any*** chromosome, the time interval, $0 \leq t \leq t_{f0}$ (t_{f0}, an initial estimate of t_f, is user-provided, and is based on the reaction time required using a uniform temperature of T_{min}), is divided into *n* (again, user-specified) equal intervals, Δt, of time. It is assumed that the temperature, T_i, is constant in any time interval, $t_i \leq t \leq t_{i+1}$. The first (at $t = 0$) value, T_1, in this chromosome is selected by the GA code randomly in the *entire* temperature range, $T_{min} \leq T \leq T_{max}$. The successive values of T_i are selected by the GA code randomly to lie in a much smaller range (ΔT say, $\pm$ 1 °C) of temperature *around the previous value*, T_{i-1} (but subject to the overall temperature constraint in Eqn. (4.7), so as to make the temperature history achievable (else, an energy balance equation will have to be added to the set of model equations). A stopping criterion ($x_m = x_{md} \pm TOL$, where *TOL* is a user-specified tolerance) is used to end the simulation for *this* chromosome at $t = t_N$, as soon as the conversion exceeds $x_{md} + TOL$ (*TOL* is taken to be 0.001). The interval $t_{N-1} \leq t \leq t_N$ is explored further. The fitness function, *I*, defined in Eqn. (4.6), is calculated over $t_{N-1} \leq t \leq t_N$ and t_f is taken to be that value (for this chromosome) which corresponds to the minimum value of *I*. This is repeated

for every chromosome. All other steps in genetic algorithm (GA) are unchanged. The single objective optimization toolbox of MATLAB™ with GA as the solver is used. The fitness function, *I*, defined in Eqn. (4.6) is solved using GA with a user-specified value of the number of digitized decision variables. The population type, population size, fitness scaling, reproduction, mutation, crossover and stopping criteria are all user-defined.

The value of the tolerance, TOL, for conversion is taken as 0.001. This is used to ascertain if x_{mf} has attained the value of x_{md} within a small bound of $x_{md} \pm$ TOL. The tolerance specifies a narrow conversion range and gives a product of desired physical properties.

4.2 MULTI-OBJECTIVE OPTIMIZATION

The single objective function, *I*[*T*(*t*)] is further extended to two and three objective problems.

4.2.1 The *two*-objective optimization problem

The first two-objective optimization problem requires the minimization of the total reaction time, t_f, and the maximization of the number average molecular weight, $\bar{M}_{nf}$, of the product. The associated constraints are that the overall conversion of the monomers has a specified (*d*esired) value, x_{md}, and that the composition in the copolymer product has a *d*esired value, St_{cd} (mole fraction of styrene in the product). This two-objective optimization problem can be represented mathematically as

$$\text{Min } I_1^*[T(t)] = t_f \tag{4.8}$$

$$\text{Max} I_2^*[T(t)] = x_{mf} \tag{4.9}$$

subject to (s. t.)

$$\bar{M}_{nf} = \bar{M}_{nd} \tag{4.10}$$

$$St_{cf} = St_{cd} \tag{4.11}$$

$$T_{min} \le T(t) \le T_{max} \tag{4.12}$$

The conflicting nature of these two objectives gives a good opportunity to carry out multi-objective optimization. The end-point constraints in Eqns. (4.10) – (4.12) can be incorporated as penalty functions [42] in Eqns. (4.8) and (4.9) to give a modified objective functions, $I_1[T(t)]$ and $I_2[T(t)]$. The final two-objective optimization problem is then

$$\text{Min } I_1[T(t)] = t_f + w_1 \left(1 - \frac{\bar{M}_{nf}}{\bar{M}_{nd}}\right)^2 + w_2 \left(1 - \frac{St_{cf}}{St_{cd}}\right)^2 \tag{4.13}$$

$$\text{Max } I_2[T(t)] = x_{mf} + w_1 \left(1 - \frac{\bar{M}_{nf}}{\bar{M}_{nd}}\right)^2 + w_2 \left(1 - \frac{St_{cf}}{St_{cd}}\right)^2 \tag{4.14}$$

s.t.

$$T_{min} \le \text{T}(t) \le T_{max} \tag{4.15}$$

In Eqns. (4.13) and (4.14), w_1 and w_2 are (large) penalty parameters, specified by the user to satisfy the three end-point constraints.

4.2.2 The *three*-objective optimization problem

A three-objective optimization problem solved here is given by

$$\text{Min } I_1^*[T(t)] = t_f \tag{4.16}$$

$$\text{Max} I_2^*[T(t)] = x_{mf} \tag{4.17}$$

$$\text{Max} I_3^*[T(t)] = \bar{M}_{nf} \tag{4.18}$$

s. t.

$$St_{cf} = St_{cd} \tag{4.19}$$

$$T_{min} \leq T(t) \leq T_{max} \tag{4.20}$$

The conflicting nature of these objectives, again, gives a good opportunity to carry out multi-objective optimization. The end-point constraint in Eqn. 4.19 can be incorporated as a penalty function [42] in Eqns. (4.16) – (4.18) to give modified objective functions, $I_1[T(t)]$, $I_2[T(t)]$ and $I_3[T(t)]$. The final multi-objective optimization problem is then

$$\text{Min } I_1[T(t)] = t_f + w_1 \left(1 - \frac{St_{cf}}{St_{cd}}\right)^2 \tag{4.21}$$

$$\text{Max } I_2[T(t)] = x_{mf} + w_1 \left(1 - \frac{St_{cf}}{St_{cd}}\right)^2 \tag{4.22}$$

$$\text{Max } I_3[T(t)] = \bar{M}_{nf} + w_1 \left(1 - \frac{St_{cf}}{St_{cd}}\right)^2 \tag{4.23}$$

s. t.

$$T_{min} \leq \text{T}(t) \leq T_{max} \tag{4.24}$$

In Eqns. (4.21) − (4.23), w_1 is a (large) penalty parameter, specified by the user to satisfy the three end-point constraint.

Chapter 5

RESULTS AND DISCUSSION

The parameters, θ_{tc11}, θ_{p11}, θ_{p22} and θ_f, for the gel, glass and cage effects are obtained by curve-fitting (tuning) the experimental data of Garcia-Rubio et al. [3] on SAN for (small) batch reactors under isothermal conditions.

5.1 TUNING OF MODEL PARAMETERS

The values of these parameters, which minimize the *normalized* sum of square errors, E, between the experimental data, *exp*, and the model-predicted values, *mod*, are computed for **each** individual experimental run at 40 ℃ and 60 ℃ with 10 mM and 50 mM initial concentrations, I_0, of the initiator (AIBN) for four different mole fractions (f_{10} = 0.6, 0.7, 0.8 and 0.9), f_{10}, of styrene in the feed.

$$Min\ E\left(\theta_{tc11}, \theta_{p11}, \theta_{p22}, \theta_f\right)$$

$$= \sum_{i=1}^{a} w_i \left(\frac{x_{m,i}^{exp} - x_{m,i}^{mod}}{x_{m,i}^{mod}}\right)^2 + \sum_{j=1}^{b} w_j \left(\frac{\bar{M}_{n,j}^{exp} - \bar{M}_{n,j}^{mod}}{\bar{M}_{n,j}^{mod}}\right)^2$$

$$+ \sum_{k=1}^{c} w_k \left(\frac{\bar{M}_{w,k}^{exp} - \bar{M}_{w,k}^{mod}}{\bar{M}_{w,k}^{mod}}\right)^2 + \sum_{l=1}^{d} w_l \left(\frac{St_{c,l}^{exp} - St_{c,l}^{mod}}{St_{c,l}^{mod}}\right)^2 \qquad (5.1)$$

$$+ \sum_{p=1}^{e} w_p \left(\frac{St_{rm,p}^{exp} - St_{rm,p}^{mod}}{St_{rm,p}^{mod}}\right)^2$$

In Eqn. (5.1), a, b, c, d and e are the number of discrete points for the overall monomer conversion, x_m, the number average molecular weight, $\bar{M}_n$, the

weight average molecular weight, $\bar{M}_w$, styrene mole fraction, St_{rm}, in the unreacted monomer mixture and the styrene composition, St_c, in the copolymer, in any experimental run. The weighting factors, w_i, w_j, w_k, w_l and w_p have been used to provide proper weightings to the different errors and are user-specified.

5.1.1 Individually optimized parameters (IOPs)

The bulk copolymerization of SAN proceeds in a single phase when the initial mole fraction, f_{10}, of styrene is larger than about 50%, as discussed by Garcia-Rubio et al. [3]. Experimental data on x_m, $\bar{M}_n$, $\bar{M}_w$, St_c and St_{rm} for initial styrene mole fractions of 0.6, 0.7, 0.8 and 0.9 have been used to estimate the parameters, θ_{tc11}, θ_{p11}, θ_{p22} and θ_f. These values are referred to as individually optimized parameters (IOPs). The IOPs for these cases are given in Table 5.1. Figs. A-3 (a-d) in Appendix A-3 represent the histories (variation with time) of x_m for different values of f_{10} at 40 ºC and 60 ºC with 10 mM and 50 mM initial initiator concentration (I_0). The discrete points represent experimental data of Garcia-Rubio et al. [3], while the continuous curves denote the model-predictions using the IOPs. The initial conversion increases linearly with time and then, there is a sharp rise in conversion in the middle is due to the diffusional limitations (cage, gel and the glass effects) due to the increase in viscosity of the reaction mass. The reaction ends due to the glass effect before 100% completion. The time required to attain the desired conversion decreases with the increase in temperature for the given initial molar concentration of initiator and initial mole fraction of styrene in the reaction mass. At a given temperature and initial molar concentration of initiator, time required to attain

Table 5.1. IOPs for Bulk Copolymerization of SAN*

T	I_0 (mM)	f_{10}	θ_{tc11} (s)	θ_{p11} (s)	θ_{p22} (s)	θ_f (s)
313 K (40°C)	10	0.6	2.84×10^{48}	9.23×10^{24}	2.24×10^{24}	1.08×10^{12}
		0.7	4.04×10^{47}	9.23×10^{24}	2.24×10^{24}	1.08×10^{12}
		0.8	5.64×10^{45}	9.23×10^{24}	2.24×10^{24}	1.08×10^{12}
		0.9	9.89×10^{42}	9.23×10^{24}	2.24×10^{24}	1.08×10^{12}
	50	0.6	1.27×10^{48}	9.23×10^{24}	2.24×10^{24}	1.08×10^{12}
		0.7	9.97×10^{46}	9.23×10^{24}	2.24×10^{24}	1.08×10^{12}
		0.8	1.80×10^{45}	9.23×10^{24}	2.24×10^{24}	1.08×10^{12}
		0.9	4.93×10^{42}	9.23×10^{24}	2.24×10^{24}	1.08×10^{12}
333 K (60°C)	10	0.6	1.86×10^{25}	8.83×10^{14}	2.94×10^{15}	6.08×10^{4}
		0.7	5.67×10^{24}	8.83×10^{14}	2.94×10^{15}	6.08×10^{4}
		0.8	8.87×10^{23}	8.83×10^{14}	2.94×10^{15}	6.08×10^{4}
		0.9	4.93×10^{22}	8.83×10^{14}	2.94×10^{15}	6.08×10^{4}
	50	0.6	8.44×10^{24}	8.83×10^{14}	2.94×10^{15}	6.08×10^{4}
		0.7	2.89×10^{24}	8.83×10^{14}	2.94×10^{15}	6.08×10^{4}
		0.8	5.04×10^{23}	8.83×10^{14}	2.94×10^{15}	6.08×10^{4}
		0.9	4.04×10^{22}	8.83×10^{14}	2.94×10^{15}	6.08×10^{4}

*$\theta_{tc11} = \theta_{tc22} = \theta_{tc12}$, $\theta_{p11} = \theta_{p12}$, $\theta_{p21} = \theta_{p22}$

the desired conversion decreases with the increase in initial mole fraction of styrene in the reaction mixture. The agreement between the best-fit model predictions and experimental data are quite good.

Figs. A-3 (e-h) and Figs. A-3 (i-l) represent $\bar{M}_n$ and $\bar{M}_w$ as a function of x_m for initial styrene mole fractions of 0.8 and 0.9 at 40 ºC and 60 ºC with 10 mM and 50 mM initial initiator concentration (I_0). For the given temperature and initial molar concentration of initiator, the number- and weight-average molecular weights increases with the increase in the initial mole fraction of styrene in the reaction mass. The model predictions agree with experimental data at low conversions but there are slight discrepancies at higher monomer conversions. These discrepancies are due to the increase in reaction mass and the phenomenon will become very complex. This is similar to the disagreement observed for homopolymerizations by Ray et al. [16]

In Figs. A-3 (m-p) and A-3 (q-t), the histories of St_c and St_{rm} are shown for different values of f_{10} at 40 ºC and 60 ºC with 10 mM and 50 mM initial initiator concentration. The model predicts these variations excellently.

The IOPs in Table 5.1 give model predictions which are in reasonable accord with experimental data. However, it is necessary to develop a *generalized* correlation for the parameters, θ_{tc11}, θ_{p11}, θ_{p22}, and θ_f, to increase the usefulness of the model and make it applicable for more generalized operating conditions of non-isothermal operations. It may be emphasized that in any *real-life* optimization problem involving large sets of information/data, one must solve simpler problems to obtain suitable ranges of parameters. These have been generated using the IOPs first.

5.1.2 Best-fit *correlations* (BFCs)

The IOP values of θ_{tc11} are a function of T, f_{10}, and I_0, whereas the IOP values

42

of θ_{p11}, θ_{p22} and θ_f are functions of T alone and are independent of f_{10} and I_0, as predicted by the present model. They may be written in terms of an *empirical* curve-fit equation as

$$log\theta_{tc11} = \frac{\left(A + \frac{B}{T} + \frac{C}{T^2}\right) \times (D + E f_{10} + F f_{10}^2) \times (G + H T I_0)}{I + J \frac{f_{10}}{T}} \quad (5.2)$$

$$log\theta_{p11} = K + \frac{L}{T} + \frac{M}{T^2} \quad (5.3)$$

$$log\theta_{p22} = N + \frac{O}{T} + \frac{P}{T^2} \quad (5.4)$$

$$log\theta_f = Q + \frac{R}{T} \quad (5.5)$$

Tuning of these parameters is done by minimizing the cumulative weighted sum-of-square errors between the model predicted results and experimental values. The values of the different constants in Eqns. (5.2)-(5.5) are optimized using the single-objective optimization toolbox of MATLAB with the genetic algorithm (GA) solver to give the generalized *b*est-*f*it *c*orrelations (BFCs) as

$log\theta_{tc11}$

$$= \frac{\left(3094.7613 - \frac{2096103.1846}{T} + \frac{3.576389 \times 10^8}{T^2}\right) \times}{(0.8685 + 0.5979 f_{10} - 0.6345 f_{10}^2) \times (0.9773 - 4.4861 \times 10^-}{0.9749 + 0.9263 \frac{f_{10}}{T}} \quad (5.6)$$

$$log\theta_{p11} = 1055.99 - \frac{7.243 \times 10^5}{T} + \frac{1.2577 \times 10^8}{T^2} \quad (5.7)$$

$$log\theta_{p22} = 1174.232 - \frac{7.925 \times 10^5}{T} + \frac{1.3545 \times 10^8}{T^2} \quad (5.8)$$

$$log\theta_f = -106.594 + \frac{36440.8117}{T} \quad (5.9)$$

The experimental data with two initial mole fractions of styrene ($f_{10} = 0.6$ and 0.9) at 40 ℃ and 60 ℃ with 10 mM and 50 mM initial initiator concentration is used to *tune* the BFCs. The remaining two values of the initial mole fractions of styrene ($f_{10} = 0.7$ and 0.8) at 40 ℃ and 60 ℃ with 10 mM and 50 mM initial initiator concentration are *predicted*. The plots of different sets of tuned and predicted values of the BFCs are presented in Appendix A-4 as Figs. A-4 (a-t). It may be added that the forms used in Eqns. (5.2) - (5.5) have been developed by a trial and error procedure starting with simpler linear forms, with further terms added one by one based on the results obtained. Also, the *entire* set of experimental data points have been used to obtain Eqns. (5.6) - (5.9). For such *highly non-linear* behavior (as for SAN polymerization), this is most essential.

Figs. A-4 (a-d) in Appendix A-4 represent the time histories for different values of f_{10} at 40 ℃ and 60 ℃ with 10 mM and 50 mM initial initiator concentration (I_0). The discrete points represent experimental data [3] while the continuous curves denote the model-predictions using the BFCs. The model predicts these variations *reasonably* well. Figs. A-4 (e-h) and A-4 (i-l) show $\bar{M}_n$ and $\bar{M}_w$ as a function of x_m for different values of f_{10} at 40 ℃ and 60 ℃ with 10 mM and 50 mM initial initiator concentration (I_0). The model predictions are in concurrence with experimental data [3] at low conversions but there are slight discrepancies at higher monomer conversions. This is similar to the disagreement observed for homopolymerizations by Ray et al. [16] In Figs. A-4 (m-p) and A-4 (q-t), the time histories of St_c and St_{rm} are shown for different values of f_{10} at 40 ℃ and 60 ℃ with 10 mM and 50 mM initial initiator concentration. The model predictions are in accord with

experimental data. Clearly, the fit of the generalized correlations is not as good as for the case of the IOPs. This is expected and can possibly be improved (but only *somewhat*) by adding more terms in Eqns. (5.2) − (5.5) or by changing the weightage factors in Eqn. (5.1).

5.2   OPTIMIZATION   OF   BULK   COPOLYMERIZATION REACTORS FOR SAN

Several checks are made to ensure that the code prepared to generate the optimal temperature histories in the non-isothermal batch reactor for the copolymerization of SAN, is free of errors. One of these checks was that the values obtained by simulation for x_m, $\bar{M}_n$ and St_c, *at isothermal conditions*, were consistent with values obtained using a simulation code. The match was excellent. The other is [for Eqn. (4.6)] that when the values of x_{md}, $\bar{M}_{nd}$ and St_{cd} are taken as those corresponding to isothermal conditions (say, 40 ºC), the optimization code gives an isothermal temperature history of 40 ºC, etc.

The total reaction time, t_f, for the copolymerization of SAN is minimized (Eqn. 4.6) with an initiator loading of 50 mM AIBN and for an initial mole fraction of styrene (f_{10}) of 0.6. The temperature difference (ΔT) between two successive values of t_i should be small and the temperature should also lie within the overall range, $T_{min} \leq T \leq T_{max}$. The effect of the temperature difference, ΔT, on the optimal temperature history for the desired overall monomer conversion (x_{md}) of 0.94, the styrene mole fraction in the copolymer (St_{cd}) of 0.597 and the number average molecular weight ($\bar{M}_{nd}$) of 48,000 kg/kmol, is shown in Fig. 5.1. The oscillations obtained at ΔT of ± 2 °C and ± 3 °C are quite large whereas with $\Delta T = \pm 1$ °C, a reasonably smooth temperature history is obtained. Therefore, $\Delta T == \pm 1$ ^{0}C is used for (most of
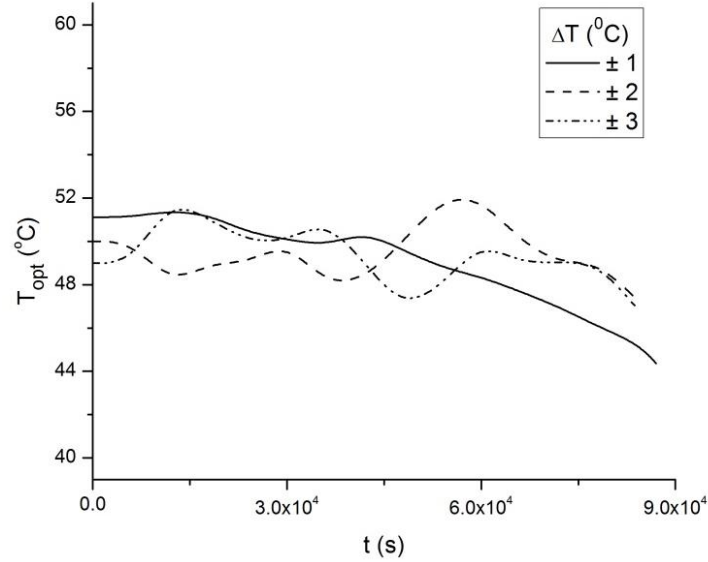
45

Figure 5.1. Optimal temperature histories [for Eqn. (4.6)] obtained for different values of ΔT for the desired overall monomer conversion (x_{md}) of 0.94, the styrene mole fraction in the copolymer (St_{cd}) of 0.597 and the number average molecular weight ($\bar{M}_{nf}$) of 48,000 kg/kmol. $\Delta t = 6{,}000$ s, $t_{f0} = 1.5 \times 10^5$ s, $w_1 = w_2 = w_3 = 10^{12}$

the) further optimization studies since it is a good compromise between the computational effort and the temperature histories.

The optimal temperature histories obtained for the single objective problem (Eqn. 4.6) for different values of $\bar{M}_{nd}$ are shown in Fig. 5.2 for a constant *desired* overall monomer conversion (x_{md}) of 0.94 and the styrene mole fraction in the copolymer (St_{cd}) of 0.597 (this value is near the azeotropic composition of SAN under non-bulk polymerizations, and is useful to avoid composition drift).

The corresponding final values of the conversion (x_{mf}), styrene mole fraction in the copolymer (St_{cf}), number average molecular weight ($\bar{M}_{nf}$) and time (t_f) are given in Table 5.2. The agreement between the final values and the desired
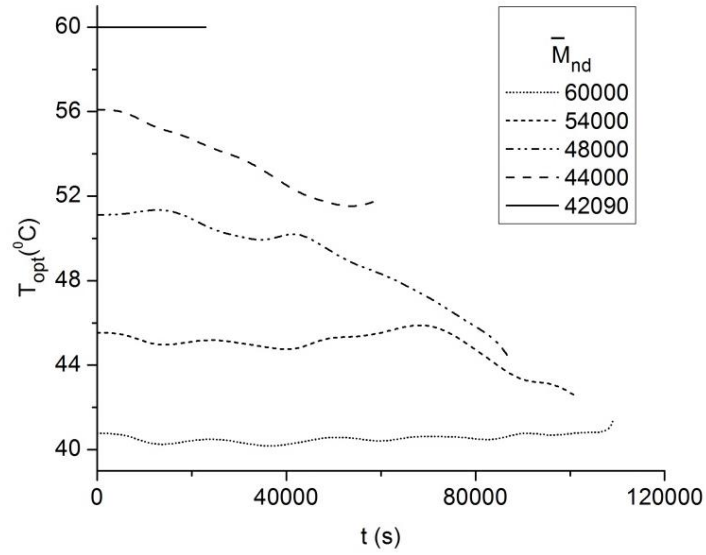
Figure 5.2. Optimal temperature histories [Eqn. (4.6)] of SAN copolymerization with an initiator loading of 50 mM AIBN and for an initial mole fraction of styrene (f_{10}) of 0.6. The desired overall monomer conversion (x_{md}) is 0.94 and the desired styrene mole fraction in the copolymer (St_{cd}) is 0.597. Plots for different values of $\bar{M}_{nd}$ shown. $\Delta t = 6{,}000$ s, $t_{f0} = 1.5 \times 10^5$ s, $w_1 = w_2 = w_3 = 10^{12}$

Table 5.2 Final values of the conversion (x_{mf}), styrene mole fraction in copolymer (St_{cf}), number average molecular weight ($\bar{M}_{nf}$) and time (t_f) for x_{md} = 0.94 and St_{cd} = 0.597 for the optimal temperature histories of Fig. 5.2

x_{mf}	St_{cf}	$\left(\bar{M}_{nf}\right)$ (kg/kmol)	t_f (s)
0.94	0.597	60,000	109,194
0.94	0.597	54,000	100,782
0.94	0.597	48,000	87,036
0.94	0.597	44,000	58,812
0.94	0.597	42,090	22,956
x_{md} = 0.94	St_{cd} = 0.597	$\bar{M}_{nd}$ = 42,090-60,000	--

values is quite good. The minimum value of $\bar{M}_{nf}$ obtained is 42,090 kg/kmol

with a *uniform* temperature of 60 ºC in a short time of 22,956 s, whereas the

maximum value $\bar{M}_{nf}$ obtained is 60,000 kg/kmol, obtained with the lowest

temperature of 40 ºC requiring a maximum t_f of 109,194 s. Thus, a lower value

of the desired number average molecular weight, $\bar{M}_{nd}$, requires higher

temperatures and lower reaction times. Plots of the overall conversion history

(x_m vs. t), $\bar{M}_{nd}$ vs. t and $\bar{M}_{wd}$ vs. t corresponding to the optimum temperature

histories of Fig. 5.2 are shown in Fig. 5.3. Plots of St_c vs. time are not shown

since they are almost constant at its desired value (confirming polymerization

near the azeotropic composition).

Eqn. (4.6) has also been solved for different values of x_{md} and for a constant

value of $\bar{M}_{nd} = 48,000$ and $St_{cd} = 0.597$ (instead of for several $\bar{M}_{nd}$ but for x_{md}

$= 0.94$ and $St_{cd} = 0.597$, as in Fig. 5.2).

The optimal temperature histories [Eqn. (4.6)] for $\bar{M}_{nd}$ and St_{cd} of 48,000

kg/kmol and 0.597, respectively, using an initiator loading of 50 mM AIBN

and for an initial mole fraction of styrene (f_{10}) of 0.6, are shown in Fig. 5.4 for

different values of x_{md}. The final values of x_{mf}, St_{cf}, $\bar{M}_{nf}$ and t_f are given in

Table 5.3.

It is observed that for some of the choices of x_{md}, e.g., $x_{md} = 0.80$, the final

value of $\bar{M}_{nf}$ does not attain the desired value of 48,000 kg/kmol (and the

weightages, w_i, in Eqn. 4.6 need to be increased). It may be added that the

value of ΔT had to be decreased to ±0.5 ºC, so as to obtain smooth

temperature histories in Fig. 5.4 (for x_{md} of 0.89).
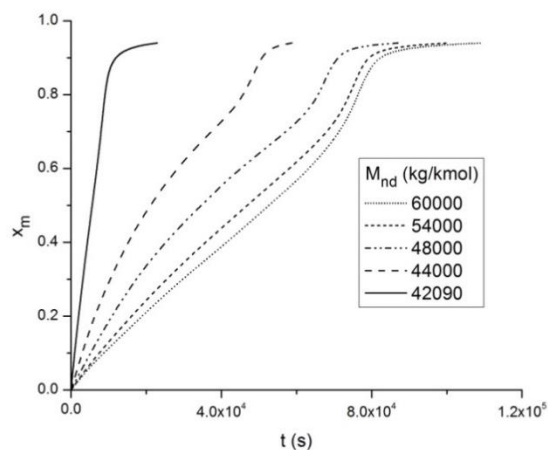
(a) Conversion history
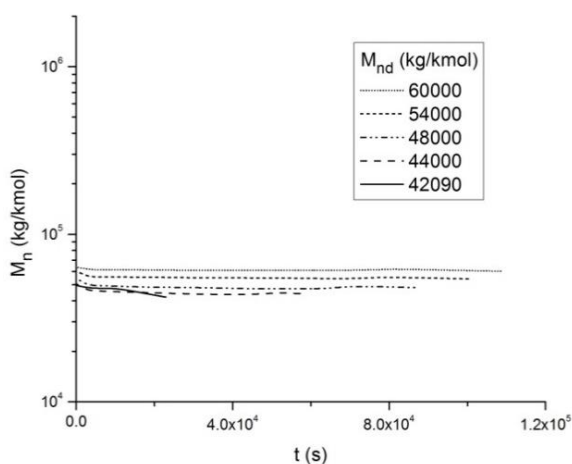
(b) Number average molecular weight *vs*. time
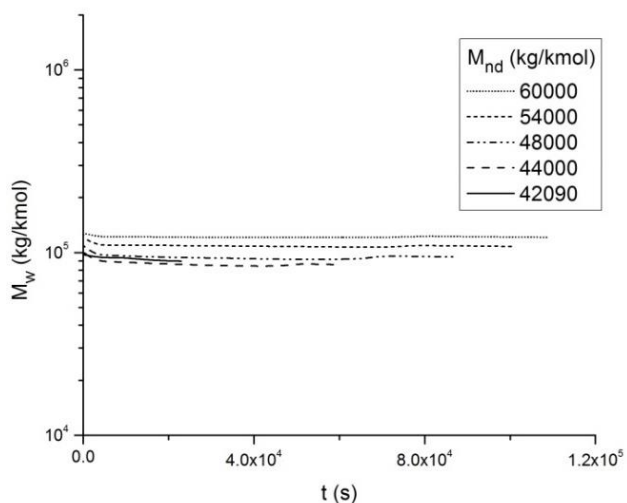
(c) Weight average molecular weight *vs*. time

Figure 5.3. Results of SAN copolymerization [Eqn. (4.6)] for the optimal temperature histories in Fig. 5.2 (initiator loading = 50 mM AIBN, f_{10} = 0.6). x_{md} is 0.94 and St_{cd} is 0.597. Plots for different values of $\bar{M}_{nd}$ shown.
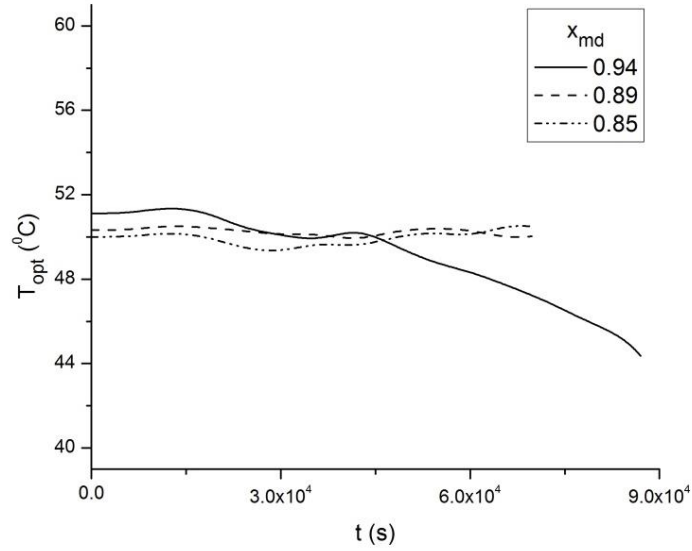
Figure 5.4. Optimal temperature histories for SAN copolymerization [Eqn. (4.6)] with an initiator loading of 50 mM AIBN and f_{10} = 0.6. The values of $\bar{M}_{nd}$ and St_{cd} are 48,000 kg/kmol and 0.597, respectively. Results shown for three different values of x_{md}.

Table 5.3 Final values [for Eqn. (4.6)] of conversion (x_{mf}), styrene mole fraction in copolymer (St_{cf}), number average molecular weight ($\bar{M}_{nf}$) and time (t_f) for $\bar{M}_{nd}$ = 48,000 kg/kmol and St_{cd} = 0.597; x_{md} = 0.85-0.94

x_{mf}	St_{cf}	$\bar{M}_{nf}$ (kg/kmol)	t_f (s)
0.85	0.5963	48,000	69,810
0.89	0.5767	48,000	69,762
0.94	0.5973	48,000	83,712
x_{md} = 0.85-0.94	St_{cd} = 0.597	$\bar{M}_{nd}$ = 48,000	--

The two-objective optimization problem [Eqns. (4.13) and (4.14)], minimization of the final reaction time, t_f, and maximization of the final value of the number average molecular weight, $\bar{M}_{nf}$, is then solved.

Table 5.4 Values of the computational parameters used for the two-objective optimization problem [Eqns. (4.13) and (4.14)]

Parameter	Value
Population size	300
Cross over fraction	0.90
Mutation fraction	Constraint dependent
Migration (forward) fraction	0.2
Pareto front population fraction	0.35
Number of generations	2,000

This MOO problem is solved with the constraints of $x_{mf} = 0.94$, and $S_{tcf} = 0.597$, with the temperature bounds of 40 to 60 ^{o}C. The optimization toolbox of MATLAB with the genetic algorithm as solver was used to obtain the Pareto set of optimal solutions for this two-objective problem. The computational parameters used for this problem are given in Table 5.4.

For this two-objective optimization problem, a *seed* of one chromosome (isothermal, 40 ^{o}C) is provided so as to obtain the *entire* Pareto set. The remaining chromosomes are created by the *creation function* in MATLAB.

Fig. 5.5 shows the converged Pareto set for this problem. It is observed that as $\bar{M}_{nf}$ increases (desirable), t_f also increases (undesirable), and so this plot, indeed, represents a Pareto set.

Points A, B, C, D and E marked on the Pareto set in Fig. 5.5 represent five of the Pareto-optimal solutions for this two-objective optimization problem. Points A and E represent the two extreme isothermal conditions of 60 $^{\circ}$C and
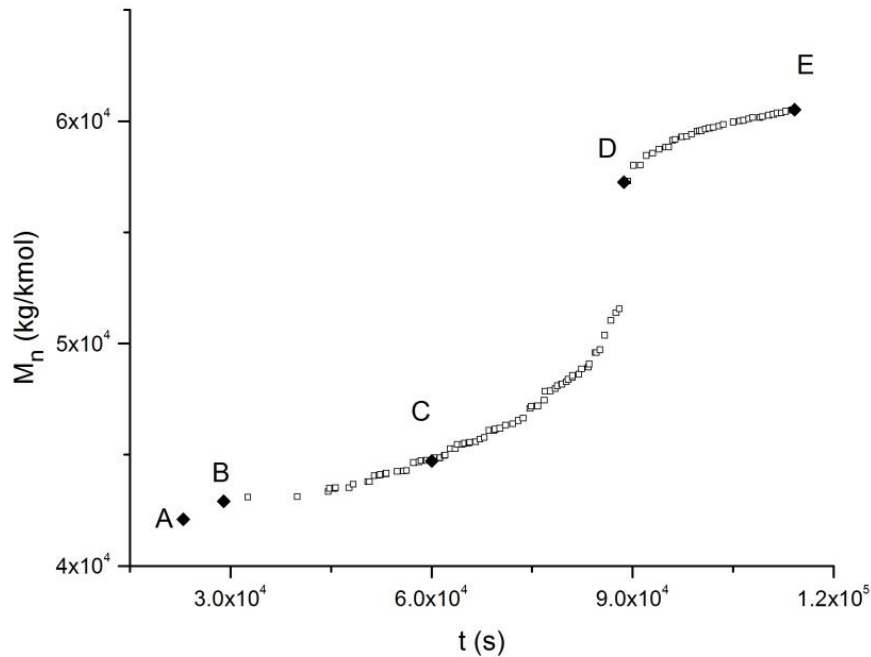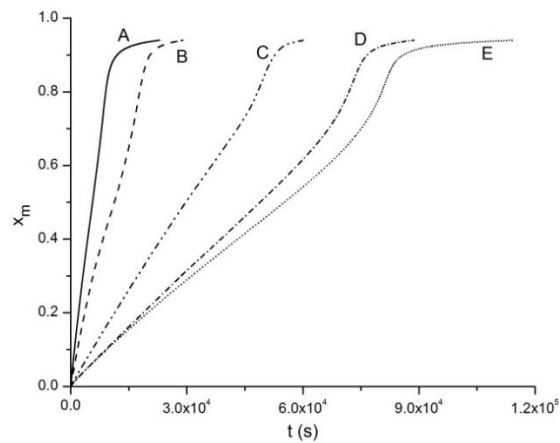

Figure 5.5. Pareto set of optimal solutions for the two-objective optimization problem [Eqns. (4.13) and (4.14)] for SAN copolymerization with an initiator loading of 50 mM AIBN and for an initial mole fraction of styrene (f_{10}) of 0.6. $x_{md} = 0.94$ and $St_{cd} = 0.597$. $w_1 = w_2 = 10^{12}$.

40 $^{\circ}$C, respectively. Plots of the histories of the temperature, overall monomer conversion and the number average molecular weight for these five points, A – E, are shown in Fig. 5.6.

The three-objective optimization problem [Eqns. (4.21) – (4.23)], namely, minimization of the final reaction time, t_f, maximization of the final value of the number average molecular weight, $\overline{M}_{nf}$, and maximization of the final value of the overall conversion, x_{mf}, is then solved. The only constraint used in this three-objective optimization problem is the desired final value of the mole fraction of styrene in the copolymer ($St_{cd} = 0.597$), with the temperature

52
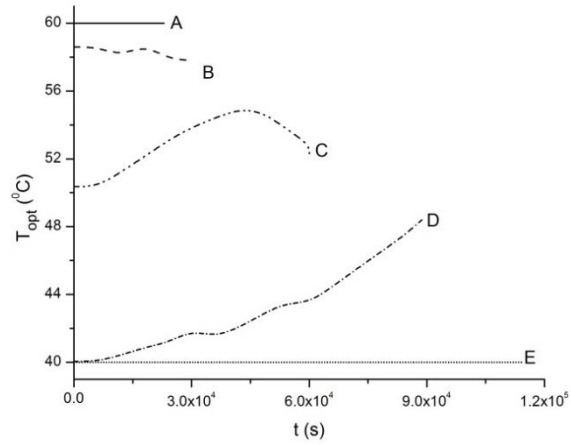
(a) Optimum temperature histories for points A-E in Fig. 5

(b) Conversion histories for points A-E in Fig. 5
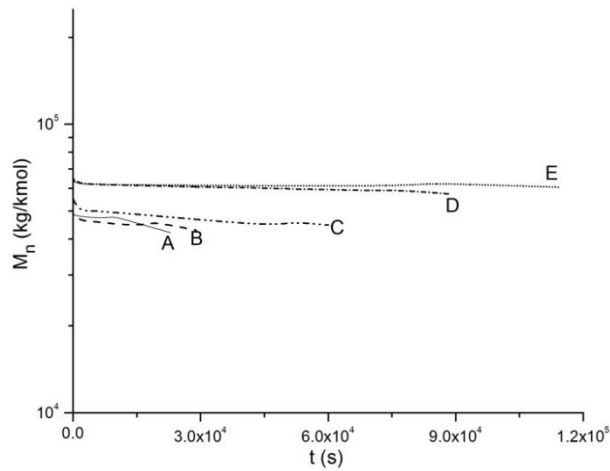
(c) Histories of the number average molecular weight for points A-E in Fig. 5

Figure 5.6. Histories $[T(t), x_m(t),$ and $\overline{M}_n]$ corresponding to optimal points A-E on the Pareto set of Fig. 5.5. SAN copolymerization with an initiator loading of 50 mM AIBN and for $f_{10} = 0.6$. The desired overall monomer conversion (x_{md}) is 0.94 and of the desired styrene mole fraction in the copolymer (St_{cd}) is 0.597.

bounds of 40 to 60 °C. The optimization toolbox of MATLAB with genetic algorithm as the solver is used to obtain the Pareto set of optimal solutions for this three-objective problem. The computational parameters used for this problem are the same as used in the two-objective problem (Table 5.4).

Fig. 5.7 shows the converged optimal solutions for this three-objective problem. The three objectives are plotted as a function of the chromosome number (with the chromosome numbers re-ordered such that the first objective function, t_f, increases continuously). This methodology of presenting Pareto solutions when more than two objective functions are involved, was suggested by Agrawal et al. [43]. This diagram shows that the abscissa can easily be partitioned into two domains: A-B and C-E. In domain A-B, t_f increases (undesirable), M_{nf} decreases (undesirable) but x_{mf} increases (desirable). So, this represents Pareto-behavior and A-B, thus, represents a (part of a) Pareto front. Similarly, in C-E, t_f increases (undesirable), M_{nf} increases (desirable) and x_{mf} decreases (undesirable). So, C-E also represents a (part of a) Pareto front. Points A-E marked in Fig. 5.7 represent five of the Pareto-optimal solutions for this three-objective optimization problem. Plots of the histories of the temperature, overall monomer conversion and the number average molecular weight for these five points are shown in Fig. 5.8. Point E represents the extreme isothermal condition of 40 °C.
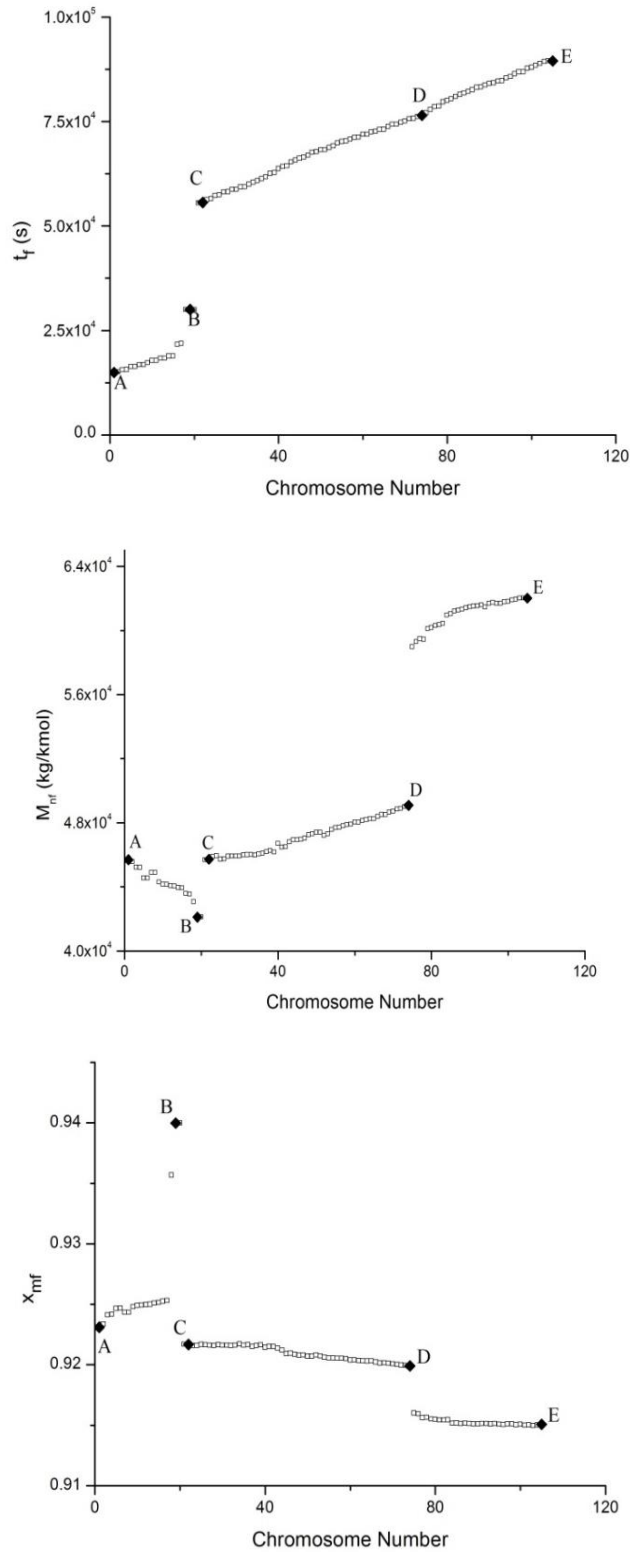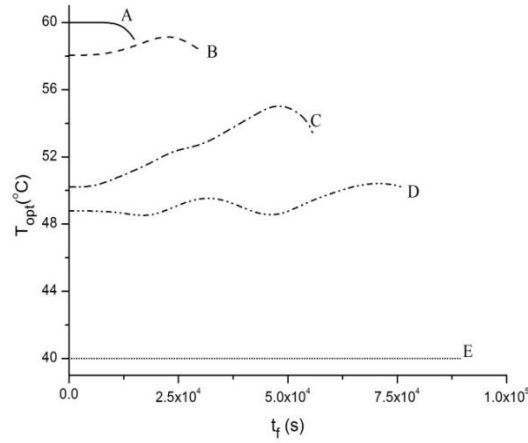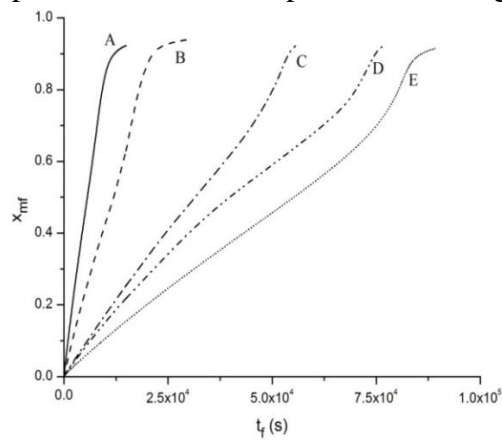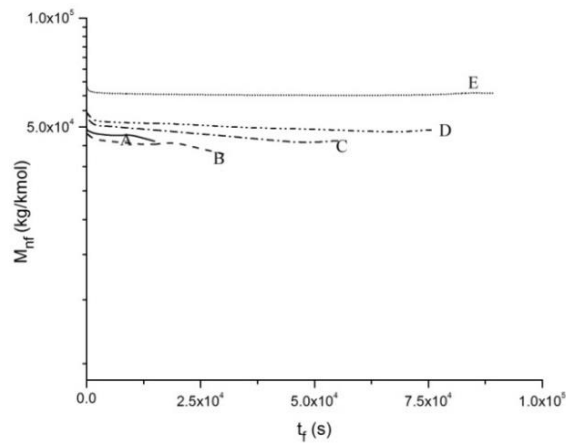
Figure 5.7. Converged optimal solutions for the three-objective optimization problem [Eqns. (4.21)−(4.23)] for SAN copolymerization with an initiator loading of 50 mM AIBN and for an initial mole fraction of styrene (f_{10}) of 0.6. $St_{cd} = 0.597$. $w_1 = w_2 = 10^{12}$

(a) Optimum temperature histories for points A-E in Fig. 5.7

(b) Conversion histories for points A-E in Fig. 5.7

(c) Histories of the number average molecular weight for points A-E in Fig. 5.7

Figure 5.8. Histories [$T(t)$, $x_{mf}(t)$, and $\bar{M}_{nf}$] corresponding to Pareto-optimal points, A-E, in Fig. 5.7. SAN copolymerization with an initiator loading of 50 mM AIBN and for f_{10} = 0.6. The desired styrene mole fraction in the copolymer (St_{cd}) is 0.597

56

Chapter 6

CONCLUSIONS AND RECOMMENDATIONS FOR FURTHER WORK

A new semi-empirical model accounting for the effects of diffusional resistances (cage, glass and Trommsdorff effects) on the rate constants of the initiation, propagation and termination reactions, respectively, in free radical bulk copolymerizations has been proposed. *Some* sets of experimental data (on the overall monomer conversion, number- and weight-average molecular weights, mole fraction of styrene in the copolymer formed and mole fraction of styrene in the reaction mixture at any time) under isothermal conditions on the SAN system have been used to 'tune' the model parameters. These have been used to predict results under *other* isothermal conditions. There is a perfect match between the experimental values and the model results for the conversion histories, mole fraction of styrene in the copolymer as a function of time and mole fraction of styrene in the unreacted reaction mass as a function of time, but show some deviation for the number- and weight-average molecular weight as a function of time for different sets of temperature and initial molar concentrations of initiator. Generalized correlations have been developed for *non-isothermal* copolymerizations of SAN, and the agreement with the experimental data is show small deviations in some of the cases. The model is an improvement and a generalization over other models since it can be used for the study of non-isothermal bulk copolymerizations of SAN.

Single and multi-objective optimizations using one, two and three objective functions are then studied using the tuned kinetic model. The optimization toolbox of MATLAB with genetic algorithm as the solver is used. The objective functions used in this study are selected from among: minimization of the reaction time, maximization of the overall monomer conversion and maximization of the number average molecular weight of the copolymer. The mole fraction of styrene in the copolymer produced, and the permissible range of temperature in the reactor are used as constraints. The optimal temperature histories are obtained for the single objective problem as well as for a few representative points on the Pareto sets. These optimal results may be used in industrial reactors.

6.1   RECOMMENDATIONS FOR FURTHER WORK

The tuned model developed in this study is applicable for the non-isothermal batch reactor for SAN copolymerization. Simulation of nonisothermal industrial reactors using our model should be done. This study needs to be extended to non-isothermal semi-batch reactors in which the monomers and/or initiator can be added to the reactor as required during the course of polymerization. Polydispersity index, using polyol solvent base and the use of new initiators needs to be added along with back-up data from industry or labs. Also, an empirical free volume-based model along the lines developed by Sangwai et al. [11] for methyl methacrylate polymerizations needs to be developed since this family of models is superior to those similar to that for homopolymerizations of Chiu et al. [4]

REFERENCES

1. Trommsdorff, V. E., Köhle, H., and Lagally, P. (1947), Zur Polymerisation Desmethacrylsäuremethylesters. *Die Makromolekulare Chemie,* Vol. 1. pp. 169-198.

2. Norrish, R. G. W. and Smith, R. R. (1942), Catalyzed Polymerization of Methyl Methacrylate in the Liquid Phase. *Nature,* Vol. 150. pp. 336-337.

3. Garcia-Rubio, L. H., Lord, M. G., MacGregor, J. F., and Hamielec, A. E. (1985), Bulk Copolymerization of Styrene and Acrylonitrile: Experimental Kinetics and Mathematical Modelling. *Polymer,* Vol. 26. pp. 2001-2013.

4. Chiu, W. Y., Carratt, G. M., and Soong, D. S. (1983), A Computer Model for the Gel Effect in Free-Radical Polymerization. *Macromolecules,* Vol. 16. pp. 348-357.

5. Bueche, F., *Physical Properties of Polymers*. Interscience, New York 1962.

6. Hui, A. W. and Hamielec, A. E. (1972), Thermal Polymerization of Styrene at High Conversions and Temperatures. An Experimental Study. *Journal of Applied Polymer Science,* Vol. 16. pp. 749-769.

7. Curteanu, S. and Bulacovschi, V. (1999), Free Radical Polymerization of Methyl Methacrylate: Modeling and Simulation under Semi-batch

and Nonisothermal Reactor Conditions. *Journal of Applied Polymer Science,* Vol. 74. pp. 2561-2570.

8.   Balke, S. T. and Hamielec, A. E. (1973), Bulk Polymerization of Methyl Methacrylate. *Journal of Applied Polymer Science,* Vol. 17. pp. 905-949.

9.   Srinivas, T., Sivakumar, S., Gupta, S. K., and Saraf, D. N. (1996), Free Radical Polymerizations Associated with the Trommsdorff Effect Under Semi-batch Reactor Conditions. II: Experimental Responses to Step Changes in Temperature. *Polymer Engineering and Science,* Vol. 36. pp. 311-321.

10.   Dua, V., Saraf, D. N., and Gupta, S. K. (1996), Free Radical Polymerizations Associated with the Trommsdorff Effect Under Semibatch Reactor Conditions - III: Experimental Responses to Step Changes in Initiator Concentration. *Journal of Applied Polymer Science,* Vol. 59. pp. 749-758.

11.   Sangwai, J. S., Bhat, S. A., Gupta, S., Saraf, D. N., and Gupta, S. K. (2005), Bulk Free Radical Polymerizations of Methyl Methacrylate under Non-isothermal Conditions and with Intermediate Addition of Initiator: Experiments and Modeling. *Polymer,* Vol. 46. pp. 11451-11462.

12.   Achilias, D. S. and Kiparissides, C. (1992), Development of a General Mathematical Framework for Modeling Diffusion-Controlled Free-Radical Polymerization Reactions. *Macromolecules,* Vol. 25. pp. 3739-3750.

13. Vrentas, J. S. and Duda, J. L. (1977), Diffusion in Polymer-Solvent Systems. II. A Predictive Theory for the Dependence of Diffusion Coefficients on Temperature, Concentration and Molecular Weight. *Journal of Polymer Science - Polymer Physics Edn.,* Vol. 15. pp. 417-439.

14. Vrentas, J. S. and Duda, J. L. (1979), Molecular Diffusion in Polymer Solutions. *AIChE Journal,* Vol. 25. pp. 1-24.

15. Seth, V. and Gupta, S. K. (1995), Free Radical Polymerizations Associated with the Trommsdorff Effect Under Semi-Batch Reactor Conditions: An Improved Model. *Journal of Polymer Engineering,* Vol. 15. pp. 283-326.

16. Ray, A. B., Saraf, D. N., and Gupta, S. K. (1995), Free Radical Polymerizations Associated With the Trommsdorff Effect Under Semibatch Reactor Conditions. I: Modeling. *Polymer Engineering and Science,* Vol. 35. pp. 1290-1299.

17. Schulz, G. V. and Harborth, G. (1947), Über Den Mechanismus Des Explosiven Polymerisationsverlaufes Des Methacrylsäuremethylesters. *Die Makromolekulare Chemie,* Vol. 1. pp. 106-139.

18. Marten, F. L. and Hamielec, A. E. (1982), High Conversion Diffusion-Controlled Polymerization of Styrene. *Journal of Applied Polymer Science,* Vol. 27. pp. 489-505.

19. Marten, F. L. and Hamielec, A. E. (1979), High Conversion Diffusion-Controlled Polymerization. *ACS Symposium Series,* Vol. 104. pp. 43-70.

20. Sharma, D. K. and Soane, D. S. (1988), High-Conversion Diffusion-Controlled Copolymerization Kinetics. *Macromolecules,* Vol. 21. pp. 700-710.

21. Hwang, W. H., Yoo, K. Y., and Rhee, H. K. (1997), Modeling of Bulk Copolymerization Reactor Using Chain-Length-Dependent Rate Constants. *Journal of Applied Polymer Science,* Vol. 64. pp. 1015-1027.

22. Keramopoulos, A. and Kiparissides, C. (2002), Development of a Comprehensive Model for Diffusion-Controlled Free-Radical Copolymerization Reactions. *Macromolecules,* Vol. 35. pp. 4155-4166.

23. Scorah, M. J., Dhib, R., and Penlidis, A. (2006), Modelling of Free Radical Polymerization of Styrene and Methyl Methacrylate by a Tetrafunctional Initiator. *Chemical Engineering Science,* Vol. 61. pp. 4827-4859.

24. Jalili, K., Abbasi, F., and Nasiri, M. (2011), Copolymerization of Styrene and Methyl Methacrylate. Part I: Experimental Kinetics and Mathematical Modeling. *Polymer,* Vol. 52. pp. 4362-4376.

25. Costa, L. I., Storti, G., Morbidelli, M., Ferro, L., Galia, A., Scialdone, O., and Filardo, G. (2012), Copolymerization of VDF and HFP in Supercritical Carbon Dioxide: A Robust Approach for Modeling Precipitation and Dispersion Kinetics. *Macromolecular Reaction Engineering,* Vol. 6. pp. 24-44.

26. Li, L., Wu, L., Bu, Z., Gong, C., Li, B.-G., and Hungenberg, K.-D. (2012), Graft Copolymerization of Styrene and Acrylonitrile in the

Presence of Poly(propylene glycol): Kinetics and Modeling. *Macromolecular Reaction Engineering,* Vol. 6. pp. 365-383.

27. Chakravarthy, S. S. S., Saraf, D. N., and Gupta, S. K. (1997), Use of Genetic Algorithms in the Optimization of Free Radical Polymerizations Exhibiting the Trommsdorff Effect. *Journal of Applied Polymer Science,* Vol. 63. pp. 529–548.

28. Garg, S. and Gupta, S. K. (1999), Multiobjective Optimization of a Free Radical Bulk Polymerization Reactor Using Genetic Algorithm. *Macromolecular Theory and Simulations,* Vol. 8. pp. 46-53.

29. Mitra, K., Deb, K., and Gupta, S. K. (1998), Multiobjective Dynamic Optimization of an Industrial Nylon 6 Semibatch Reactor Using Genetic Algorithm. *Journal of Applied Polymer Science,* Vol. 69. pp. 69-87.

30. Merquior, D. M., Fontoura, J. M. R., Pinto, J. C., and Lima, E. L. (2001), Studies of Multiobjective Optimization of Batch Free Radical Polymerization Process. *Latin American Applied Research,* Vol. 31. pp. 513-517.

31. Bhat, S. A., Sharma, R., and Gupta, S. K. (2004), Simulation and Multiobjective Optimization of the Continuous Tower Process for Styrene Polymerization. *Journal of Applied Polymer Science,* Vol. 94. pp. 775-788.

32. Mitra, K., Majumdar, S., and Raha, S. (2004), Multiobjective Optimization of a Semibatch Epoxy Polymerization Process Using the Elitist Genetic Algorithm. *Industrial and Engineering Chemistry Research,* Vol. 43. pp. 6055-6063.

33.   Tsoukas, A., Tirrell, M., and Stephanopoulos, G. (1982), Multiobjective Dynamic Optimization of Reactors. *Chemical Engineering Science,* Vol. 37. pp. 1785-1795.

34.   Farber, J. N. (1986), Steady State Multiobjective Optimization of Continuous Copolymerization Reactors. *Polymer Engineering and Science,* Vol. 26. pp. 499-507.

35.   Butala, D., Fan, M. K. H., and Choi, K. Y. (1988), Multiobjective Dynamic Optimization of a Semibatch Free Radical Copolymerization Process with Interactive CAD Tools. *Computers and Chemical Engineering,* Vol. 12. pp. 1115-1127.

36.   Nayak, A. and Gupta, S. K. (2004), Multi-Objective Optimization of Semi-Batch Copolymerization Reactors Using Adaptations of Genetic Algorithm. *Macromolecular Theory and Simulations,* Vol. 13. pp. 73-85.

37.   Amaro, B., Immanuel, C. D., Pistikopoulos, E. N., Andreas, D., Hungenberg, K., and Saraiva, P. A. (2010), Dynamic Process Optimization in Free Radical Multicomponent Polymerization: Butyl Methacrylate and Butyl Acrylate Case Study. *20th European Symposium on Computer Aided Process Engineering-ESCAPE20.*

38.   Toledo M. R and Castellanos, G. M. (2013), Generation of Efficient Solutions in Multiobjective Optimization for Copolymerization Processes. *1ST International Symosium on Innovative Technologies in Engineering and Science, at Sakarya University Congress and Culture Center Sakarya – Turkey.*

39. Anand, P., Venkateswarlu, C., and Bhagvanth Rao, M. (2013), Multistage Dynamic Optimization of a Copolymerization Reactor Using Differential Evolution. *Asia-Pacific Journal of Chemical Engineering,* Vol. 8. pp. 687-698.

40. Aggarwal, M., Modeling of Diffusional Limitations in Styrene-Acrylonitrile (SAN) Co-polymerization. *Department of Chemical Engineering,* M. Tech. dissertation, Indian Institute of Technology, Kanpur (2012).

41. Suzuki, H. and Mathot, V. B. F. (1989), An Insight into the Barten Equation for Copolymer Glass Transition. *Macromolecules,* Vol. 22. pp. 1380-1384.

42. Beveridge, G. S. G. and Schechter, R. S., *Optimization: Theory and Practice* 1970, New York: McGraw-Hill Book Company.

43. Agrawal, N., Rangaiah, G. P., Ray, A. K., and Gupta, S. K. (2006), Multi-objective Optimization of the Operation of an Industrial Low-density Polyethylene Tubular Reactor using Genetic Algorithm and its Jumping Gene Adaptations. *Industrial and Engineering Chemistry Research,* Vol. 45. pp. 3182-3199.

INDEX OF APPENDICES

APPENDIX A-1. Species Balance Equations and Moment (and Associated) Equations for Free Radical Bulk Copolymerizations in Batch Reactors

Appendix A-1a Species Balance Equations for SAN Bulk Copolymerization [40]

$$\frac{dI}{dt} = -k_d I \tag{A1a.1}$$

$$\frac{dM_1}{dt} = -k_{I1}\frac{RM_1}{V_L} - (k_{p11} + k_{f11})\frac{\lambda_{0,0} M_1}{V_L} - (k_{p21} + k_{f21})\frac{\mu_{0,0} M_1}{V_L} \tag{A1a.2}$$

$$\frac{dM_2}{dt} = -k_{I2}\frac{RM_2}{V_L} - (k_{p12} + k_{f12})\frac{\lambda_{0,0} M_2}{V_L} - (k_{p22} + k_{f22})\frac{\mu_{0,0} M_2}{V_L} \tag{A1a.3}$$

$$\frac{dR}{dt} = 2 f k_d I - k_{I1}\frac{RM_1}{V_L} - k_{I2}\frac{RM_2}{V_L} \tag{A1a.4}$$

$$\begin{aligned}
\frac{dP_{1,0}}{dt} = {} & k_{I1}\frac{RM_1}{V_L} + (k_{f11}\lambda_{0,0} + k_{f21}\mu_{0,0})\frac{M_1}{V_L} \\
& - [(k_{p11} + k_{f11})M_1 + (k_{p12} + k_{f12})M_2 \\
& + (k_{tc11} + k_{td11})\lambda_{0,0} + (k_{tc12} + k_{td12})\mu_{0,0}]\frac{P_{1,0}}{V_L}
\end{aligned} \tag{A1a.5}$$

For $n \geq 2$, $m = 0$:

$$\begin{aligned}
\frac{dP_{n,0}}{dt} = {} & k_{p11}\frac{M_1 P_{n-1,0}}{V_L} \\
& - [(k_{p11} + k_{f11})M_1 + (k_{p12} + k_{f12})M_2 \\
& + (k_{tc11} + k_{td11})\lambda_{0,0} + (k_{tc12} + k_{td12})\mu_{0,0}]\frac{P_{n,0}}{V_L}
\end{aligned} \tag{A1a.6}$$

For $n = 1$, $m \geq 1$

$$\begin{aligned}
\frac{dP_{1,m}}{dt} = {} & k_{p21}\frac{M_1 Q_{0,m}}{V_L} \\
& - [(k_{p11} + k_{f11})M_1 + (k_{p12} + k_{f12})M_2 \\
& + (k_{tc11} + k_{td11})\lambda_{0,0} + (k_{tc12} + k_{td12})\mu_{0,0}]\frac{P_{1,m}}{V_L}
\end{aligned} \tag{A1a.7}$$

For $n \geq 2$, $m \geq 1$

$$\frac{dP_{n,m}}{dt} = \left(k_{p11}P_{n-1,m} + k_{p21}Q_{n-1,m}\right)\frac{M_1}{V_L}$$
$$- \left[\left(k_{p11} + k_{f11}\right)M_1 + \left(k_{p12} + k_{f12}\right)M_2\right.$$
$$\left. + \left(k_{tc11} + k_{td11}\right)\lambda_{0,0} + \left(k_{tc12} + k_{td12}\right)\mu_{0,0}\right]\frac{P_{n,m}}{V_L} \quad \text{(A1a.8)}$$

$$\frac{dQ_{0,1}}{dt} = k_{I2}\frac{RM_2}{V_L} + \left(k_{f12}\lambda_{0,0} + k_{f22}\mu_{0,0}\right)\frac{M_2}{V_L}$$
$$- \left[\left(k_{p21} + k_{f21}\right)M_1 + \left(k_{p22} + k_{f22}\right)M_2\right.$$
$$\left. + \left(k_{tc12} + k_{td12}\right)\lambda_{0,0} + \left(k_{tc22} + k_{td22}\right)\mu_{0,0}\right]\frac{Q_{0,1}}{V_L} \quad \text{(A1a.9)}$$

For $n = 0$, $m \geq 2$:

$$\frac{dQ_{0,m}}{dt} = k_{p22}\frac{Q_{0,m-1}\,M_2}{V_L}$$
$$- \left[\left(k_{p21} + k_{f21}\right)M_1 + \left(k_{p22} + k_{f22}\right)M_2\right.$$
$$\left. + \left(k_{tc12} + k_{td12}\right)\lambda_{0,0} + \left(k_{tc22} + k_{td22}\right)\mu_{0,0}\right]\frac{Q_{0,m}}{V_L} \quad \text{(A1a.10)}$$

For $n \geq 1$, $m = 1$:

$$\frac{dQ_{n,1}}{dt} = k_{p12}\frac{P_{n,0}\,M_2}{V_L}$$
$$- \left[\left(k_{p21} + k_{f21}\right)M_1 + \left(k_{p22} + k_{f22}\right)M_2\right.$$
$$\left. + \left(k_{tc12} + k_{td12}\right)\lambda_{0,0} + \left(k_{tc22} + k_{td22}\right)\mu_{0,0}\right]\frac{Q_{n,1}}{V_L} \quad \text{(A1a.11)}$$

For $n \geq 1$, $m \geq 2$:

$$\frac{dQ_{n,m}}{dt} = \left(k_{p12}P_{n,m-1} + k_{p22}Q_{n,m-1}\right)\frac{M_2}{V_L}$$
$$- \left[\left(k_{p21} + k_{f21}\right)M_1 + \left(k_{p22} + k_{f22}\right)M_2\right.$$
$$\left. + \left(k_{tc12} + k_{td12}\right)\lambda_{0,0} + \left(k_{tc22} + k_{td22}\right)\mu_{0,0}\right]\frac{Q_{n,m}}{V_L} \quad \text{(A1a.12)}$$

$$\frac{dD_{1,0}}{dt} = \left[\left(k_{f11}M_1 + k_{f12}M_2\right) + \left(k_{td11}\lambda_{0,0} + k_{td12}\mu_{0,0}\right)\right]\frac{P_{1,0}}{V_L} \qquad \text{(A1a.13)}$$

$$\frac{dD_{0,1}}{dt} = \left[\left(k_{f21}M_1 + k_{f22}M_2\right) + \left(k_{td12}\lambda_{0,0} + k_{td22}\mu_{0,0}\right)\right]\frac{Q_{0,1}}{V_L} \qquad \text{(A1a.14)}$$

For $n = 0$, $m \geq 2$:

$$\frac{dD_{0,m}}{dt} = \frac{1}{2}\frac{k_{tc22}}{V_L}\sum_{q=1}^{m-1} Q_{0,q}\, Q_{0,m-q}$$

$$+ \left[\left(k_{f21}M_1 + k_{f22}M_2\right)\right.$$

$$\left. + \left(k_{td12}\lambda_{0,0} + k_{td22}\mu_{0,0}\right)\right]\frac{Q_{0,m}}{V_L} \qquad \text{(A1a.15)}$$

For n $\geq$ 2, m= 0 :

$$\frac{dD_{n,0}}{dt} = \frac{1}{2}\frac{k_{tc11}}{V_L}\sum_{r=1}^{n-1} P_{n-r,0}\, P_{r,0}$$

$$+ \left[\left(k_{f11}M_1 + k_{f12}M_2\right)\right.$$

$$\left. + \left(k_{td11}\lambda_{0,0} + k_{td12}\mu_{0,0}\right)\right]\frac{P_{n,0}}{V_L} \qquad \text{(A1a.16)}$$

For n = 1, $m \geq 2$:

$$\frac{dD_{1,m}}{dt} = \frac{k_{tc12}}{V_L}\sum_{q=1}^{m} P_{1,m-q}\, Q_{0,q} + \frac{k_{tc22}}{V_L}\sum_{q=1}^{m-1} Q_{1,m-q}\, Q_{0,q}$$

$$+ \left[\left(k_{f11}M_1 + k_{f12}M_2\right) + \left(k_{td11}\lambda_{0,0} + k_{td12}\mu_{0,0}\right)\right]\frac{P_{1,m}}{V_L}$$

$$+ \left[\left(k_{f21}M_1 + k_{f22}M_2\right)\right.$$

$$\left. + \left(k_{td12}\lambda_{0,0} + k_{td22}\mu_{0,0}\right)\right]\frac{Q_{1,m}}{V_L} \qquad \text{(A1a.17)}$$

$$\frac{dD_{1,1}}{dt} = \frac{k_{tc12}}{V_L}P_{1,0}Q_{0,1}$$

$$+ \left[\left(k_{f11}M_1 + k_{f12}M_2\right) + \left(k_{td11}\lambda_{0,0} + k_{td12}\mu_{0,0}\right)\right]\frac{P_{1,1}}{V_L} \qquad \text{(A1a.18)}$$

$$+ \left[\left(k_{f21}M_1 + k_{f22}M_2\right) + \left(k_{td12}\lambda_{0,0} + k_{td22}\mu_{0,0}\right)\right]\frac{Q_{1,1}}{V_L}$$

For n ≥ 2, $m = 1$:

$$\frac{dD_{n,1}}{dt} = \frac{k_{tc12}}{V_L}\sum_{r=1}^{n} P_{r,0}\, Q_{n-r,1} + \frac{k_{tc11}}{V_L}\sum_{r=1}^{n-1} P_{r,0}\, P_{n-r,1}$$

$$+ \left[(k_{f11}M_1 + k_{f12}M_2) + (k_{td11}\lambda_{0,0} + k_{td12}\mu_{0,0})\right]\frac{P_{n,1}}{V_L}$$

$$+ \left[(k_{f21}M_1 + k_{f22}M_2) + (k_{td12}\lambda_{0,0} + k_{td22}\mu_{0,0})\right]\frac{Q_{n,1}}{V_L}$$

(A1a.19)

For n ≥ 2, $m \geq 2$:

$$\frac{dD_{n,m}}{dt} = \frac{1}{2}\frac{k_{tc11}}{V_L}\sum_{r=1}^{n-1}\sum_{q=0}^{m} P_{r,q}\, P_{n-r,m-q} + \frac{1}{2}\frac{k_{tc22}}{V_L}\sum_{r=0}^{n}\sum_{q=1}^{m-1} Q_{r,q}\, Q_{n-r,m-q}$$

$$+ \frac{k_{tc12}}{V_L}\sum_{r=0}^{n-1}\sum_{q=1}^{m} P_{n-r,m-q}\, Q_{r,q}$$

(A1a.20)

$$+ \left[(k_{f11}M_1 + k_{f12}M_2) + (k_{td11}\lambda_{0,0} + k_{td12}\mu_{0,0})\right]\frac{P_{n,m}}{V_L}$$

$$+ \left[(k_{f21}M_1 + k_{f22}M_2)\right.$$

$$\left. + (k_{td12}\lambda_{0,0} + k_{td22}\mu_{0,0})\right]\frac{Q_{n,m}}{V_L}$$

Appendix A-1b   Moment   (and   Associated)   Equations   for   SAN
Copolymerizations

$$\frac{d\lambda_{0,0}}{dt} = k_{I1}\frac{RM_1}{V_L} + \{(k_{p11} + k_{f11})\lambda_{0,0} + (k_{p21} + k_{f21})\mu_{0,0}\}\frac{M_1}{V_L}$$
$$- \{(k_{p11} + k_{f11})M_1 + (k_{p12} + k_{f12})M_2 \qquad \text{(A1b.1)}$$
$$+ (k_{td11} + k_{tc11})\lambda_{0,0} + (k_{td12} + k_{tc12})\mu_{0,0}\}\frac{\lambda_{0,0}}{V_L}$$

$$\frac{d\lambda_{1,0}}{dt} = k_{I1}\frac{RM_1}{V_L}$$
$$+ (k_{f11}\lambda_{0,0} + k_{f21}\mu_{0,0})\frac{M_1}{V_L} + k_{p11}(\lambda_{0,0}$$
$$+ \lambda_{1,0})\frac{M_1}{V_L} + k_{p21}(\mu_{0,0} + \mu_{1,0})\frac{M_1}{V_L} \qquad \text{(A1b.2)}$$
$$- \{(k_{p11} + k_{f11})M_1 + (k_{p12} + k_{f12})M_2$$
$$+ (k_{td11} + k_{tc11})\lambda_{0,0} + (k_{td12} + k_{tc12})\mu_{0,0}\}\frac{\lambda_{1,0}}{V_L}$$

$$\frac{d\lambda_{0,1}}{dt} = (k_{p11}\lambda_{0,1} + k_{p21}\mu_{0,1})\frac{M_1}{V_L}$$
$$- \{(k_{p11} + k_{f11})M_1 + (k_{p12} + k_{f12})M_2 \qquad \text{(A1b.3)}$$
$$+ (k_{td11} + k_{tc11})\lambda_{0,0} + (k_{td12} + k_{tc12})\mu_{0,0}\}\frac{\lambda_{0,1}}{V_L}$$

$$\frac{d\lambda_{1,1}}{dt} = k_{p11}(\lambda_{0,1} + \lambda_{1,1})\frac{M_1}{V_L} + k_{p21}(\mu_{0,1} + \mu_{1,1})\frac{M_1}{V_L}$$
$$- \{(k_{p11} + k_{f11})M_1 + (k_{p12} + k_{f12})M_2 \qquad \text{(A1b.4)}$$
$$+ (k_{td11} + k_{tc11})\lambda_{0,0} + (k_{td12} + k_{tc12})\mu_{0,0}\}\frac{\lambda_{1,1}}{V_L}$$

$$\frac{d\lambda_{2,0}}{dt} = k_{I1}\frac{M_1}{V_L}$$
$$- \{(k_{p11} + k_{f11})M_1 + (k_{p12} + k_{f12})M_2 \qquad \text{(A1b.5)}$$
$$+ (k_{td11} + k_{tc11})\lambda_{0,0} + (k_{td12} + k_{tc12})\mu_{0,0}\}\frac{\lambda_{2,0}}{V_L}$$

$$\frac{d\lambda_{0,2}}{dt} = k_{p11}\frac{\lambda_{0,2}M_1}{V_L} + k_{p21}\frac{\mu_{0,2}M_1}{V_L}$$
$$- \{(k_{p11} + k_{f11})M_1 + (k_{p12} + k_{f12})M_2 \qquad\qquad \text{(A1b.6)}$$
$$+ (k_{td11} + k_{tc11})\lambda_{0,0} + (k_{td12} + k_{tc12})\mu_{0,0}\}\frac{\lambda_{1,1}}{V_L}$$

$$\frac{d\mu_{0,0}}{dt} = k_{I2}\frac{RM_2}{V_L} + \{(k_{f12} + k_{p12})\lambda_{0,0} + (k_{f22} + k_{p22})\mu_{0,0}\}\frac{M_2}{V_L}$$
$$- \{(k_{p21} + k_{f21})M_1 + (k_{p22} + k_{f22})M_2 \qquad\qquad \text{(A1b.7)}$$
$$+ (k_{td12} + k_{tc12})\lambda_{0,0} + (k_{td22} + k_{tc22})\mu_{0,0}\}\frac{\mu_{0,0}}{V_L}$$

$$\frac{d\mu_{1,0}}{dt} = (k_{p12}\lambda_{1,0} + k_{p22}\mu_{1,0})\frac{M_2}{V_L}$$
$$- \{(k_{p21} + k_{f21})M_1 + (k_{p22} + k_{f22})M_2 \qquad\qquad \text{(A1b.8)}$$
$$+ (k_{td12} + k_{tc12})\lambda_{0,0} + (k_{td22} + k_{tc22})\mu_{0,0}\}\frac{\mu_{1,0}}{V_L}$$

$$\frac{d\mu_{0,1}}{dt} = k_{I2}\frac{RM_2}{V_L} + (k_{f12}\lambda_{0,0} + k_{f22}\mu_{0,0})\frac{M_2}{V_L}$$
$$+ k_{p12}(\lambda_{0,0} + \lambda_{0,1})\frac{M_2}{V_L} + k_{p22}(\mu_{0,0} + \mu_{0,1})\frac{M_2}{V_L} \qquad \text{(A1b.9)}$$
$$- \{(k_{p21} + k_{f21})M_1 + (k_{p22} + k_{f22})M_2$$
$$+ (k_{td12} + k_{tc12})\lambda_{0,0} + (k_{td22} + k_{tc22})\mu_{0,0}\}\frac{\mu_{0,1}}{V_L}$$

$$\frac{d\mu_{1,1}}{dt} = k_{p12}(\lambda_{1,0} + \lambda_{1,1})\frac{M_2}{V_L} + k_{p22}(\mu_{1,0} + \mu_{1,1})\frac{M_2}{V_L}$$
$$- \{(k_{p21} + k_{f21})M_1 + (k_{p22} + k_{f22})M_2 \qquad\qquad \text{(A1b.10)}$$
$$+ (k_{td12} + k_{tc12})\lambda_{0,0} + (k_{td22} + k_{tc22})\mu_{0,0}\}\frac{\mu_{1,1}}{V_L}$$

$$\frac{d\mu_{2,0}}{dt} = k_{p12}\frac{\lambda_{2,0}M_2}{V_L} + k_{p22}\frac{\mu_{2,0}M_2}{V_L}$$
$$- \{(k_{p21} + k_{f21})M_1 + (k_{p22} + k_{f22})M_2 \qquad\qquad \text{(A1b.11)}$$
$$+ (k_{td12} + k_{tc12})\lambda_{0,0} + (k_{td22} + k_{tc22})\mu_{0,0}\}\frac{\mu_{1,1}}{V_L}$$

$$\frac{d\mu_{0,2}}{dt} = k_{I2}\frac{RM_2}{V_L} + \left(k_{f12}\lambda_{0,0} + k_{f22}\mu_{0,0}\right)\frac{M_2}{V_L}$$

$$+ k_{p12}\left(\lambda_{0,0} + 2\lambda_{0,1} + \lambda_{0,2}\right)\frac{M_2}{V_L}$$

$$+ k_{p22}\left(\mu_{0,0} + 2\mu_{0,1} + \mu_{0,2}\right)\frac{M_2}{V_L} \qquad \text{(A1b.12)}$$

$$- \{\left(k_{p21} + k_{f21}\right)M_1 + \left(k_{p22} + k_{f22}\right)M_2$$

$$+ \left(k_{td12} + k_{tc12}\right)\lambda_{0,0} + \left(k_{td22} + k_{tc22}\right)\mu_{0,0}\}\frac{\mu_{0,1}}{V_L}$$

$$\frac{d\tau_{0,0}}{dt} = \left(k_{td11}\lambda_{0,0} + k_{td12}\mu_{0,0} + k_{f11}M_1 + k_{f12}M_2\right)\frac{\lambda_{0,0}}{V_L}$$

$$+ \left(k_{td12}\lambda_{0,0} + k_{td22}\mu_{0,0} + k_{f21}M_1 + k_{f22}M_2\right)\frac{\mu_{0,0}}{V_L} \qquad \text{(A1b.13)}$$

$$+ \frac{1}{2}k_{tc11}\frac{\lambda_{0,0}^2}{V_L} + \frac{1}{2}k_{tc22}\frac{\mu_{0,0}^2}{V_L} + k_{tc12}\frac{\lambda_{0,0}\mu_{0,0}}{V_L}$$

$$\frac{d\tau_{1,0}}{dt} = \left(k_{td11}\lambda_{0,0} + k_{td12}\mu_{0,0} + k_{f11}M_1 + k_{f12}M_2\right)\frac{\lambda_{1,0}}{V_L}$$

$$+ \left(k_{td12}\lambda_{0,0} + k_{td22}\mu_{0,0} + k_{f21}M_1 + k_{f22}M_2\right)\frac{\mu_{1,0}}{V_L}$$

$$+ k_{tc11}\frac{\lambda_{0,0}\,\lambda_{1,0}}{V_L} + k_{tc22}\frac{\mu_{0,0}\,\mu_{1,0}}{V_L} \qquad \text{(A1b.14)}$$

$$+ \frac{k_{tc12}}{V_L}\left(\lambda_{1,0}\mu_{0,0} + \lambda_{0,0}\mu_{1,0}\right)$$

$$\frac{d\tau_{0,1}}{dt} = \left(k_{td11}\lambda_{0,0} + k_{td12}\mu_{0,0} + k_{f11}M_1 + k_{f12}M_2\right)\frac{\lambda_{0,1}}{V_L}$$

$$+ \left(k_{td12}\lambda_{0,0} + k_{td22}\mu_{0,0} + k_{f21}M_1 + k_{f22}M_2\right)\frac{\mu_{0,1}}{V_L}$$

$$+ k_{tc11}\frac{\lambda_{0,0}\,\lambda_{1,0}}{V_L} + k_{tc22}\frac{\mu_{0,0}\,\mu_{1,0}}{V_L} \qquad \text{(A1b.15)}$$

$$+ \frac{k_{tc12}}{V_L}\left(\lambda_{1,0}\mu_{0,0} + \lambda_{0,0}\mu_{1,0}\right)$$

$$\frac{d\tau_{1,1}}{dt} = \left(k_{td11}\lambda_{0,0} + k_{td12}\mu_{0,0} + k_{f11}M_1 + k_{f12}M_2 \right)\frac{\lambda_{1,1}}{V_L}$$

$$+ \left(k_{td12}\lambda_{0,0} + k_{td22}\mu_{0,0} + k_{f21}M_1 + k_{f22}M_2 \right)\frac{\mu_{1,1}}{V_L}$$

$$+ \frac{k_{tc11}}{V_L}\left(\lambda_{0,0}\,\lambda_{1,1} + \lambda_{0,1}\,\lambda_{1,0} \right) \tag{A1b.16}$$

$$+ \frac{k_{tc22}}{V_L}\left(\mu_{0,0}\,\mu_{1,1} + \mu_{0,1}\,\mu_{1,0} \right)$$

$$+ \frac{k_{tc12}}{V_L}\left(\lambda_{1,0}\mu_{0,1} + \lambda_{0,0}\mu_{1,1} + \lambda_{1,1}\mu_{0,0} + \lambda_{0,1}\mu_{1,0} \right)$$

$$\frac{d\tau_{2,0}}{dt} = \left(k_{td11}\lambda_{0,0} + k_{td12}\mu_{0,0} + k_{f11}M_1 + k_{f12}M_2 \right)\frac{\lambda_{2,0}}{V_L}$$

$$+ \left(k_{td12}\lambda_{0,0} + k_{td22}\mu_{0,0} + k_{f21}M_1 + k_{f22}M_2 \right)\frac{\mu_{2,0}}{V_L}$$

$$+ \frac{k_{tc11}}{V_L}\left(\lambda_{1,0}^2 + \lambda_{0,0}\,\lambda_{2,0} \right) + \frac{k_{tc22}}{V_L}\left(\mu_{1,0}^2 + \mu_{0,0}\,\mu_{2,0} \right) \tag{A1b.17}$$

$$+ \frac{k_{tc12}}{V_L}\left(\lambda_{2,0}\mu_{0,0} + 2\,\lambda_{1,0}\mu_{1,0} + \lambda_{0,0}\mu_{2,0} \right)$$

$$\frac{d\tau_{0,2}}{dt} = \left(k_{td11}\lambda_{0,0} + k_{td12}\mu_{0,0} + k_{f11}M_1 + k_{f12}M_2 \right)\frac{\lambda_{0,2}}{V_L}$$

$$+ \left(k_{td12}\lambda_{0,0} + k_{td22}\mu_{0,0} + k_{f21}M_1 + k_{f22}M_2 \right)\frac{\mu_{0,2}}{V_L}$$

$$+ \frac{k_{tc11}}{V_L}\left(\lambda_{0,1}^2 + \lambda_{0,0}\,\lambda_{0,2} \right) + \frac{k_{tc22}}{V_L}\left(\mu_{0,1}^2 + \mu_{0,0}\,\mu_{0,2} \right) \tag{A1b.18}$$

$$+ \frac{k_{tc12}}{V_L}\left(\lambda_{0,2}\mu_{0,0} + 2\,\lambda_{0,1}\mu_{0,1} + \lambda_{0,0}\mu_{0,2} \right)$$

$$V_L = \frac{M_1(MW)_{m1}}{\rho_{m1}} + \frac{M_2(MW)_{m2}}{\rho_{m2}} + \frac{(M_{1,0} - M_1)(MW)_{m1}}{\rho_{p1}}$$

$$+ \frac{(M_{2,0} - M_2)(MW)_{m2}}{\rho_{p2}} \tag{A1b.19}$$

$$\rho_p = \frac{(M_{1,0} - M_1)(MW)_{m1} + (M_{2,0} - M_2)(MW)_{m2}}{\dfrac{(M_{1,0} - M_1)(MW)_{m1}}{\rho_{p1}} + \dfrac{(M_{2,0} - M_2)(MW)_{m2}}{\rho_{p2}}} \tag{A1b.20}$$

$$\phi_{m1} = \frac{M_1(MW)_{m1}/\rho_{m1}}{V_L} \tag{A1b.21}$$

$$\phi_{m2} = \frac{M_2(MW)_{m2}/\rho_{m2}}{V_L} \tag{A1b.22}$$

$$\phi_p = 1 - \phi_{m1} - \phi_{m2} \tag{A1b.23}$$

* * *

APPENDIX A-2. Gel, Glass and Cage Effect and Other Associated Equations for SAN Copolymerization

$$\frac{1}{k_{tc11}} = \frac{1}{k_{tc11,0}} + \theta_{tc11}(T, I_o, f_{10})\bar{M}_w^2 \frac{\lambda_{0,0}^2}{V_L(\lambda_{0,0} + \mu_{0,0})} \frac{1}{exp(-\Psi + \Psi_{ref})} \qquad (A2.1)$$

$$\frac{1}{k_{tc22}} = \frac{1}{k_{tc22,0}} + \theta_{tc11}(T, I_o, f_{10})\bar{M}_w^2 \frac{\mu_{0,0}^2}{V_L(\lambda_{0,0} + \mu_{0,0})} \frac{1}{exp(-\Psi + \Psi_{ref})} \qquad (A2.2)$$

$$k_{tc12} = \phi_t \left[2(k_{tc11} \, k_{tc22})^{1/2}\right] \qquad (A2.3)$$

$$k_{td11} = k_{td12} = k_{td21} = k_{td22} = 0 \qquad (A2.4)$$

$$\frac{1}{k_{p11}} = \frac{1}{k_{p11,0}} + \theta_{p11}(T) \frac{\lambda_{0,0}}{V_L} \frac{1}{exp[\xi_{m1p}(-\Psi' + \Psi'_{ref})]} \qquad (A2.5)$$

$$\frac{1}{k_{p22}} = \frac{1}{k_{22,0}} + \theta_{p22}(T) \frac{\mu_{0,0}}{V_L} \frac{1}{exp[\xi_{m2p}(-\Psi' + \Psi'_{ref})]} \qquad (A2.6)$$

$$k_{p12} = \frac{k_{p11}}{r_1} \qquad (A2.7)$$

$$k_{p21} = \frac{k_{p22}}{r_2} \qquad (A2.8)$$

$$\frac{1}{f} = \frac{1}{f_0}\left(1 + \theta_f(T) \frac{(k_{I1,0}M_1 + k_{I2,0}M_2)}{V_L} \frac{1}{exp[\xi_{Ip}(-\Psi'' + \Psi''_{ref})]}\right) \qquad (A2.9)$$

$$\Psi = \frac{\gamma_p \left\{\frac{\rho_{m1} \phi_{m1}\hat{V}_{m1}^*}{\xi_{m1p}} + \frac{\rho_{m2}\phi_{m2}\hat{V}_{m2}^*}{\xi_{m2p}} + \rho_p\phi_p\hat{V}_p^*\right\}}{\rho_{m1} \phi_{m1}\hat{V}_{m1}^*V_{fm1} + \rho_{m2}\phi_{m2}\hat{V}_{m2}^*V_{fm2} + \rho_p\phi_p\hat{V}_p^*V_{fp}} \qquad (A2.10)$$

$$\Psi_{ref} = \frac{\gamma_p}{V_{fp}} \qquad (A2.11)$$

$$\Psi' = \frac{\gamma_m \left\{\frac{\rho_{m1} \phi_{m1}\hat{V}_{m1}^*}{\xi_{m1p}} + \frac{\rho_{m2}\phi_{m2}\hat{V}_{m2}^*}{\xi_{m2p}} + \rho_p\phi_p\hat{V}_p^*\right\}}{\rho_{m1} \phi_{m1}\hat{V}_{m1}^*V_{fm1} + \rho_{m2}\phi_{m2}\hat{V}_{m2}^*V_{fm2} + \rho_p\phi_p\hat{V}_p^*V_{fp}} \qquad (A2.12)$$

$$\Psi'_{ref} = \frac{\gamma_m}{V_{fp}} \qquad (A2.13)$$

$$\Psi'' = \frac{\gamma_I \left\{\frac{\rho_{m1} \phi_{m1}\hat{V}_{m1}^*}{\xi_{m1p}} + \frac{\rho_{m2}\phi_{m2}\hat{V}_{m2}^*}{\xi_{m2p}} + \rho_p\phi_p\hat{V}_p^*\right\}}{\rho_{m1} \phi_{m1}\hat{V}_{m1}^*V_{fm1} + \rho_{m2}\phi_{m2}\hat{V}_{m2}^*V_{fm2} + \rho_p\phi_p\hat{V}_p^*V_{fp}} \qquad (A2.14)$$

$$\Psi''_{ref} = \frac{\gamma_I}{V_{fp}} \qquad (A2.15)$$

$$\xi_{m1p} = \frac{\hat{V}^*_{m1}\,(MW)_{m1}}{\hat{V}^*_p\,M_{jp}} \qquad (A2.16)$$

$$\xi_{m2p} = \frac{\hat{V}^*_{m2}\,(MW)_{m2}}{\hat{V}^*_p\,M_{jp}} \qquad (A2.17)$$

$$\xi_{Ip} = \frac{\hat{V}^*_I\,(MW)_I}{\hat{V}^*_p\,M_{jp}} \qquad (A2.18)$$

$$\frac{k_{f11}}{k_{f11,0}} = \frac{k_{p11}}{k_{p11,0}} \qquad (A2.19)$$

$$\frac{k_{f12}}{k_{f12,0}} = \frac{k_{p12}}{k_{p12,0}} \qquad (A2.20)$$

$$\frac{k_{f21}}{k_{f21,0}} = \frac{k_{p21}}{k_{p21,0}} \qquad (A2.21)$$

$$\frac{k_{f22}}{k_{f22,0}} = \frac{k_{p22}}{k_{p22,0}} \qquad (A2.22)$$

$$k_d = k_d^0\,exp\left[-E_d/R_gT\right] \qquad (A2.23)$$

$$k_{p11,0} = k_{p11,0}^0\,exp\left[-E_{p11}/R_gT\right] \qquad (A2.24)$$

$$k_{p22,0} = k_{p22,0}^0\,exp\left[-E_{p22}/R_gT\right] \qquad (A2.25)$$

$$k_{tc11,0} = k_{tc11,0}^0\,exp\left[-E_{tc11}/R_gT\right] \qquad (A2.26)$$

$$k_{tc22,0} = k_{tc22,0}^0\,exp\left[-E_{tc22}/R_gT\right] \qquad (A2.27)$$

$$k_{f11,0} = k_{f11,0}^0\,exp\left[-E_{f11}/R_gT\right] \qquad (A2.28)$$

$$k_{f21,0} = k_{f21,0}^0\,exp\left[-E_{f21}/R_gT\right] \qquad (A2.29)$$

$$k_{f12,0} = k_{f12,0}^0\,exp\left[-E_{f12}/R_gT\right] \qquad (A2.30)$$

$$k_{f22,0} = k_{f22,0}^0\,exp\left[-E_{f22}/R_gT\right] \qquad (A2.31)$$

$$k_{p12,0} = k_{p11,0}^0/r_1 \qquad (A2.32)$$

$$k_{p21,0} = k_{p22,0}^0/r_2 \tag{A2.33}$$

$$k_{tc12,0} = 2\,\phi_t \sqrt{k_{tc11,0}^0\,k_{tc22,0}^0} \tag{A2.34}$$

$$\phi_t = 16\,\frac{\{0.625\,(1 - f_{10}) + r_1 f_{10}\}}{(1 - f_{10}) + r_1 f_{10}} \tag{A2.35}$$

$$k_{I1,0} = k_{p11,0} \tag{A2.36}$$

$$k_{I2,0} = k_{p22,0} \tag{A2.37}$$

$$\hat{V}_p^* = \frac{(\zeta_{m1} - M_1)(MW)_{m1}\hat{V}_{p1}^* + (\zeta_{m2} - M_2)(MW)_{m2}\hat{V}_{p2}^*}{(\zeta_{m1} - M_1)(MW)_{m1} + (\zeta_{m2} - M_2)(MW)_{m2}} \tag{A2.38}$$

$$T_{gp} = (1 - (AN)_m)T_{gp1} + (AN)_m T_{gp2} + \frac{R^*}{100}(T_{gp12} + \bar{T}_{gp}) \tag{A2.39}$$

$$\bar{T}_{gp} = \left(T_{gp1} + T_{gp2}\right)/2 \tag{A2.40}$$

$$R^* = \frac{400\,(AN)_m\,(1 - (AN)_m)}{[1 + \{1 + 4\,(AN)_m(1 - (AN)_m)(r_1 r_2 - 1)\}^{1/2}]} \tag{A2.41}$$

$$(AN)_m = 1 - St_c \tag{A2.42}$$

* * *

APPENDIX A-3. Experimental Results and Model Predictions for Copolymerization of SAN using IOPs
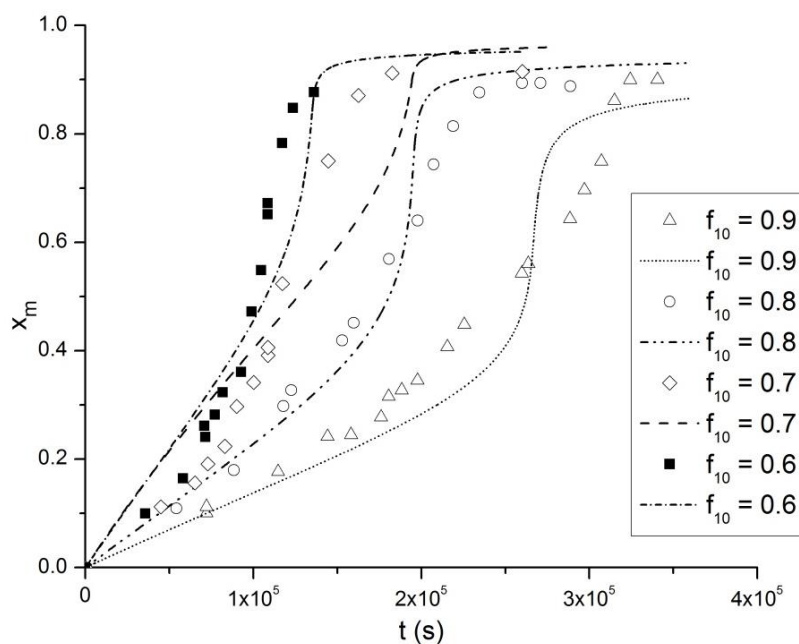
Figure A-3 (a). Conversion histories for SAN copolymerization at 40 ºC with 10 mM AIBN for different initial mole fractions of styrene (f_{10})
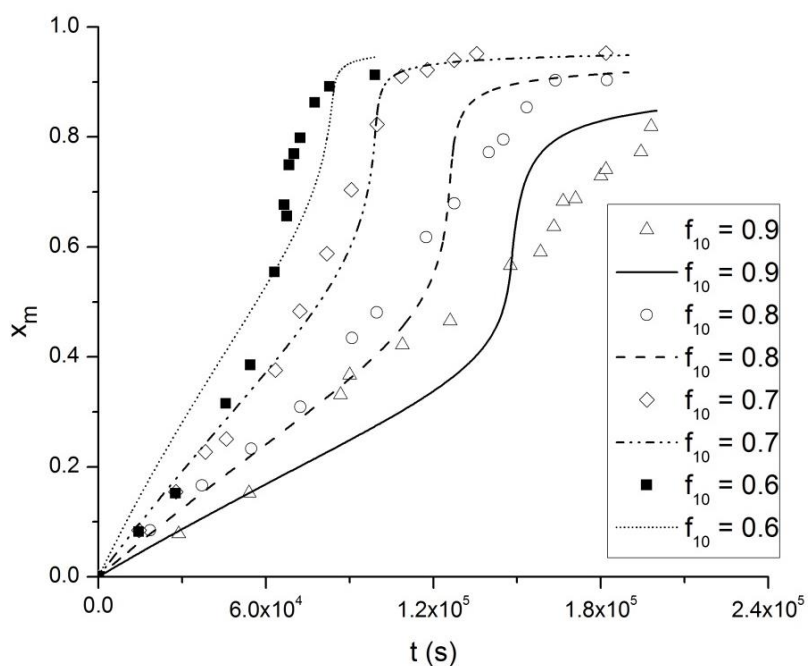
Figure A-3 (b). Conversion histories for SAN copolymerization at 40 ºC with 50 mM AIBN for different initial mole fractions of styrene (f_{10})
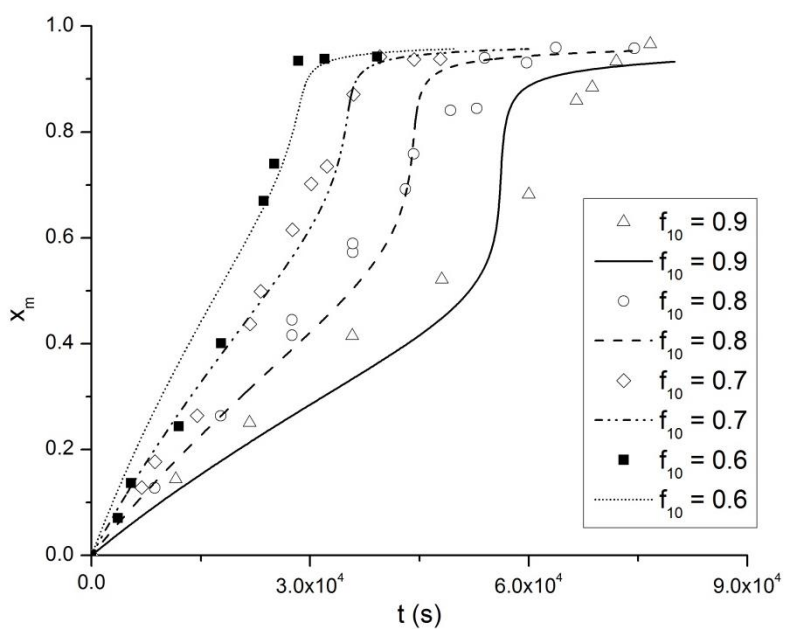
Figure A-3 (c). Conversion histories for SAN copolymerization at 60 ºC with 10 mM AIBN for different initial mole fractions of styrene (f_{10})

Figure A-3 (d). Conversion histories for SAN copolymerization at 60 ºC with 50 mM AIBN for different initial mole fractions of styrene (f_{10})
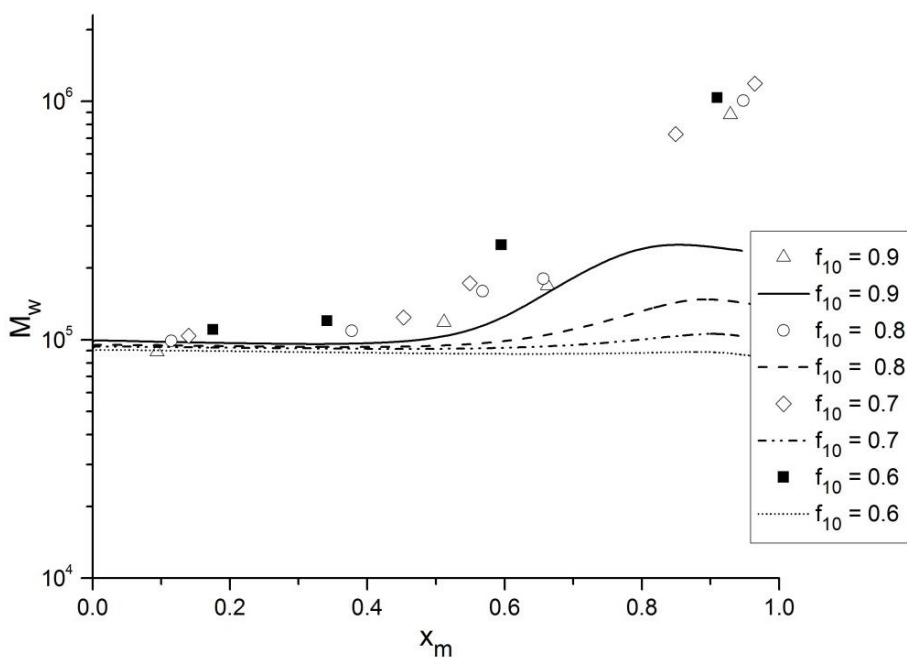
Figure A-3 (e). Number average molecular weight (M_n) as a function of the overall monomer conversion (x_m) for SAN copolymerization at 40 °C with 10 mM AIBN for different initial mole fractions of styrene (f_{10}). Data for two other values of f_{10} are not available.
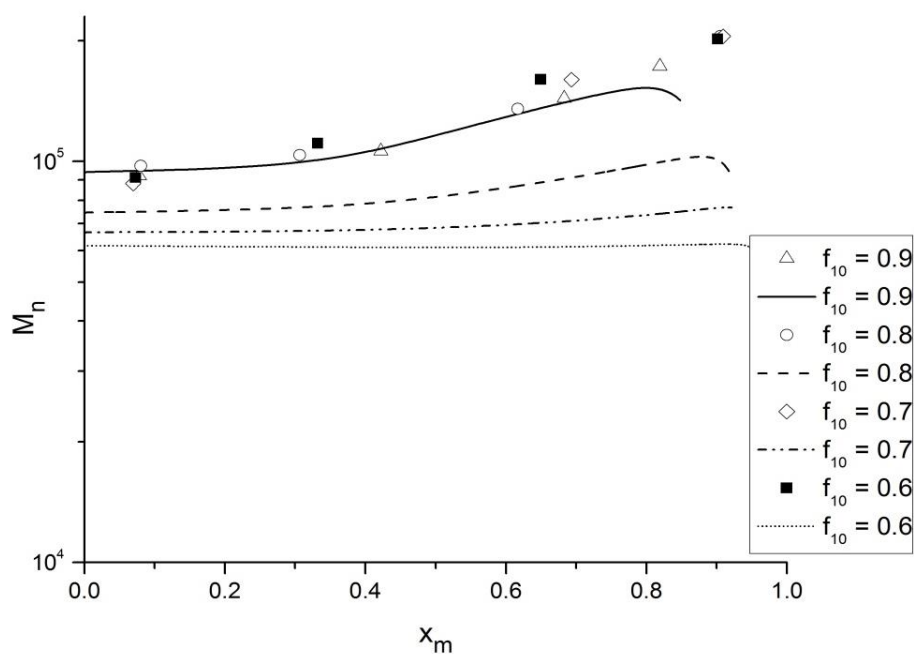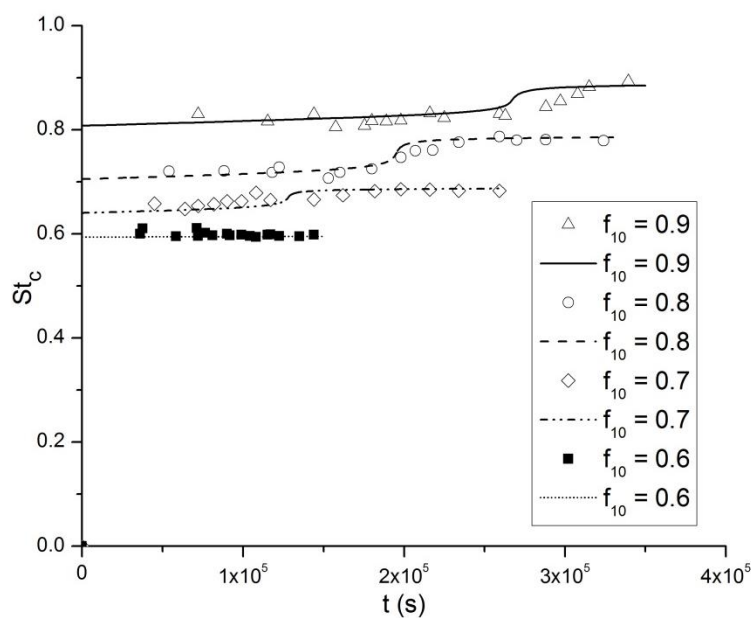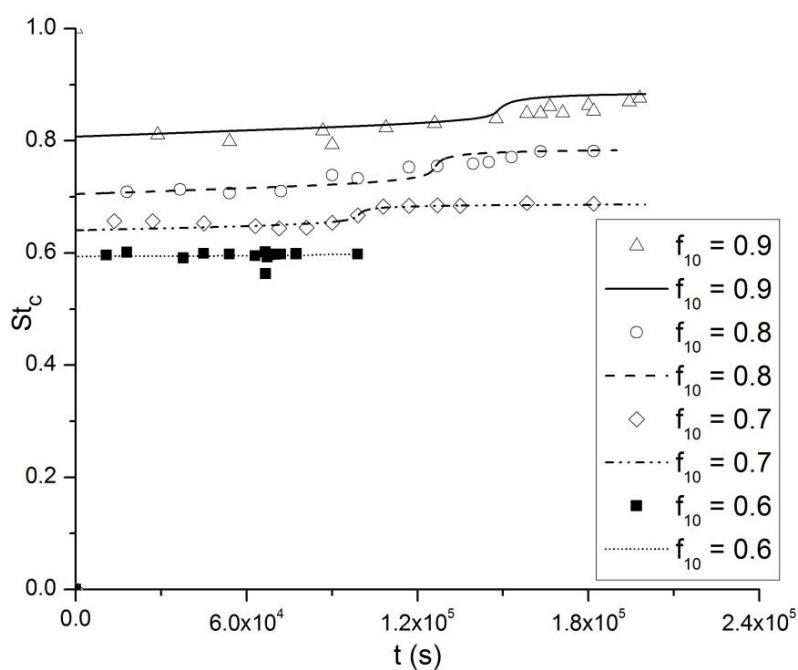

Figure A-3 (f). Number average molecular weight (M_n) as a function of the overall monomer conversion (x_m) for SAN copolymerization at 40 °C with 50 mM AIBN for different initial mole fractions of styrene (f_{10}).
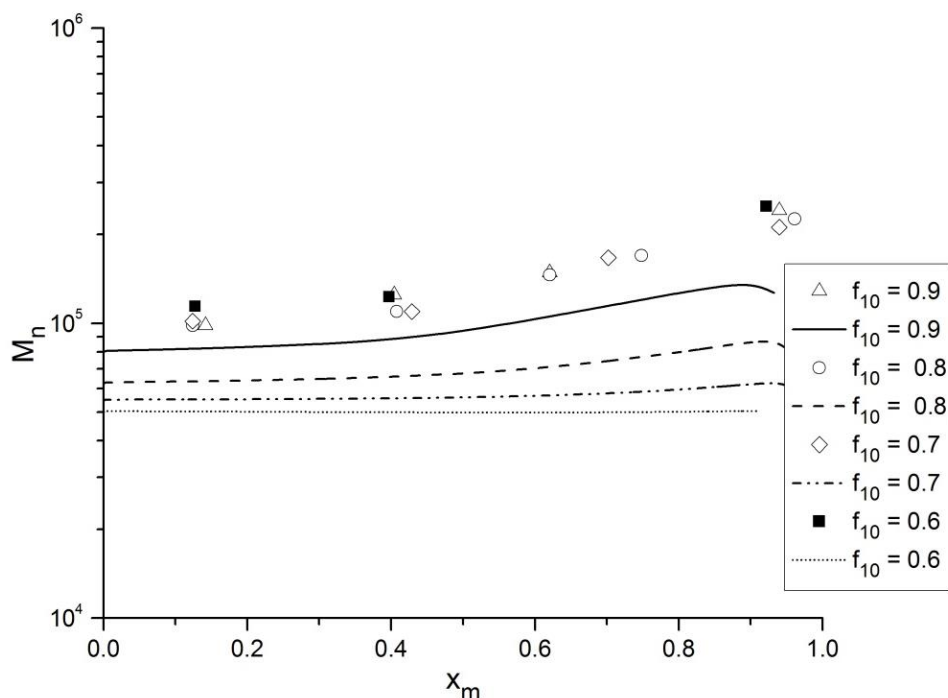
**Figure A-3 (g).** Number average molecular weight (M_n) as a function of the overall monomer conversion (x_m) for SAN copolymerization at 60 ºC with 10 mM AIBN for different initial mole fractions of styrene (f_{10}).

Figure A-3 (h). Number average molecular weight (M_n) as a function of the overall monomer conversion (x_m) for SAN copolymerization at 60 ºC with 50 mM AIBN for different initial mole fractions of styrene (f_{10}).

Figure A-3 (i). Weight average molecular weight (M_w) as a function of the overall monomer conversion (x_m) for SAN copolymerization at 40 ℃ with 10 mM AIBN for different initial mole fractions of styrene (f_{10}). Data for two other values of f_{10} are not available.
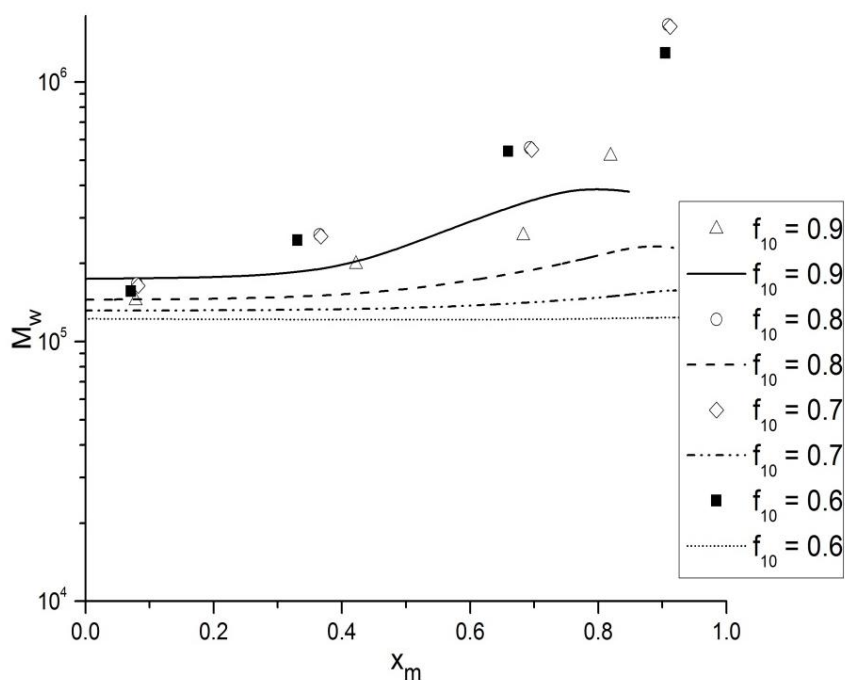
Figure A-3 (j). Weight average molecular weight (M_w) as a function of the overall monomer conversion (x_m) for SAN copolymerization at 40 ℃ with 50 mM AIBN for different initial mole fractions of styrene (f_{10}).
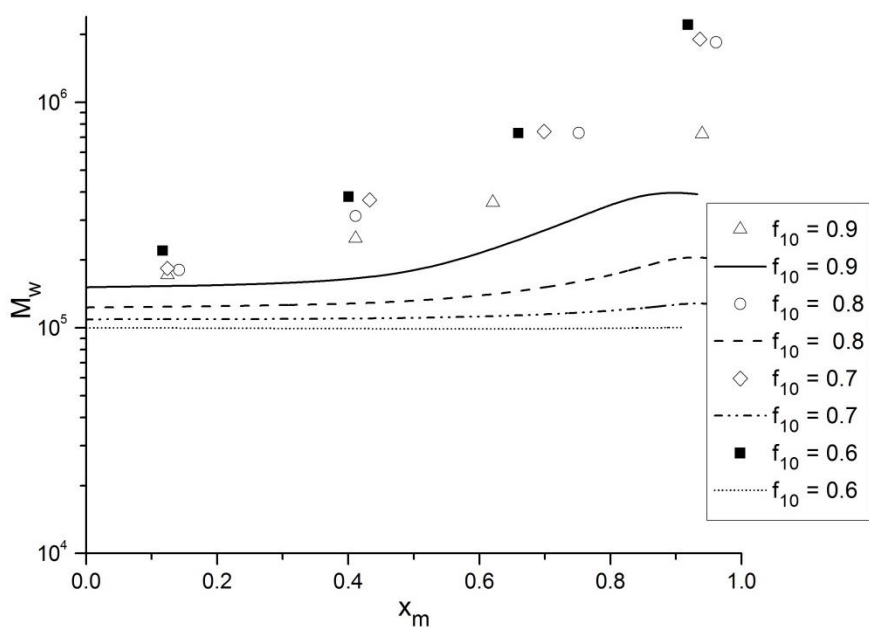
Figure A-3 (k). Weight average molecular weight (M_w) as a function of the overall monomer conversion (x_m) for SAN copolymerization at 60 °C with 10 mM AIBN for different initial mole fractions of styrene (f_{10}).

Figure A-3 (l). Weight average molecular weight (M_w) as a function of the overall monomer conversion (x_m) for SAN copolymerization at 60 °C with 50 mM AIBN for different initial mole fractions of styrene (f_{10}).

Figure A-3 (m). Mole fraction of styrene in the copolymer formed as a function of time for SAN copolymerization at 40 ºC with 10 mM AIBN, for different initial mole fractions of styrene (f_{10})
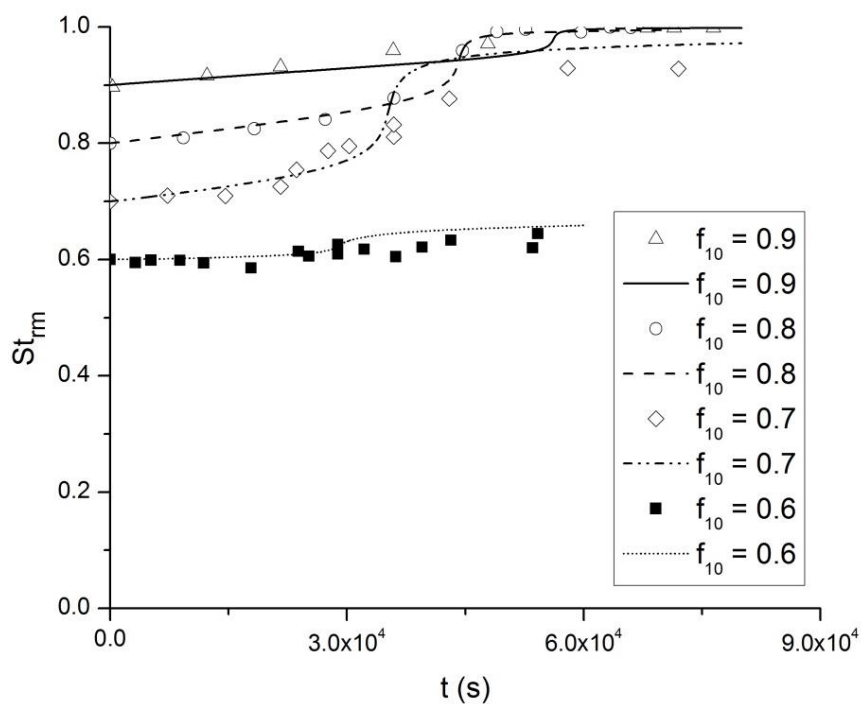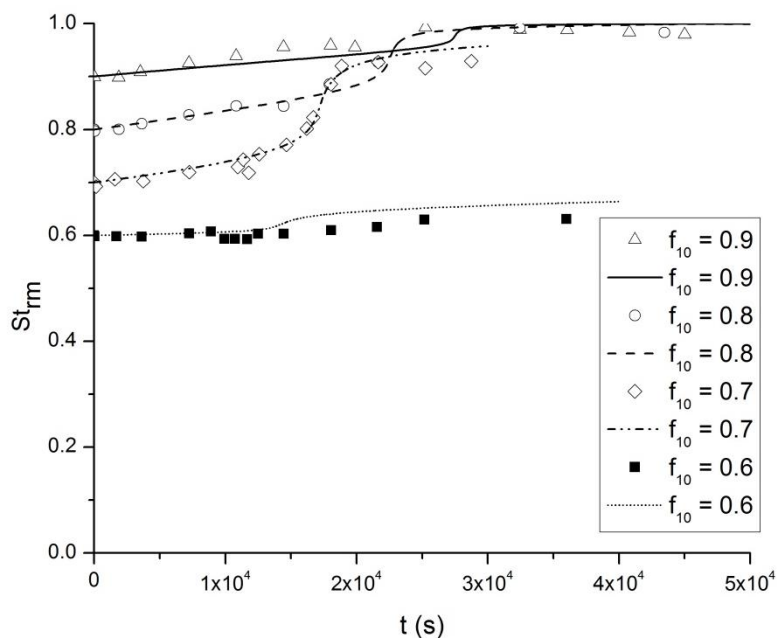

Figure A-3 (n). Mole fraction of styrene in the copolymer formed as a function of time for SAN copolymerization at 40 ºC with 50 mM AIBN, for different initial mole fractions of styrene (f_{10})
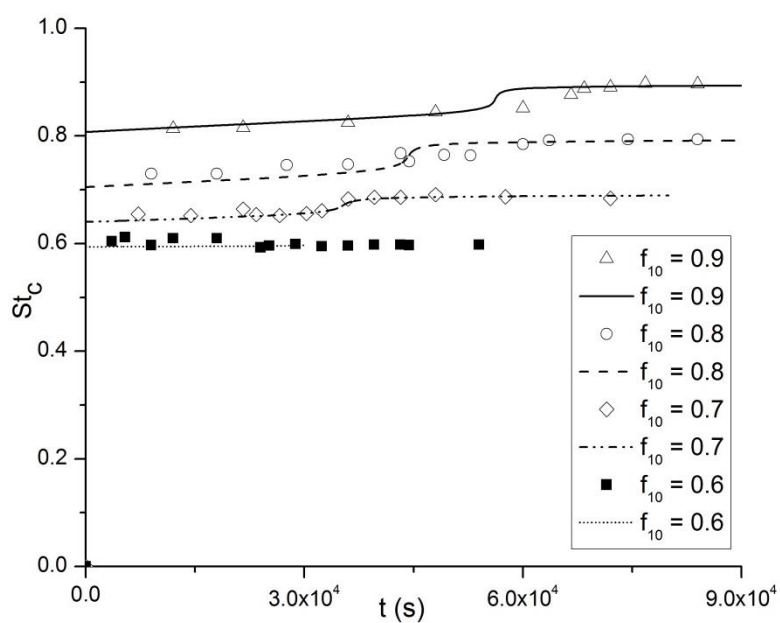
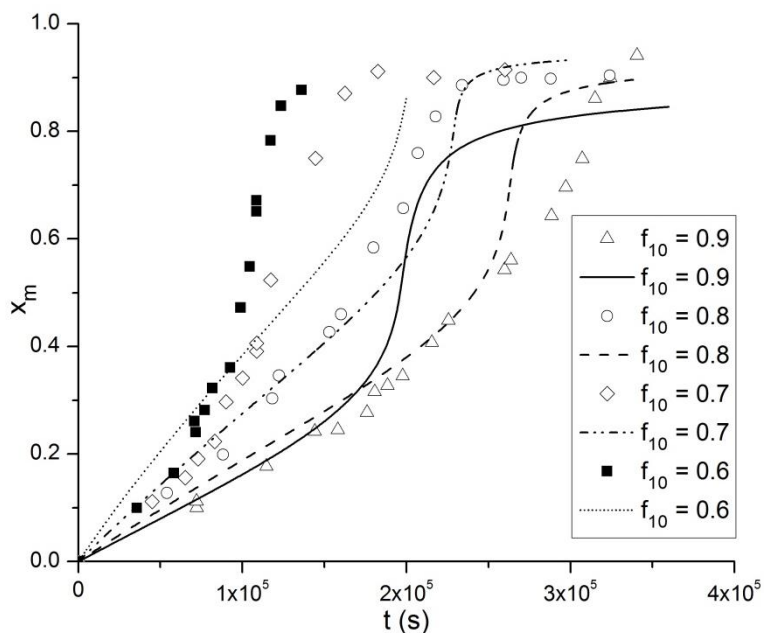**Figure A-3 (o).** Mole fraction of styrene in the copolymer formed as a function of time for SAN copolymerization at 60 ℃ with 10 mM AIBN, for different initial mole fractions of styrene (f_{10})

Figure A-3 (p). Mole fraction of styrene in the copolymer formed as a function of time for SAN copolymerization at 60 ℃ with 50 mM AIBN, for different initial mole fractions of styrene (f_{10})

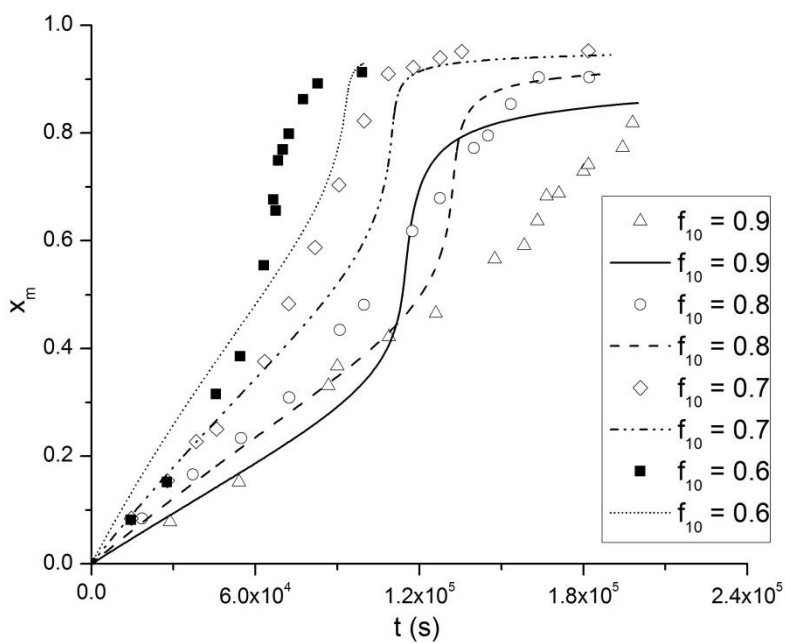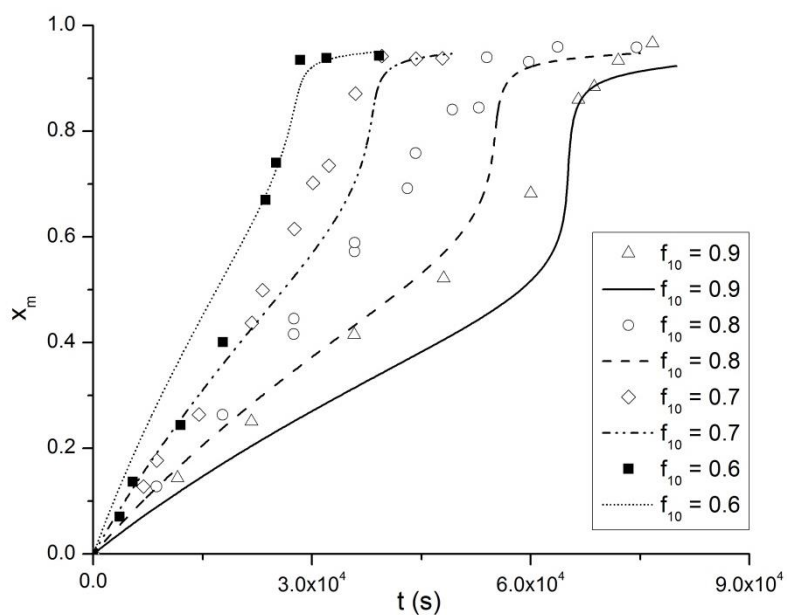**Figure A-3 (q).** Mole fraction of styrene in the (unreacted) reaction mass as a function of time for SAN copolymerization at 40 ℃ with 10 mM AIBN, for different initial mole fractions of styrene (f_{10})
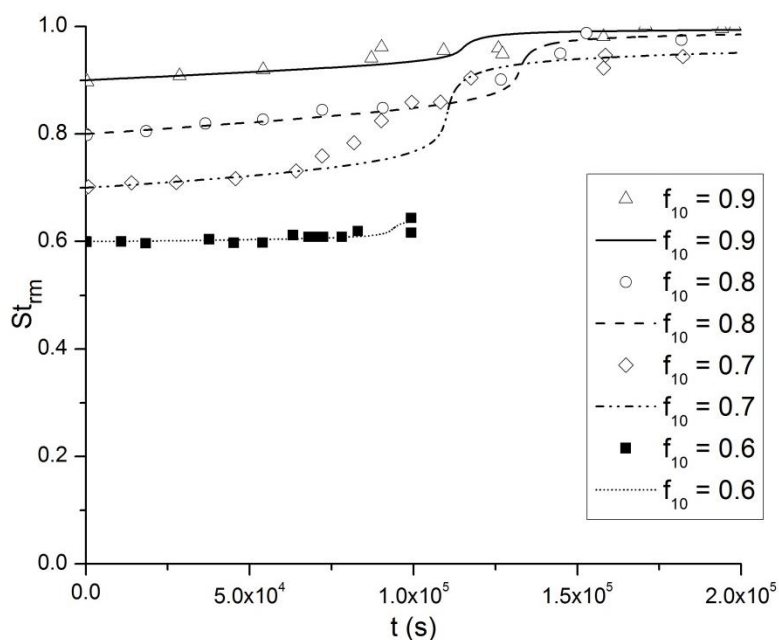
Figure A-3 (r). Mole fraction of styrene in the (unreacted) reaction mass as a function of time for SAN copolymerization at 40 ℃ with 50 mM AIBN, for different initial mole fractions of styrene (f_{10})

Figure A-3 (s). Mole fraction of styrene in the (unreacted) reaction mass as a function of time for SAN copolymerization at 60 ºC with 10 mM AIBN, for different initial mole fractions of styrene (f_{10})

Figure A-3 (t). Mole fraction of styrene in the (unreacted) reaction mass as a function of time for SAN copolymerization at 60 ºC with 50 mM AIBN, for different initial mole fractions of styrene (f_{10})

APPENDIX A-4. Experimental Results and Model Predictions for Copolymerization of SAN using BFCs

Figure A-4 (a). Conversion histories for SAN copolymerization at 40 ℃ with 10 mM AIBN for different initial mole fractions of styrene (f_{10})
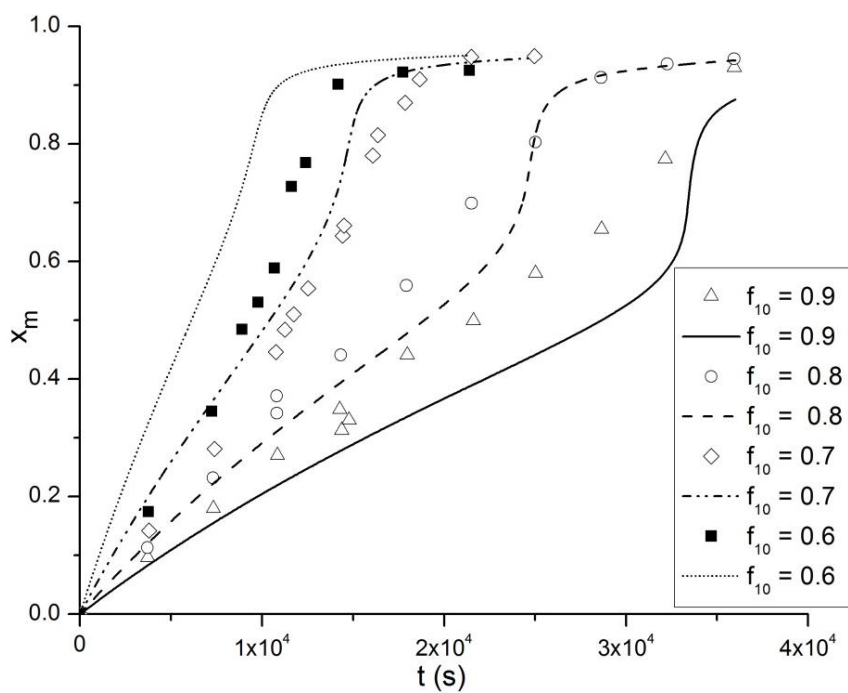

Figure A-4 (b). Conversion histories for SAN copolymerization at 40 ℃ with 50 mM AIBN for different initial mole fractions of styrene (f_{10})
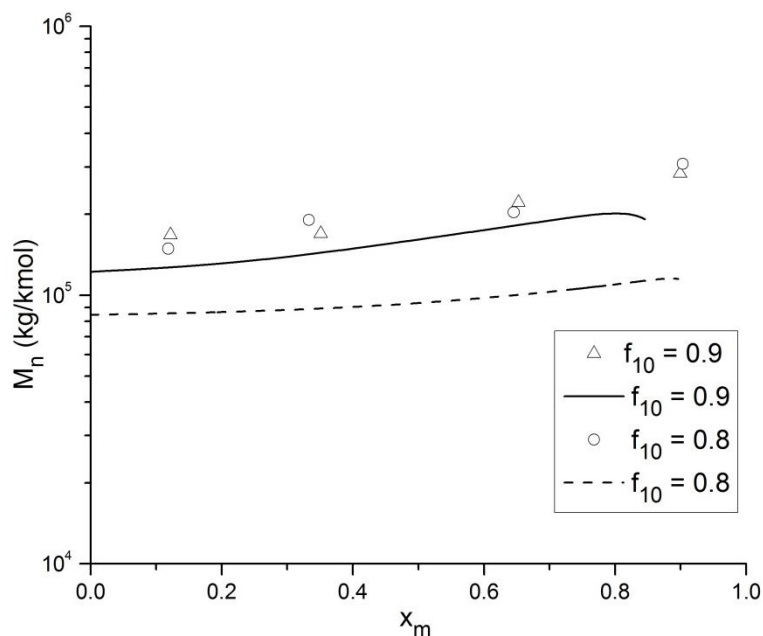
Figure A-4 (c). Conversion histories for SAN copolymerization at 60 ℃ with 10 mM AIBN for different initial mole fractions of styrene (f_{10})

Figure A-4 (d). Conversion histories for SAN copolymerization at 60 ℃ with 50 mM AIBN for different initial mole fractions of styrene (f_{10})
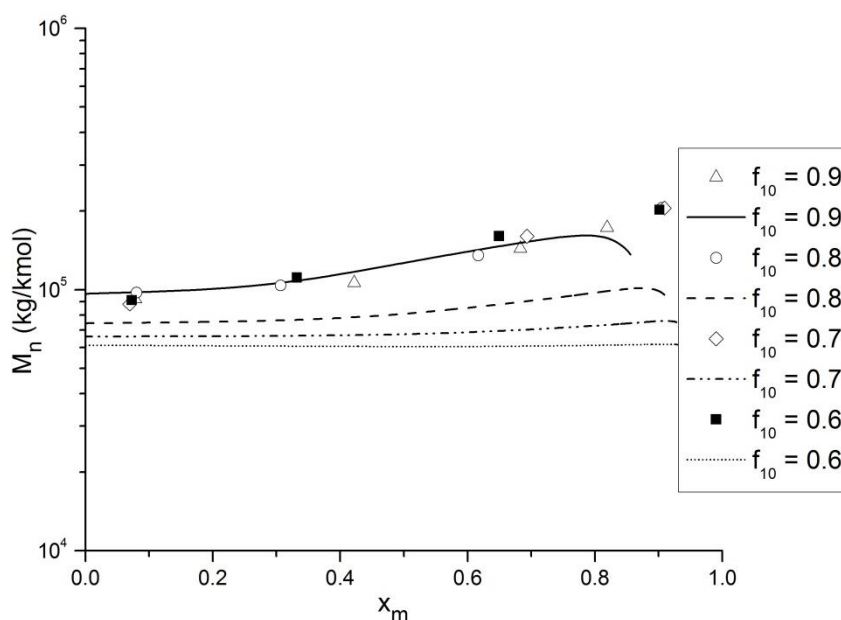
Figure A-4 (e). Number average molecular weight (M_n) as a function of the overall monomer conversion (x_m) for SAN copolymerization at 40 ℃ with 10 mM AIBN for different initial mole fractions of styrene (f_{10}). Data for two other values of f_{10} are not available.
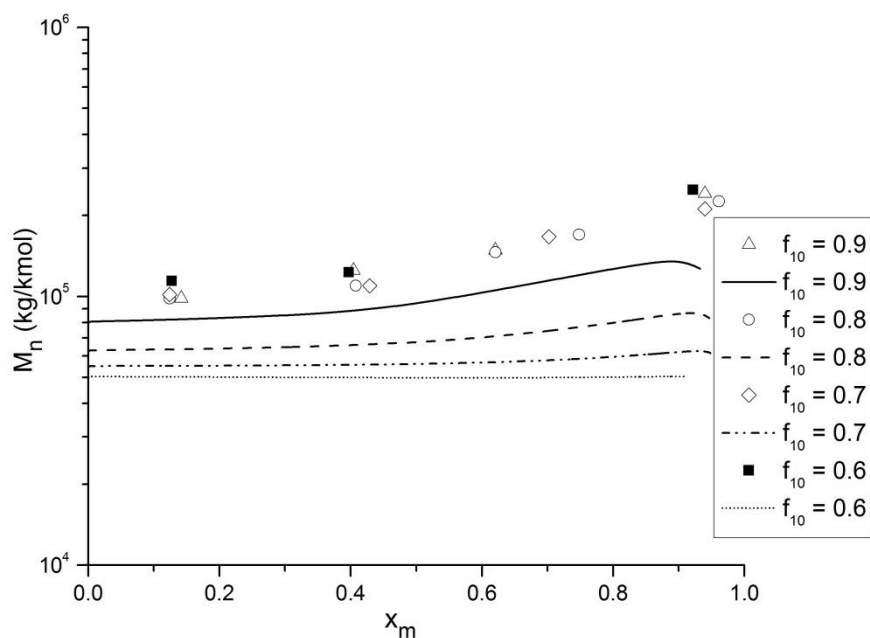

Figure A-4 (f). Number average molecular weight (M_n) as a function of the overall monomer conversion (x_m) for SAN copolymerization at 40 ℃ with 50 mM AIBN for different initial mole fractions of styrene (f_{10}).
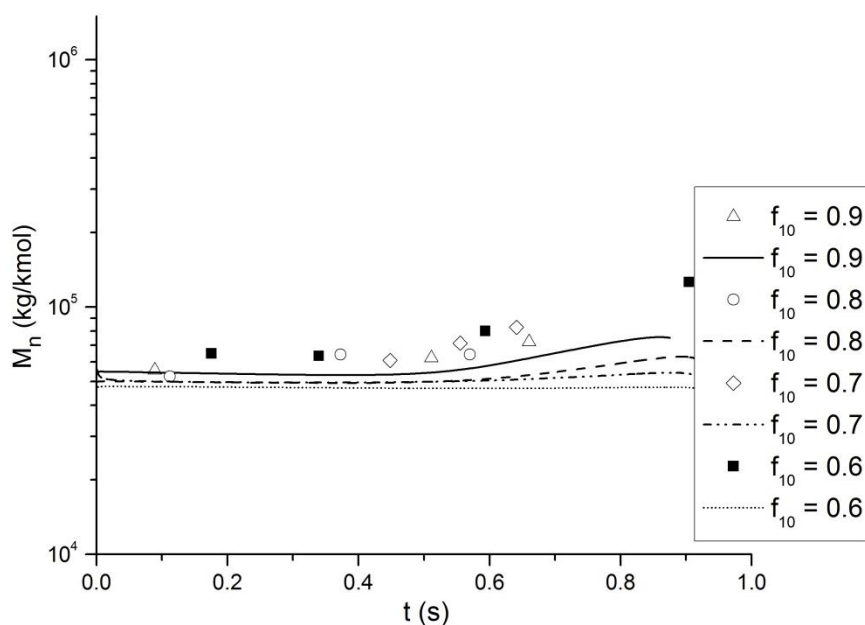
Figure A-4 (g). Number average molecular weight (M_n) as a function of the overall monomer conversion (x_m) for SAN copolymerization at 60 ºC with 10 mM AIBN for different initial mole fractions of styrene (f_{10}).
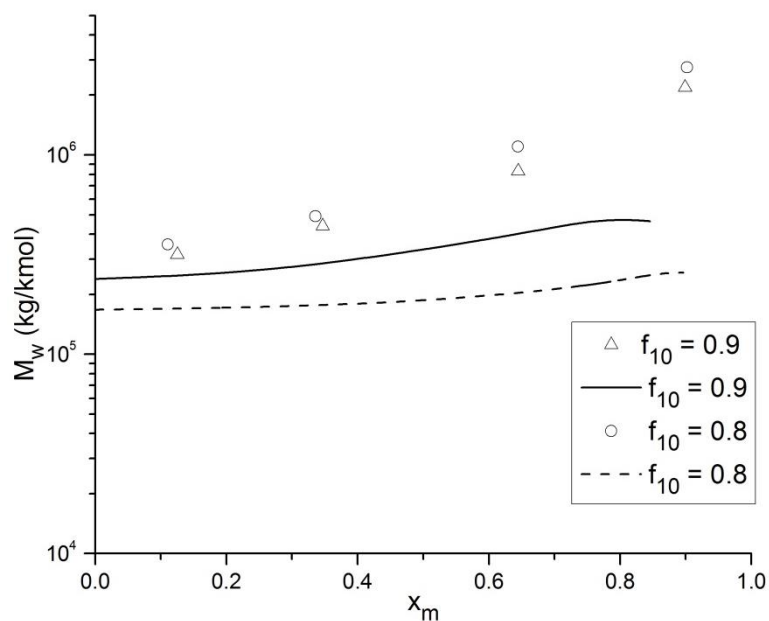

Figure A-4 (h). Number average molecular weight (M_n) as a function of the overall monomer conversion (x_m) for SAN copolymerization at 60 ºC with 50 mM AIBN for different initial mole fractions of styrene (f_{10}).

Figure A-4 (i). Weight average molecular weight (M_w) as a function of the overall monomer conversion (x_m) for SAN copolymerization at 40 °C with 10 mM AIBN for different initial mole fractions of styrene (f_{10}). Data for two other values of f_{10} are not available.
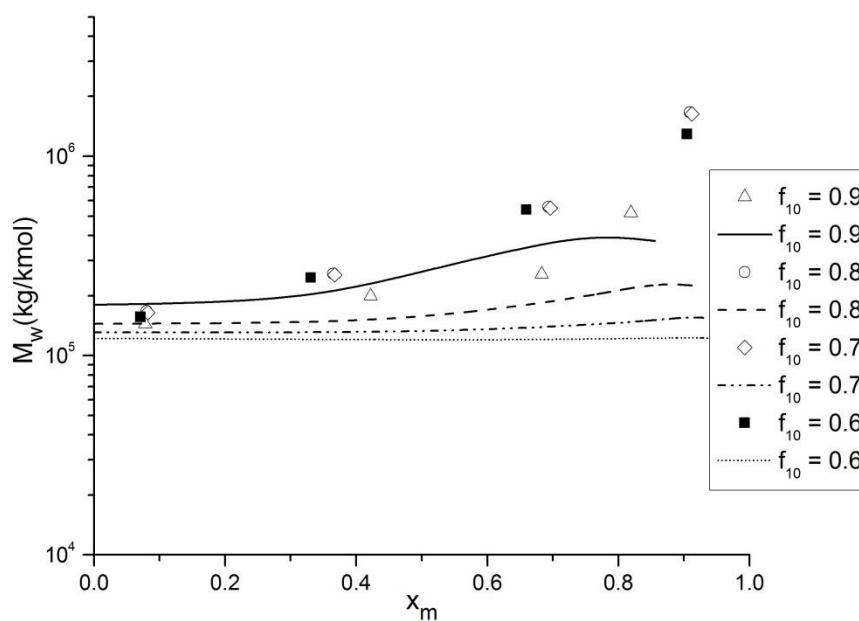

Figure A-4 (j). Weight average molecular weight (M_w) as a function of the overall monomer conversion (x_m) for SAN copolymerization at 40 °C with 50 mM AIBN for different initial mole fractions of styrene (f_{10}).
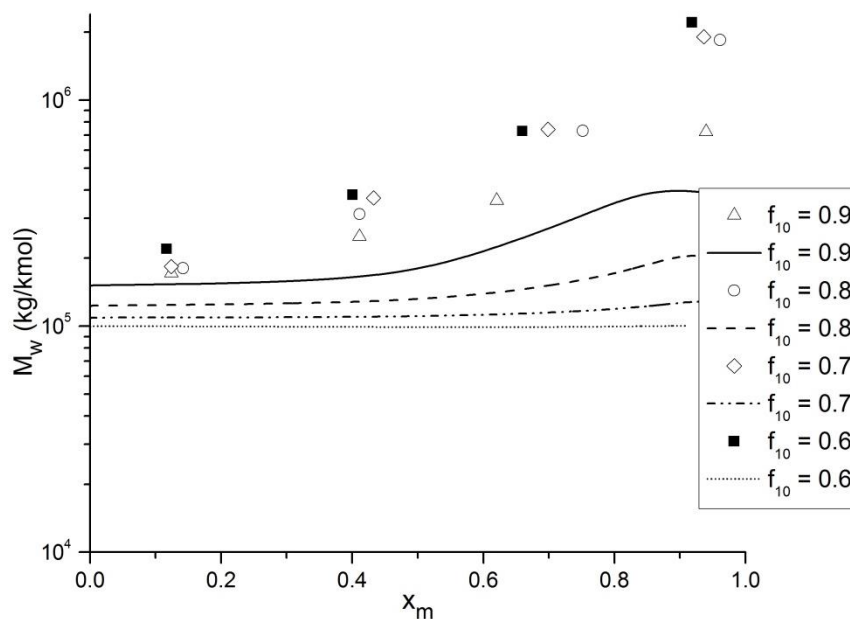
Figure A-4 (k). Weight average molecular weight (M_w) as a function of the overall monomer conversion (x_m) for SAN copolymerization at 60 ºC with 10 mM AIBN for different initial mole fractions of styrene (f_{10}).

Figure A-4 (l). Weight average molecular weight (M_w) as a function of the overall monomer conversion (x_m) for SAN copolymerization at 60 ºC with 50 mM AIBN for different initial mole fractions of styrene (f_{10}).
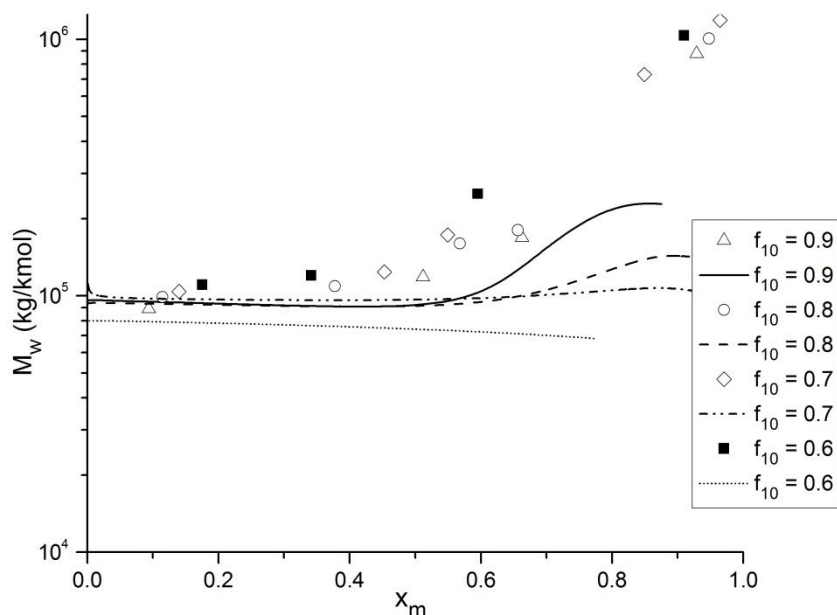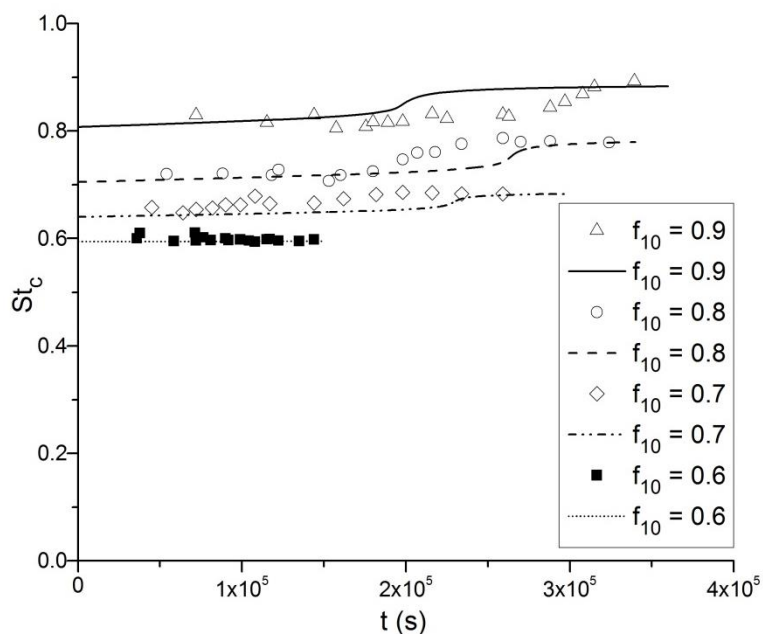
Figure A-4 (m). Mole fraction of styrene in the copolymer formed as a function of time for SAN copolymerization at 40 ℃ with 10 mM AIBN, for different initial mole fractions of styrene (f_{10})

Figure A-4 (n). Mole fraction of styrene in the copolymer formed as a function of time for SAN copolymerization at 40 ℃ with 50 mM AIBN, for different initial mole fractions of styrene (f_{10})

Figure A-4 (o). Mole fraction of styrene in the copolymer formed as a function of time for SAN copolymerization at 60 ℃ with 10 mM AIBN, for different initial mole fractions of styrene (f_{10})
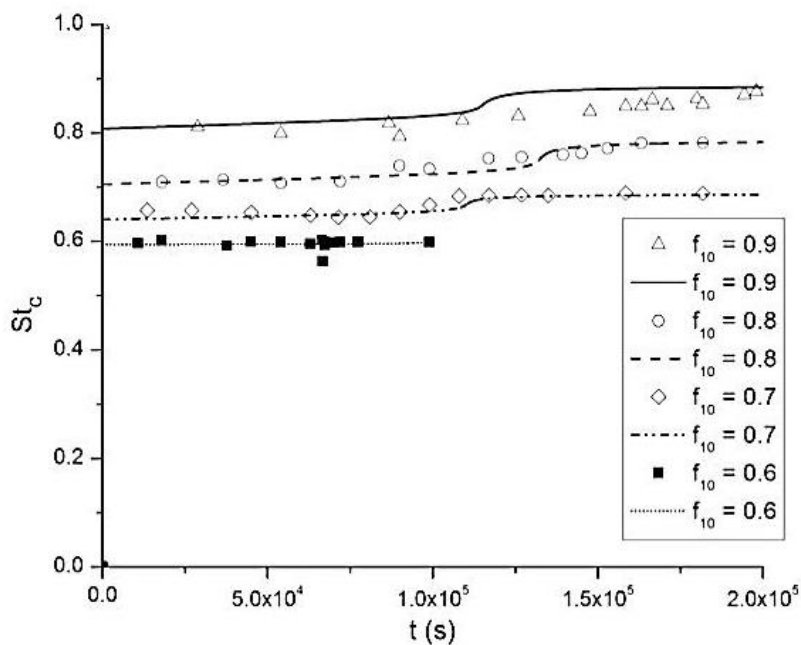

Figure A-4 (p). Mole fraction of styrene in the copolymer formed as a function of time for SAN copolymerization at 60 ℃ with 50 mM AIBN, for different initial mole fractions of styrene (f_{10})
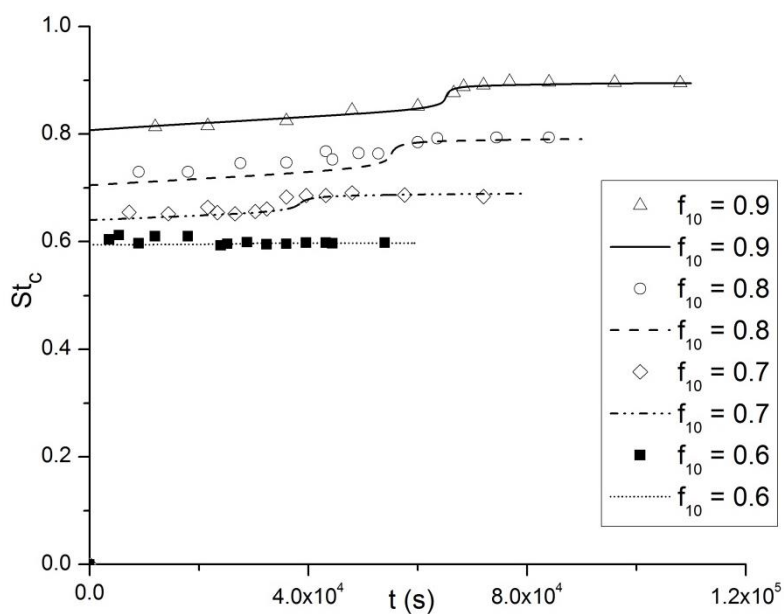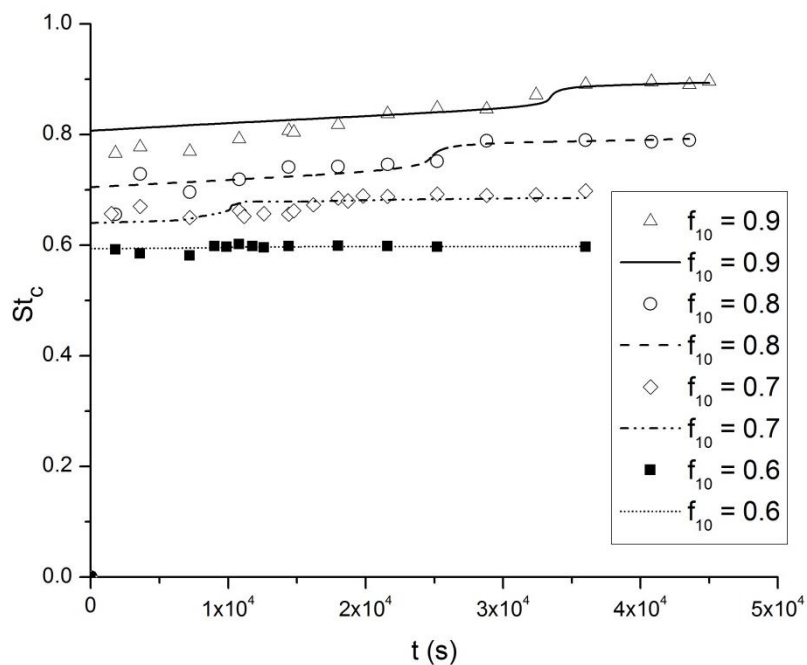
95

Figure A-4 (q). Mole fraction of styrene in the (unreacted) reaction mass as a function of time for SAN copolymerization at 40 ℃ with 10 mM AIBN, for different initial mole fractions of styrene (f_{10})
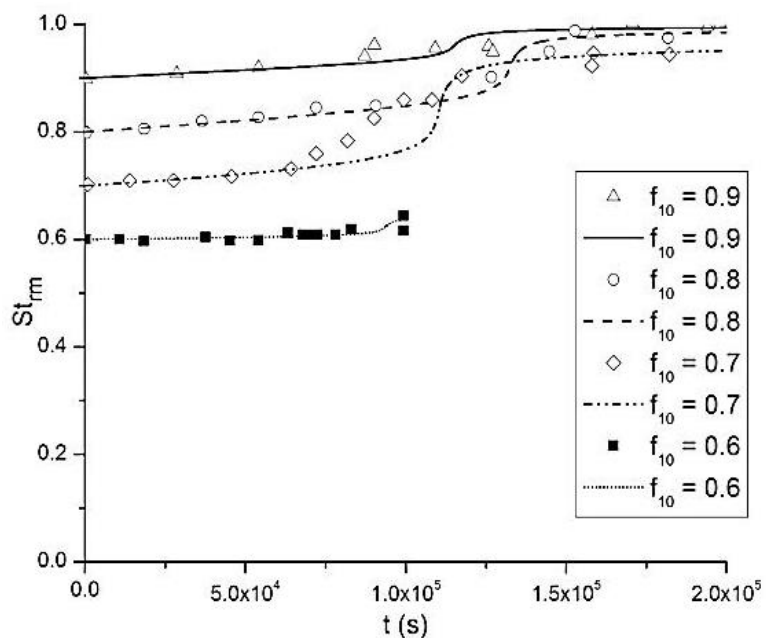
Figure A-4 (r). Mole fraction of styrene in the (unreacted) reaction mass as a function of time for SAN copolymerization at 40 ℃ with 50 mM AIBN, for different initial mole fractions of styrene (f_{10})

Figure A-4 (s). Mole fraction of styrene in the (unreacted) reaction mass as a function of time for SAN copolymerization at 60 ℃ with 10 mM AIBN, for different initial mole fractions of styrene (f_{10})
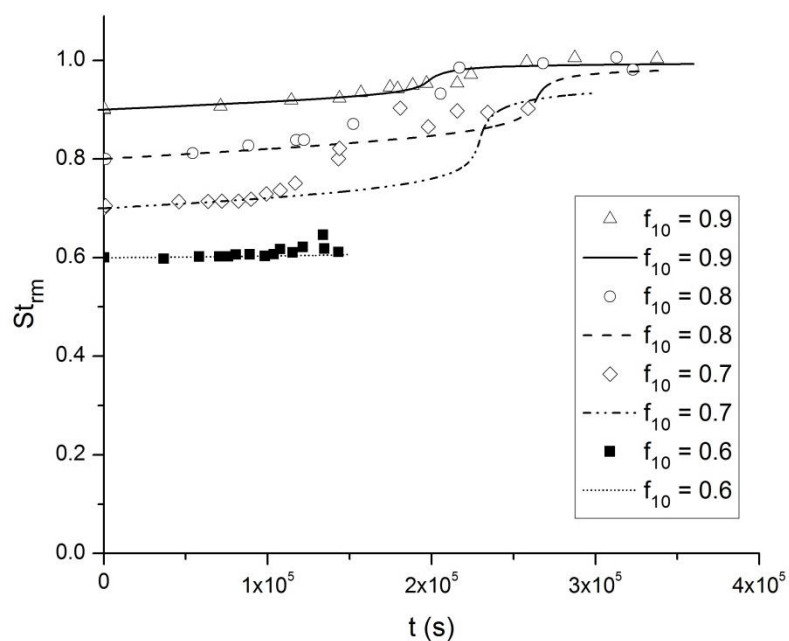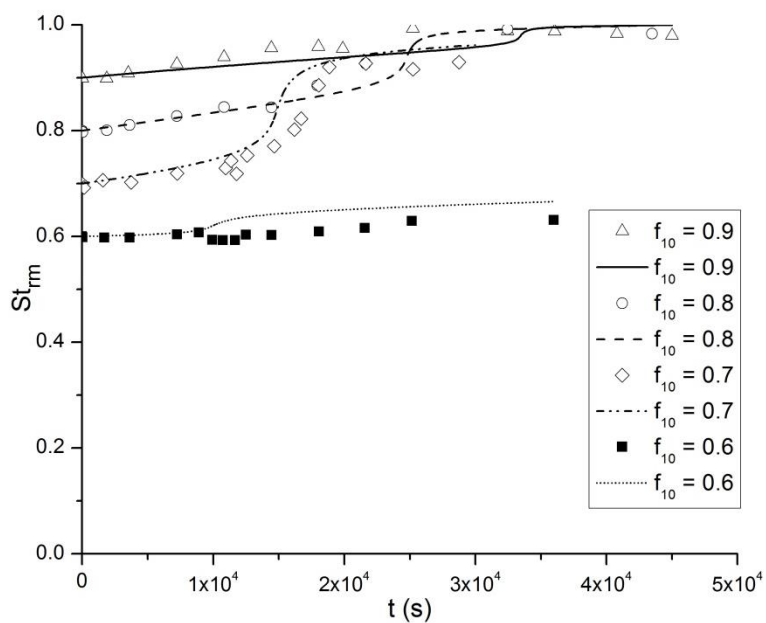

Figure A-4 (t). Mole fraction of styrene in the (unreacted) reaction mass as a function of time for SAN copolymerization at 60 ℃ with 50 mM AIBN, for different initial mole fractions of styrene (f_{10})
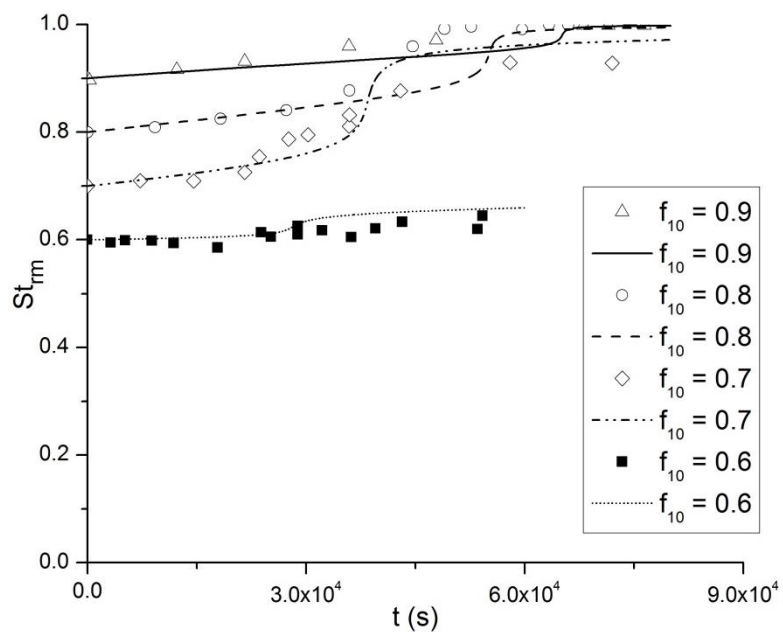
APPENDIX A-5.   Research Publications from this Thesis and Resume of the Author

RESEARCH PUBLICATIONS FROM THIS THESIS

➢ Mahajan, R., and Gupta, S. K. (2014). Modeling of Diffusional Limitations in Styrene Acrylonitrile (SAN) Random Bulk Copolymerizations. *Polymer Engineering and Science*, in press; doi No.: 10.1002/pen.24051.

➢ Mahajan, R., and Gupta, S. K. (2014). Optimization of Styrene Acrylonitrile (SAN) Random Bulk Copolymerization Reactors. *Polymer Engineering and Science,* submitted.

RESUME OF THE AUTHOR

RAJESHWAR MAHAJAN

Assistant Professor (SG)
Department of Chemical Engineering
College of Engineering Studies
University of Petroleum & Energy Studies,
Energy Acres, PO Bidholi, *via* Premnagar,
Dehradun (Uttarakhand) - 248007
Off. 0135 - 2261090, 91 (Ext. 1310)
Mob. +91 9997843732
Email: rmahajan@ddn.upes.ac.in
        rajeshwarmahajan@gmail.com

EXPERIENCE

- Assistant Professor (SG) at University of Petroleum & Energy Studies, Dehradun from 01-07-2005 onwards.

- Lecturer at Meerut Institute of Engineering & Technology, Meerut from 02-08-2004 to 30-06-2005.

- Lecturer (*ad hoc* basis) at Sant Harchand Singh Longowal Central Institute of Engineering & Technology, Longowal, Dist. Sangrur, from 12-01-2004 to 28-05-2004.

- Research Fellow in Panjab University, Chandigarh for 8 months.

PROFESSIONAL QUALIFICATIONS

- M.E. (Chemical Engg.) from Panjab University, Chandigarh with 70% marks.

- B. Tech. (Chemical Engg.) from Punjab Technical University, Jallandhar with 77.38% marks.

ACADEMIC QUALIFICATIONS

- Intermediate from Punjab School Education Board, Mohali with 75.77% marks.

- Matric from Punjab School Education Board, Mohali with 84.46% marks.

COMPUTER PROFICIENCY

Software ……………………..   Aspen Hysis, MATLAB

Operating Systems……………….   Windows, MS DOS

Programming Languages………..   C, C++, JAVA

INDUSTRIAL TRAINING

- Training at Bhabha Atomic Research Centre, Trombay from 14 June - 18 July 1999.

- In-plant training at Mukerian Papers Limited, Mukerian from 9 June to 12 July 1998.

PROJECTS UNDERTAKEN

Project during B. Tech.:   Design of Multi-component Distillation Column.

Project during M. E.:   Separation of Lead (Pb^{2+}) and Cadmium (Cd^{2+}) Ions using Bulk Liquid Membrane.

RESEARCH PUBLICATIONS

➢ Mahajan, R., and Gupta, S. K. (2014). Optimization of Styrene Acrylonitrile (SAN) Random Bulk Copolymerization Reactors. *Polymer Engineering and Science,* submitted.

➢ Mahajan, R., and Gupta, S. K. (2014). Modeling of Diffusional Limitations in Styrene Acrylonitrile (SAN) Random Bulk Copolymerizations. *Polymer Engineering and Science*, in press; doi No.: 10.1002/pen.24051.

➢ Bansal, B., Mahajan, R., Hossain, M. M., and Liaw, M. S (2006), Application of a Liquid Membrane to Recover Cadmium. *Developments in Chemical Engineering and Mineral Processing*, Vol. 14, pp. 227-238.

CONFERENCES:

➢ Mahajan, R., and Gupta, S. K., "Diffusional Limitations in Styrene Acrylonitrile (SAN) Bulk Copolymerization Reactions: A New Model" in proceedings of CHEMCON-2013, 66th Annual Session of Indian Institute

of Chemical Engineers hosted at Institute of Chemical Technology, Mumbai 400 019

➢ Bansal, B., Mahajan, R., Hossain, M. M., and Liaw, M. S, "Recovery of Cadmium using Liquid Membrane containing D2EHPA/n-Hexane," in proceeding of Chemeca 2004: Sustainable Processes: 32nd Australasian Chemical Engineering, pp.11-16, 2004.

WORKSHOPS/SHORT TERM COURSES/TRAINING PROGRAMS

➢ Delivered lectures in the DST-SERB School on Optimization (24 -29 March 2014) organized at UPES, Dehradun.

➢ Attended a two week (20-30 May 2014) ISTE workshop on Fluid Mechanics conducted by Indian Institute of Technology, Kharagpur.

➢ Attended the 3rd National Seminar on 'Bioenergy Solutions: Sustainable Supply Chains' on August 23, 2013 at the Desire Hall, Hotel Le Meridien, New Delhi, organized by Petrofed.

➢ Attended a two day (19 - 21 October 2011) Industry-Academia Workshop on "A to Z of Natural Gas and LNG" organized jointly by Petroleum Federation of India, Lovraj Kumar Memorial Trust and Petronet LNG Ltd. at Petronet LNG Terminal, Dahej.

➢ Attended a two day (26 - 27 November, 2009) workshop on "Managing Carbon Footprints in the Process Industry" organized by Lovraj Kumar Memorial Trust and EIL at India Habitat Centre, Lodhi Road, New Delhi.

➢ Attended a two day (29 June – 01 July 2009) workshop on "Natural Gas Processing and Natural Gas/LPG Pipeline Transportation" at GAIL Training Institute, Noida.

➢ Attended a two day (25 - 26 September 2008) "7th PETRO INDIA 2008" conference on "GAS IN INDIA - Issues, Opportunities and Challenges" at Hotel Hyatt Regency, New Delhi, organized by India Energy Forum (IEF) and the Observer Research Foundation (ORF).

➢ Attended a one day (14 July 2008) workshop on "IPR Sensitization" organized by Forest Research Institute, Dehradun.

- Attended a three day (7 – 9 February 2008) International Conference on "*Gas Hydrates*" organized by Directorate General of Hydrocarbon.

- Attended a workshop on "*Solid Waste Management*" organized by UPES, Dehradun in association with UCOST, Dehradun on 31 March, 2007.

- Attended a proficiency course on *"Modern Practices in Petroleum Exploration"* in IDT, ONGC from 18 – 23 September 2006.

- Attended a Summer School Programme on "*Advances in Petroleum Refining Industry*" conducted at Indian Oil Institute of Petroleum Management, Gurgaon from 3 -8 July 2006.

- Attended Dale Carnegie's *Executive Development Program* in UPES from 22 - 25 March 2006.

- Attended a two days (19 – 20 December 2005) RTI-IIP Seminar on "*Technologies For Gasification of Carbonaceous Feedstocks & Syngas Utilization*".

PERSONAL DETAILS

Father's Name……………:   Shri Satish Kumar

Date of Birth………………:   26th December 1978

Languages Known…………:   Hindi, Punjabi, English

Permanent Address…………:   House No. 274, Ward No. 2,

                                       Purana Bazar, Gurdaspur -

                                         143 521 Punjab (India).

Place**:** Dehradun

Date: 30-11-2014   (**RAJESHWAR MAHAJAN**)